

Faculty of Medicine and Health Sciences
School of Medicine.



Understanding The Biology Of CD24.

Saira Sajid.

MBBS, M.Phil. (Pathology).

Thesis submitted to the University of Nottingham for the
Degree of Doctor of Philosophy.

DEC 2017.

Declaration:

I declare that this thesis is the result of my own work during my period of study at the University of Nottingham, and it has not been submitted in any form to this, or to any other University, for a degree other than for which I am now a candidate.

Saira Sajid.

Acknowledgment:

In the first place, I must thank **ALLAH** who gave me countless blessings; one of them is the completion of this piece of work. I would like to express my deepest gratitude to my supervisor **Professor. Mohammad Ilyas** for his supervision, continuous advice, guidance, and support from the outset of this research till the end of the writing up period. Prof. Ilyas has given me endless support not only related to my work, but a lot of day to day life related guidance, advice and encouragement. I got a lot of experience being under his supervision and I consider it an honour to work with him. I am indeed grateful to him more than he knows. When I was shaken bad by my health and family crisis, his positive support played a major role, in my way back to work.

Many thanks for **Mr. Darryl Jackson** for the induction training on most of the laboratory techniques and for his continuous support with any technical queries that arose during lab work. I would also like to thank **Dr. Karin Kindle** for her expert advice and invaluable help during my experiments. I want to extend my deep gratitude to **Professor Peter Altevogt** for providing me CD24 Antibody as a gift for four years. I would like to record my deep gratitude to **all my colleagues**, in pathology research group and to **everyone** who helped me during these years enabling the successful completion of this thesis.

I am deeply thankful to the **University Of Health Sciences Lahore Pakistan/HEC Pakistan and The University of Nottingham UK**; who financially supported my PhD. Many thanks go to all members of University of Health Sciences Lahore, specially **Dr A.H .Nagi, Dr Aslam Khan, Sohail Naqvi** for the financial and moral support that they have provided me during my studies.

Dedication:

This thesis is dedicated to my ALLAH, my parents, my teachers especially DR NAGI, my husband and my son. I owe my parents, who taught me the joy of exploring and learning, and remained my support at every step of the way. My heart feels deepest gratitude to my teachers, who enlightened my way forward. My husband, whose strong belief in my abilities, sacrifices and constant support, kept me going. Last but not the least this piece of work is dedicated to my son, for whom I cannot find enough words, to express my deepest gratefulness, for his continuous patience, support, love and endless confidence in me.

Abbreviations :

AAP	Acetaminophen.
ALL	Acute lymphocytic leukaemia.
APAP	Acetyl-p-amine phenol.
BCA	Bicinchoninic Acid Protein.
Ca19-9	Cancer antigen 19-9/Carbohydrate antigen 19-9.
CD	Cluster of differentiation.
CD24	Cluster of differentiation 24 or heat stable antigen.
CEA	Carcinoembryonic antigen.
CHX	Cyclohexamide.
CLR	C-type lectin receptors.
Conc.	Concentration.
CRC	Colorectal carcinoma.
CSC	Cancer stem cells.
C-Src	Cellular Src kinase.
Cten	COOH-terminal tensin-like protein/TNS4
CXCR	Chemokine Receptor.
DAMPs	Damage associated Molecular patterns.
DRG	Dorsal root ganglion.
ECM	Extracellular Matrix.
EGFR	Epidermal Growth Factor Receptor.
EMT	Epithelial Mesenchymal transition.
FAK	Focal adhesion Kinase.
GPI ANCHOR	Glycosyl Phosphatidylinosito Anchor.
H3	Histone 3.
HMGB1	High Mobility Group Box 1 Protein.
HSP90	Heat shock protein 90.
ILK	Integrin linked Kinase.
KDa.	Kilo Daltons.
LCAM/CD171	Liver Cell Adhesion Molecule.
moAb	monoclonal Antibody.
MALDI-MS	Matrix-assisted laser desorption/ionization- Mass spectrophotometry.
MET	Mesenchymal epithelial transition.

MSCs	Mesenchymal stem cells.
NCL	Necrotic cell lysate.
NLRs	NOD like receptors.
NOD	Nucleotide-binding oligomerization domain.
ORF	Open Reading frame.
PAMPs	Pathogen associated molecular patterns.
PBS	Phosphate Buffered Saline.
PCR	Polymerase Chain Reaction.
PTB	Phosphotyrosine-binding domain.
PTEN	Phosphatase and tensin homolog.
RAGE	Receptor for Advanced Glycation End products.
SDM	Site-directed mutagenesis.
SH2	Src homology domain 2.
SIGLECS	Sialic acid binding Immunoglobulin like lectins.
SLE	Systemic lupus erythematosus.
STAT3	Signal Transducer and Activator of Transcription 3.
TBS	Tris-buffered saline.
TCF/LEF	T-cell factor/lymphoid enhancer factor.
TLR	Toll like receptors.
TNF α	Tumour necrosis factor alpha.
UC	Ulcerative colitis.
UTR	Untranslated Region.

Abstract:

Cancers are amongst the leading cause of morbidity and mortality today. Besides the tremendous amount of research, it still appears to be a long way till we can fully understand the pathology and find its cure. Scientists are still striving to find out the precise pathogenesis, factors leading to progression and the mechanisms of spread of cancers. The ultimate objective is to find out how these can be prevented and treated. Many molecules are a focus of attention in this regard and CD24 is amongst them. CD24 is normally present on haematopoietic cells and embryonal epithelial cells but the expression is generally lost with cellular maturity and differentiation.

Upregulation of CD24 has been documented in a large variety of cancers, besides non-malignant pathologies. In the recent literature, CD24 has been linked to significant cancer associated properties such as proliferation, metastasis and cancer stem cells. It is an interesting molecule with a very small protein core decorated with heavy glycosylation. The pattern and composition of CD24 glycosylation also varies within different tissues. This study attempted to explore the molecule a bit further regarding its structure, functions, molecular interactions and possible downstream signalling partners.

The first part of the project was to evaluate the possible effects of CD24 in mediating cellular response to DAMPs (Damage Associated Molecular Patterns) in colorectal cancer cell lines. Malignancies have increased CD24 levels and there is increased tissue damage and necrosis thereby release of DAMPs (Damage Associated Molecular Patterns) in their microenvironment. The effects of CD24 on modulation of DAMPs response were analysed by exposing cells to autologous DAMPs and performing functional assays (migration and proliferation assays).

Abstract.

The results of wound healing assay showed significant inhibition of colorectal cell migration by DAMPs but this was independent of CD24 status. Furthermore, transwell assays also showed significantly reduced directional motility, independent of CD24 status, in cells exposed to autologous DAMPs. The study also tested the effects of DAMPs on cellular proliferation in three colorectal cancer cell lines using Presto Blue assay. The results indicated a significant increase in cellular proliferation when exposed to DAMPs, irrespective of the CD24 status of the cell line. We proposed thereby that in colorectal cancer cells, CD24 does not appear to modulate cellular response to DAMPs unlike seen in immune cells. Nevertheless, DAMPs did show effects on autologous cell migration and proliferation. However it is acknowledged that the arguments can be strengthened by the use of purified DAMPs to demonstrate similar results and also by showing abrogation of effects after addition of anti-DAMPs antibodies to our functional assays.

Another interesting aspect of CD24 is its localisation in the cell membrane. It is attached to the cell membrane via GPI anchor and resides in lipid rafts. Interestingly, it has no cytoplasmic or transmembrane domains that are used by most signalling molecules. It is unclear how CD24 molecule mediates diverse cellular properties and molecular responses in the absence of traditional signalling domains.

The second part of this study was aimed at exploring some of the potential signalling partners and their functional relevance if any to CD24. The study explored Cten and CD24 interactions, as both molecules are proposed to be mediators of increased cellular motility. CD24 and Cten were also observed to have some common downstream signalling targets. In addition, the expression levels of both molecules also presented similar trends amid different cancer cell lines.

Abstract.

The above observations led us to contemplate if the two molecules have mutual signalling and functional relationship. We observed that CD24 up regulation led to increased levels of Cten protein, whereas, knock down of CD24 resulted in down regulation of Cten protein. Also the results of our functional studies showed that the knockdown of Cten in co-transfection experiments abrogated the increased cell motility by CD24. Based on these observations we proposed that CD24 appears to modulate Cten levels and this regulation has significant functional relevance as well. The Co-immunoprecipitation experiments indicated that these two molecules did not seem to have physical interaction with each other, suggesting the possibility that the regulation of Cten by CD24 may be arbitrated by intermediate molecules.

Similarly, we also investigated the molecular relationship between CD24, ILK and FAK using co-transfection technique. The results revealed enhanced cell migration through the membrane by CD24 but it was reduced after the knock down of both ILK and FAK. These findings provide further insight that not only these molecules are being regulated by CD24 as proposed by many recent studies but are also functionally relevant. The current study proposed that the increased cancer cell motility demonstrated by CD24 may well be mediated through FAK and ILK in addition to Cten. The argument needs further validation as the confirmation of successful transfection and expression levels by western blots are missing in this study. This is recognised as a limitation.

Being heavily glycosylated CD24 is considered a mucin- like molecule and many studies point towards the possibility of its functional diversity to be related to these sugars. But to date not much is known about this aspect of CD24. Hence, the third part of our study was aimed at finding the functional and

Abstract.

signalling significance of these sugar binding sites. CD24 has both O and N-sugar binding sites. While the molecule has multiple O-glycosylation sites, there are only two potential sites for N-glycosylation. Employing the fact that for CD24 molecule to be N-glycosylated, asparagine is a must and should be present in a specific sequence. We aimed at replacing the asparagine by glutamine, hence disabling the site to be decorated by N-sugars in CD24. We designed to mutate these N-glycosylation sites using Phusion-site directed mutagenesis kit. The procedure uses mutant primers in a PCR-based methodology to create the desired mutation. Once successful the next step of the study was to use this mutant CD24 in further experiments to explore the signalling and functional significance of these sugars in CD24 molecule. However, the results of our gene sequencing experiments showed that the attempt at generating the required clones was not successful and needed retrial. This step could not be carried out due to time limitation.

In summary, it can be said the study aimed at exploring novel aspects of CD24 biology from three different perspectives with some exciting new facts and findings. Though these are undermined by a number of limitations that can be rectified as discussed in the thesis and would generate stronger and publishable contribution to the current understanding of CD24 biology.

INDEX OF CONTENTS:

Chapter One: General Introduction.	1
General over view of CD24:.....	2
Genome of CD24:	2
CD24 m-RNA:.....	3
Protein structure:.....	3
Sequence comparison of Murine HSA and Human CD24:.....	5
Ligands of CD24:	6
Expression of CD24:	8
Role of CD24 in Immune system:.....	9
Role of CD24 in neuronal tissue:	11
Role of CD24 in Autoimmune diseases:	12
Stem cells and cancer stem cells:.....	12
Current controversies about role of CD24 :.....	19
Study Aims:	21
Chapter Two: Materials and Methods.....	23
Cell Lines:	24
Cell cultures:	26
Transient forced expression of CD24 by transfection:	27
Transfection:	27
Total RNA extraction:	30
RNA/DNA quantification and quality check:	31
Synthesis of complementary DNA from RNA:	32
Q-PCR:	33
Set up of PCR reaction:.....	34
Western blot:	35
Cell migration assays:	43
Methylene blue proliferation assay:	44
Trypan blue exclusion assay for counting dead cells:	46
Knock down of CD24:	47
Statistical Analysis:	48
Chapter Three: DAMPs and CD24.....	49
Introduction:	50
Materials and methods:	59
Results:	65
Discussion:	82
Chapter Four: CD24 Signalling Partners.	87
Introduction:	88
Material and methods:	98
Results:	107

Discussion:	123
Chapter Five: Mutating N-glycosylation sites of CD24.	127
Introduction:	128
Materials and methods:	140
Results:	164
Conclusions of transformation reactions:.....	171
Discussion:	182
Chapter six: General Discussion.	188
General discussion:	189
Conclusions:.....	199
Potential strengths:	200
Study limitations:.....	200
Future Suggestions and Recommendations:	203
References.	207
References:	208
Appendix.	218
Appendix:	219

INDEX OF FIGURES:

FIGURE 1: SIMPLIFIED CARTOON OF CD24 PROTEIN.	4
FIGURE 2: SIMPLIFIED DIAGRAM SHOWING EXTENSIVE GLYCOSYLATION SITES OF CD24 ⁽⁸⁾	5
FIGURE 3: PRIMARY AMINO ACID SEQUENCES FOR HSA (MOUSE) AND HUMAN CD24 ⁽⁸⁾	6
FIGURE 4: EXPRESSION OF CD24 FOUND IN MURINE AND HUMAN CELLS. ⁽²⁴⁾	8
FIGURE 5: L1 AND CD24 INTERACTIONS IN THE BRAIN ^(18, 43)	11
FIGURE 6: CANCER STEM CELLS AS A CAUSE OF TUMOUR RE-GROWTH ⁽⁵⁰⁾	14
FIGURE 7: SIALIDASE INHIBITORS DAMPEN SEPSIS. ⁽⁶⁶⁾	19
FIGURE 8: RELEASE OF DAMPS FROM NECROTIC CELLS TO INDUCE STERILE INFLAMMATION. ⁽⁷⁶⁾	52
FIGURE 9: SIMPLIFIED MODEL OF CD24/SIGLEC/DAMP INTERACTION.	53
FIGURE 10: FLOW DIAGRAM OF POTENTIAL OUTCOMES OF TISSUE INJURY ⁽⁷⁹⁾	56
FIGURE 11: TRANS WELL MIGRATION.	62
FIGURE 12 : WESTERN BLOT SHOWING DAMPS IN SUPERNATANTS (SW620).	66
FIGURE 13: WESTERN BLOT SHOWING DAMPS IN SUPERNATANTS (DLD1 AND HCT116).	66
FIGURE 14: OPTIMISATION OF SUPERNATANT CONC. FOR FUNCTIONAL ASSAYS.	67
FIGURE 15: WESTERN BLOTS OF CELL LINES SHOWING CD24 EXPRESSION LEVELS.	70
FIGURE 16: DAMPS REDUCED CELL MIGRATION ACROSS THE WOUND.	71
FIGURE 17: WOUND HEALING ASSAY IN FOUR COLORECTAL CELL LINES.	72
FIGURE 18: DAMPS INHIBIT DIRECTIONAL MOTILITY AS WELL IN AUTOLOGOUS CELL LINES.	73
FIGURE 19: DAMPS DECREASE CELL MOTILITY BY INHIBITING EPITHELIAL MESENCHYMAL TRANSITION.	75
FIGURE 20: INHIBITION OF TRANSWELL MIGRATION BY DAMPS IS NOT MEDIATED THROUGH CD24.	76
FIGURE 21: WESTERN BLOT SHOWING CD24 KNOCK DOWN.	77
FIGURE 22: FORCED EXPRESSION OF CD24 WAS CONFIRMED BY WESTERN BLOT.	78
FIGURE 23: DAMPS INHIBITORY EFFECT ON MOTILITY APPEARS INDEPENDENT OF CD24.	79
FIGURE 24: DAMPS INDUCE SIGNIFICANT INCREASE IN CELLULAR PROLIFERATION.	81
FIGURE 25: SCHEMATIC CARTOON OF LIPID RAFTS SHOWING GPI ANCHORED PROTEINS. ⁽⁹¹⁾	90
FIGURE 26: SCHEMATIC DIAGRAM ILLUSTRATING A FOCAL ADHESION COMPLEX.	91
FIGURE 27: SELECTION OF CD24 EXPRESSION VECTOR.	108
FIGURE 28: CD24 CAUSES UPREGULATION OF CTEN.	109
FIGURE 29: KNOCK DOWN OF CD24 CAUSES DOWN REGULATION OF CTEN.	110
FIGURE 30: INVESTIGATION OF PHYSICAL INTERACTION BETWEEN CD24 AND CTEN PROTEINS.	111
FIGURE 31: TRANSWELL MIGRATION ASSAY AFTER CO TRANSFECTION WITH CD24 AND CTEN.	114
FIGURE 32: WESTERN BLOT FOR CO TRANSFECTIONS.	115
FIGURE 33: CD24 INCREASES MOTILITY VIA ILK.	119
FIGURE 34: CD24 MEDIATES CELL MOTILITY VIA FAK AND ILK IN HCT116.	121
FIGURE 35: CD24 HAS A FUNCTIONAL RELATIONSHIP WITH FAK AND ILK IN RKO.	122
FIGURE 36: SCHEMATIC DIAGRAM FOR PROPOSED LINK BETWEEN CD24 AND CTEN/ILK AND FAK.	124
FIGURE 37: STEPS OF PROTEIN N-GLYCOSYLATION ⁽¹²²⁾	129
FIGURE 38: CD24 AND COMMON SUGARS ON THE HUMAN CELL SURFACE .MODIFIED IMAGE ⁽¹³⁶⁾	133
FIGURE 39 : GPI ANCHORAGE AND GLYCOSYLATION OF CD24. ⁽¹⁴⁶⁾	138
FIGURE 40: FLOW DIAGRAM SHOWING THE EXPERIMENTAL PLAN FOR SITE DIRECTED MUTAGENESIS.	143
FIGURE 41: SITE DIRECTED MUTAGENESIS FLOW CHART:	147
FIGURE 42: DIAGRAM INDICATING EXPECTED PRODUCT SIZES USING T7 AND BGH PRIMERS.	160
FIGURE 43: SCREENSHOTS OF SDM-ASSIST WHILE CREATING PRIMERS.	163
FIGURE 44: N36 PRIMER OPTIMIZATION.	164
FIGURE 45: N36 PRIMER OPTIMIZATION WITH ADDED MgCl ₂	166
FIGURE 46: TEMPERATURE GRADIENT FOR N36 REDESIGNED PRIMER.	166
FIGURE 47: N52 PRIMER OPTIMISATION.	167
FIGURE 48: TEMPLATE CONCENTRATION OPTIMISATION.	169
FIGURE 49: TEMPLATE CONCENTRATION OPTIMISATION.	170
FIGURE 50: BLAST 2 ANALYSES OF CD24 REFERENCE GENE AND WT CD24 CLONE	175
FIGURE 51: SEQUENCE ALIGNMENT OF CD24 REFERENCE GENE AND WT CD24.	176
FIGURE 52: MEGA6 ALIGNMENT ANALYSIS OF N-36 CLONES.	178
FIGURE 53: MEGA6 ANALYSIS OF N-52 MUTANT CLONES.	179
FIGURE 54: SCREEN SHOT OF NCBI BLAST2 OF N-52 CLONE WITH CD24 ORF.	180

INDEX OF TABLES:

TABLE 1: STATUS OF SIGNIFICANT ONCOGENES IN THE CELL LINES USED ⁽⁶⁹⁾.	26
TABLE 2: MASTER MIX MADE FOR THE REVERSE TRANSCRIPTION REACTION.	33
TABLE 3: MASTER MIX MADE FOR THE RT- NEGATIVE REACTIONS.	33
TABLE 4: PRIMERS USED FOR QPCR.	33
TABLE 5: MASTER MIX FOR QPCR	35
TABLE 6 : SUMMARY OF ANTIBODIES USED IN THE STUDY.	40
TABLE 7: TIMINGS OF MEDIA CHANGES DURING CO-TRANFECTIONS.	100
TABLE 8: SCALING CONCENTRATIONS FOR TRANSFECTION COMPONENTS	100
TABLE 9: PLATE SET UP FOR CO TRANSFECTIONS USING CD24 AND CTEN.	101
TABLE 10: PLATE SET UP FOR CO TRANSFECTIONS USING CD24 AND FAK/ILK.	102
TABLE 11: SEQUENCE OF siRNAs USED IN CO TRANSFECTIONS AND KNOCK DOWN.	102
TABLE 12: CODONS AND THE CORRESPONDING AMINO-ACID SEQUENCE FOR CD24 MATURE PEPTIDE.	145
TABLE 13: PRIMERS USED IN OUR SITE DIRECTED MUTAGENESIS EXPERIMENTS.	151
TABLE 14: COMPONENTS AND CONCENTRATIONS OF MUTAGENESIS REACTION.	153
TABLE 15: COMPONENTS AND CONCENTRATIONS OF DIGESTION REACTION.	155
TABLE 16: COMPONENTS AND CONCENTRATIONS OF LIGATION REACTION.	156
TABLE 17 : HRM REACTION COMPONENTS.	160

Chapter One: General Introduction.

General over view of CD24:

CD24 is also known as Heat Stable antigen (HSA) and was first discovered in mice by Springer et al in 1978. Mouse CD24 gene was cloned in 1990 and the human analogue of the gene was discovered a year later. Initially, it was thought to be a marker of immune cells but in the recent years, a whole multitude of potential roles have been attributed to this molecule. These encompass roles in immunity, inflammation, auto immunity, tumour metastasis and progression. CD24 is also proposed to be a marker of cancer stem cells in recent literature. This stemness potential may confer features like resistance to chemotherapy and hence linking CD24 with poorer prognosis in a wide spectrum of haematological and solid tumours. There is yet much to explore about this tiny molecule, in order to understand the diversity presented by the literature regarding its potential roles.

Interesting aspects of CD24 biology include:

- Gene structure
- Protein structure
- Extensive glycosylation
- Location in lipid rafts
- Ligands of CD24

Genome of CD24:

Mouse CD24 gene cloned in 1990 was found at Chromosome 10 and very similar sequences were also observed at chromosome number 8 and 14. However, the copy at chromosome 10 is regarded as the true gene as the other two sites lack introns and do not express the protein.

Human CD24 gene has a similar situation and its location has been a debate. There are highly homologous sequences in the human genome namely at chromosome 1p (CD24L1),

chromosome 15q21-q22 (CD24L2), chromosome 20q11.21 (CD24L3) and chromosome Yq11 (CD24L4) and chromosome 6 (1). In the case of chromosome 15, it is considered as a pseudogene as the ATG start codon is replaced by a GTG codon. Looking up Yq11 reveals that it is theoretically capable of producing a protein; however, it is deficient in the TATA box which is present in the CD24 promoter on chromosome 6(2). As the level of CD24 expression does not show any gender difference between males and females, copy present on Y chromosome may also be taken as a pseudogene. This leaves most researchers to conclude that chromosomal 6q21 copy to be the true gene location for CD24(1).

CD24 m-RNA:

CD24 mRNA comprises 2179 base pairs, its ORF (open reading frame) has just 243 base pairs starting from 111 till 353 (**see Appendix i /Appendix ii**). CD24 has a particularly long 3' UTR region (1.8 kilo-bases) that provides capping and stability to the CD24 mRNA. Deletions of this 3' UTR have been linked to unstable mRNA and a higher risk of developing systemic Lupus erythematosus (SLE) and Multiple sclerosis (MS) (3). Another important feature of the CD24 mRNA is the presence of a regulator region from position -446 till -840 relative to the start codon (ATG). This is a binding site for TCF/LEF (transcription factors) and link the regulation of this gene by the Wnt canonical pathway, the signal transduction pathway also known as Wnt/ β -catenin Pathway (4).

Protein structure:

Human CD24 gene is translated into 80 amino acids but the mature peptide is just 31 amino acids (5),(6). It has an N-terminal signal peptide directing CD24 to the cell surface and

later gets removed in the endoplasmic reticulum; this signal peptide comprises of 26 amino acids.

Present at the C-terminal, is a 23 amino acids sequence that starts at position 59, it represents a pro-peptide and is called GPI-displaced tail (5). It helps in the binding of the GPI anchor to the C-terminal of CD24 protein and it is sliced off subsequently leaving the mature peptide hanging on the cell membrane through a GPI anchor **Figure 1**.

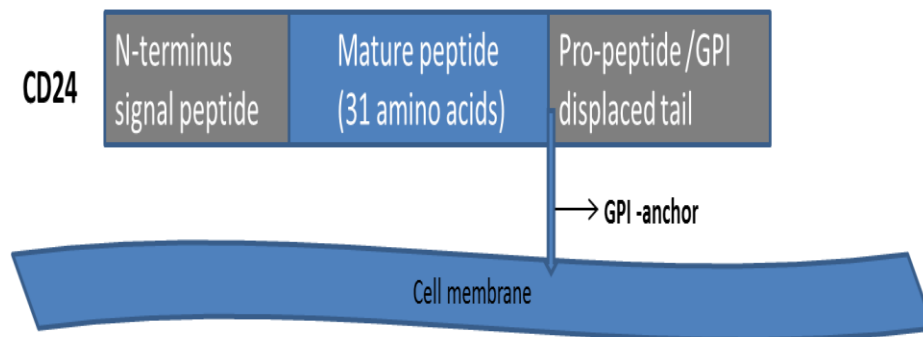


Figure 1: Simplified cartoon of CD24 protein.

CD24 undergoes extensive post translational modifications and in addition to the ones described above, there is extensive glycosylation. The molecular weight of CD24 ranges from 30 to 70 kDa (5), most of its weight and the variability of weight is due to extensive and variable N- and O-linked glycosylation in different tissues and cells. CD24 has 16 potential O- and two potential N glycosylation sites (7), **Figure 2**.

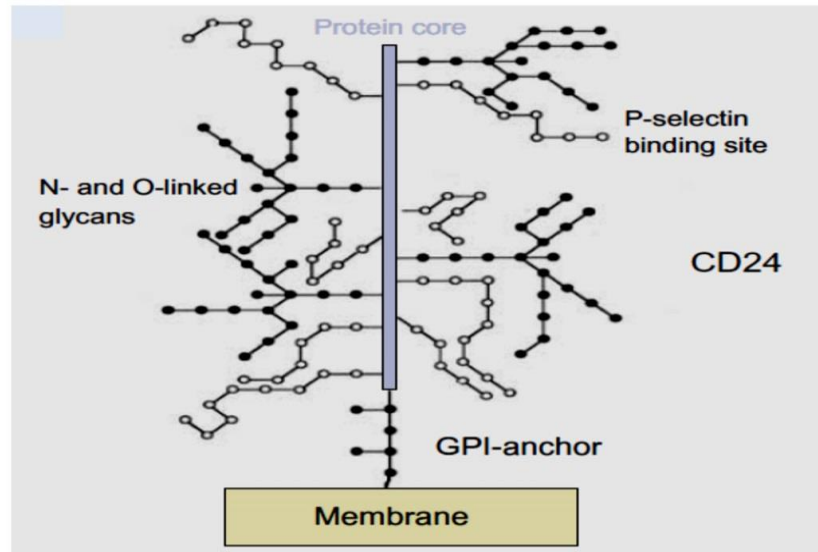


Figure 2: Simplified diagram showing extensive glycosylation sites of CD24⁽⁸⁾.

The glycosylation renders CD24 similarity to a mucin. The pattern of glycosylation of CD24 is highly variable and differs significantly between cell types and tissues (9, 10). In general, studies using MALDI-MS techniques to analyse glycosylation patterns of CD24 show that the N-glycosylation pattern of CD24 is less complex in the majority of cases when expressed in cell lines compared to the expression in brain, independent of whether the cell line is of murine or human origin(11, 12). Several studies have provided proof that at least some functions of CD24 are dependent on its glycosylation. The process takes place in endoplasmic reticulum and Golgi and will be discussed in more detail in the chapter on N-glycosylation of CD24.

Sequence comparison of Murine HSA and Human CD24:

Aigner *et al.* in 1997 presented in a study the sequence comparison of human and mouse CD24. They proposed that during evolution the human CD24 molecule has acquired additional serine and threonine residues. Making the molecule more like a typical mucin (by providing additional glycosylation

L1:

L1 is a member of the immunoglobulin superfamily (15, 16) and also known as LCAM1 and CD171. It is a 200-kDa adhesion molecule, with both homophilic and heterophilic characteristics expressed by many post-mitotic neurons in the central nervous system and also present on the lymphoid cells. According to a study, by Kadmon G *et al.* CD24 acts as a ligand for L1 (16, 17). A recent study by Kleene *et al.* also showed that L1 and CD24 cooperate with each other in neurite outgrowth and signal transduction. They also revealed that binding of CD24 to L1 depends on α 2,3-sialic acid on CD24, which determines the CD24 induced and cell type-specific promotion or inhibition of neurite outgrowth(18).

TAG-1 and Contactin:

In addition to α 2,3-linked sialic acid and L1 interaction, another important sugar present on CD24 molecule is Lewis x glycan. TAG-1 also called Axonin-1, is a cell adhesion molecule and Contactin is a lectin like molecule present in the lipid rafts (17). They interact with Lewis-X glycan and mediate **Lewis-x dependent** neurite outgrowth of cerebellar and DRG (dorsal root ganglion) neurons (19).

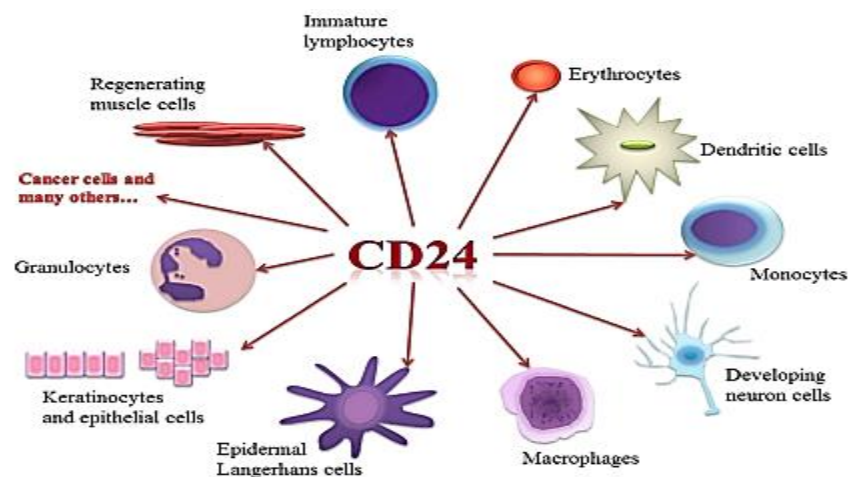
SIGLECS:

Siglecs are quite recently identified. These are **Sialic acid binding Immunoglobulin like lectins**. These are members of the Ig superfamily and are expressed on immune cell surfaces including B-cells, NK-cells, eosinophils, basophils, thymocytes and T-cells (20). In humans more than 10 types of Siglec-molecules have been identified till now. Each of these has a distinct yet sometimes overlapping tissue expression and interactions and they are believed to play a variety of significant

roles. Studies have shown that CD24 is a ligand for Siglec10 in humans and Siglec G in mice and this interaction plays a very important role regarding the physiological response of cells to tissue damage caused by non-pathogenic stimuli (DAMPs)(21). This interaction helps to discriminate between **Pathogen mediated** and **Damage mediated** tissue injury. Even though both tissue injuries lead to, Toll like receptor activation, DAMPs-Siglec and CD24 combination sends inhibitory signals to the innate immune system(21).

Expression of CD24:

In mouse CD24 is found on haematopoietic cell populations including erythrocytes, thymocytes, neutrophils, B-cells and T-cells. As its expression is developmentally regulated, it was traditionally used as a marker of differentiation for B and T-cells ontogeny(22). Later it was also found to be expressed during the embryonic stages of other tissues including neuronal tissue and certain epithelia(23).



Springer

Figure 4: Expression of CD24 found in murine and human cells.⁽²⁴⁾

In humans, CD24 is not expressed on erythrocytes or thymocytes but is highly expressed on progenitor B-cells and remains expressed on mature resting B-cells eventually waning from the plasma cells (22, 25). Being present on the activated B-cells it also acts as a co stimulatory molecule for T-cell clonal expansion. On T-cells, expression of CD24 varies with different maturation and activation states of T cells (25). Continued research has shown even broader expression of CD24 on cells and tissues including more hematopoietic cells (eosinophils, neutrophils dendritic cells and macrophages), human neuronal tissue, muscle cells, gastric parietal cells, pancreatic cells and many stem cells (26-28), **Figure 4**.

In addition to its expression in normal tissues, CD24 is shown to be up regulated in a growing list of inflammatory, autoimmune and neoplastic conditions. The list of tumours overexpressing CD24 is still growing and already includes both solid and haematological malignancies such as B-cell lymphomas, erythroleukemia, gliomas, small cell lung cancer, oesophageal squamous cell carcinoma, hepatocellular carcinoma, cholangiocarcinoma, pancreatic adenocarcinoma, urothelial carcinoma, ovarian cancer, breast cancer, gastric cancer, prostatic carcinoma and colorectal carcinoma (28-38).

[Role of CD24 in Immune system:](#)

CD24 is expressed on a variety of haemopoietic and immune cells. As a general rule, it is seen much more abundantly on the progenitor cells and in more metabolically active cells, with a gradual loss from the surface as the cells mature and differentiate. CD24 is considered as a B-cell marker and seen on very early B-cell progenitors and expression varies with stages of differentiation being highly expressed on the progenitor cells to totally absent on the plasma cells(7).

This indicates a role of CD24 in B-cell development and maturation. Several lines of evidence have pointed towards this role of CD24 and studies have also observed that CD24-deficiency resulted in a reduction in late pre-B and immature B-cell populations in the bone marrow. On activated B cells, CD24 functions as a T-cell co-stimulator for CD4⁺ T-cell clonal expansion. Research has also shown that cross linking of CD24 induces apoptosis in B-cell precursors including pre-B and pro-B ALL(Acute lymphocytic leukemia) cell lines (39).

Quite similar to B-cells, CD24 is highly expressed on immature T cells and expression gets weaker on peripheral T cells, but it is found to be upregulated in activated T cells. Li *et al.* found that a functional CD24 gene is essential for optimal homeostatic proliferation of T cells in a lymphopenic host (40). Interestingly, on the dendritic cells, CD24 is a negative regulator of T-cell homeostatic proliferation and thereby prevents fatal damage associated with the uncontrolled homeostatic proliferation of T-cells in lymphopenic hosts (7).

Very recently another important role has been attributed to CD24 i.e. discriminating between the PAMPs (Pathogen associated molecular patterns) and DAMPs (Damage/Danger associated molecular patterns) responses by the immune cells and it has been shown that the CD24-siglec axis provides the negative feedback mechanism for release of inflammatory cytokines after non-pathogenic cell injury(21). In addition, CD24 is shown by recent research to be the negative mediator of inflammation in sepsis and potentially important in the treatment of sepsis (21, 41).

Role of CD24 in neuronal tissue:

Besides immune cells, CD24 has been implicated to play a significant role in neuronal development. Keeping its general trend of expression being related to immature cells, studies on mouse brain have revealed that CD24 is transiently but extensively expressed in developing neurons and glial tissue. In an adult brain, its expression is lost from the developed neurons but still remains present on immature brain cells, and ciliated ependymal cells (42). Kadmon *et al.* explored the interaction between CD24 and L1 in neurons (16, 37). They provided evidence that in neuroblastoma N2A cells and cerebellar neurons, L1 and CD24 interact with one another and there is a significant increase in intracellular Ca^{++} concentration (16). Kleene *et al.* showed that binding of CD24 to L1 depends on its glycan chains and sialic acid residues on CD24 are essential for the binding to L1. They also showed that trans-interaction takes place between both molecules and being present in lipid rafts is also an important factor in determining the outcome of these interactions (18), **Figure 5.**

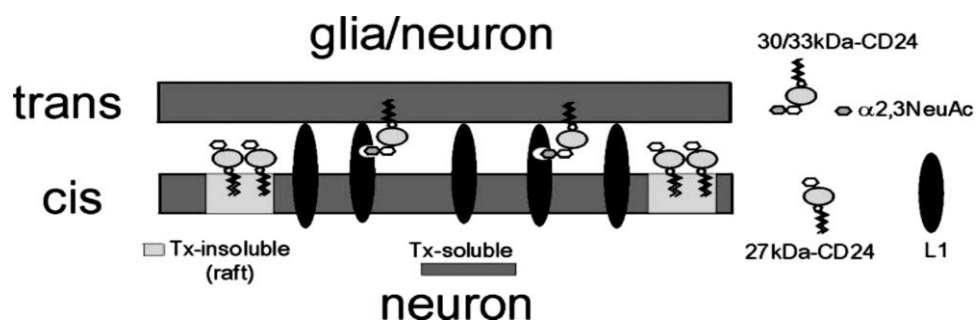


Figure 5: L1 and CD24 interactions in the brain^(18, 43).

The trans-interaction between the 30- and 33-kDa glycoforms of CD24 and L1 depends on $\alpha 2,3$ -linked sialic acid (NeuAc) residues and being located in lipid rafts region. This trans-interaction determines the CD24 induced and cell type-specific promotion or inhibition of neurite outgrowth. These CD24 glycoforms could be located either on neurons or glia(18).

Role of CD24 in Autoimmune diseases:

In general, autoimmune diseases are thought to be polygenic and multiple genes are being associated with each type of autoimmune disease, however, few have shown to employ direct significant impact and CD24 provides one such example. It has been linked to multiple autoimmune diseases including Systemic lupus erythematosus (SLE), Multiple sclerosis (MS), Autoimmune encephalitis, Rheumatoid arthritis, Crohn's disease and ulcerative colitis to name a few (44, 45).

Through a detailed pedigree analysis of families with SLE and MS, Wang *et al.* found that a destabilizing dinucleotide deletion in the 3' UTR of CD24 mRNA lead to significant protection against both MS and SLE (3). Similarly, Zhou *et al.* found a single nucleotide polymorphism of CD24 to be related with the risk and progression of MS. They found that CD24 v/v renders a >2-fold increase in the relative risk of MS even in the general population (P=0.023) with greater disability in familial cases (46). A meta-analysis published in 2015 proposed that CD24 C170T polymorphism might contribute to higher risk UC (ulcerative colitis), and the CD24 TG1527del polymorphism might be associated with the risk of Crohn's disease (47, 45).

Stem cells and cancer stem cells:

Many human tissues undergo rapid and continuous cell turnover. One of a good example is colonic mucosa where, for example, the average life span of a mature, differentiated cell (for exemple a goblet cell in a crypt of the large intestine) can be measured in days or even hours. Under physiological conditions, this process is sustained by a small minority of long-lived cells with extraordinary expansion potential, known as stem cells.

Stem cells have three main properties:

1. Differentiation:

The ability to give rise to a heterogeneous progeny of cells, which progressively diversify and specialize according to a hierarchical process, constantly replenishing the tissue of short-lived, mature elements;

2. Self-renewal:

The ability to form new stem cells with identical, intact potential for proliferation, expansion, and differentiation, thus maintaining the stem cell pool.

3. Homeostatic control:

The ability to modulate and balance differentiation and self-renewal according to environmental stimuli and genetic constraints (48).

In the past few decades, owing to dramatic improvements in techniques of molecular biology, the underlying mechanisms of cancers are gradually being uncovered. There is evidence that many cancers are composed of heterogeneous sub populations of tumour cells and these cells differ from each other not only in molecular markers but also in their abilities of growth and differentiation (49).

There are undifferentiated cells which, when xeno-transplanted into immunocompromised mice result in the formation of tumours which resemble the primary tumour from which they were isolated. These cells are called Cancer stem cells (CSC) due to the characteristics of self-renewal and ability to produce mature cells through differentiation just like normal stem cells(50, 51).

Cancer stem cells (CSC) are thus a small number of cells in a tumour with tumour initiation ability and can give rise to progeny that then differentiates into mature tumour cells, besides their own renewal. According to this concept, cancers

are not mere monoclonal expansions of transformed cells, but rather complex tri-dimensional tissues where cancer cells become functionally heterogeneous as a result of differentiation (48).

These cancer stem cells are getting immense attention due to their probable role in tumour formation , metastasis and resistance to currently available forms of chemotherapy(50). The evidence is increasing regarding each role of cancer stem cells (49) (52). It has been proposed now that the current chemotherapies only de-bulk the tumour and the stem cells are the ones that need eradication in order to prevent tumour relapse after treatment (50, 53), **Figure 6**.

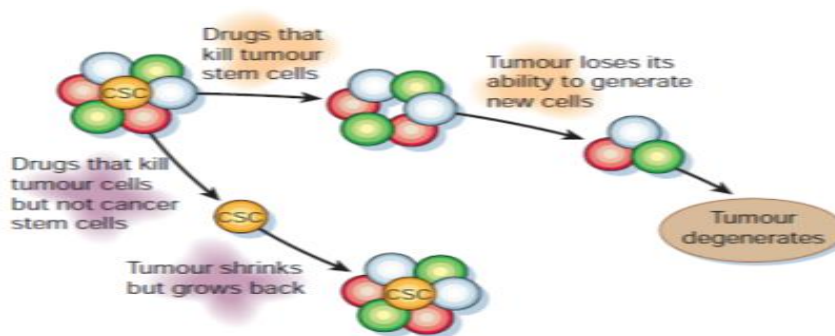


Figure 6: Cancer stem cells as a cause of tumour re-growth⁽⁵⁰⁾.

In order to develop specific and effective treatment of cancers there is need to further uncover the cancer stem cell properties including understanding of their signalling mechanisms, their interacting molecular partners and thereby developing specific targeted therapy. In the recent literature several molecular markers have been attributed to represent stem cells in solid tumours, and some of them differ in different tissues(53).

CD24 positive cells as cancer stem cells:

Ovarian Cancer:

Gao *et al.* in a recent study identified a sub-population enriched for ovarian CSCs defined by CD24 phenotype(37). Experiments

in vitro demonstrated that the CD24+ sub-population possessed stem cell-like characteristics of remaining quiescent and more chemo resistance compared with CD24– fraction, as well as a specific capacity for self-renewal and differentiation.

In addition, injection of 5×10^3 CD24+ cells was able to form tumour xenografts in nude mice, whereas an equal number of CD24– cells remained non-tumorigenic. They also found that CD24+ cells expressed higher mRNA levels of some 'stemness' genes, including Nestin, β -catenin, Bmi-1, Oct4, Oct3/4, Notch1 and Notch4 (37).

Colorectal Carcinoma:

To further add to the concept of cancer stem cells, a study by Vermeulen *et al.* used colon cancer undifferentiated stem cells and revealed that even a single CSC (cancer stem cell) can generate the tumour of origin on xenotransplantation. It was also proved that CD24 in addition to CDq133 was the marker of cancer stem cell(49).

Pancreatic Carcinoma:

Li *et al.* found that the pancreatic cancer cells with the CD44+CD24+ESA+ phenotype (constituting 0.2–0.8% of the pancreatic cancer cells) had a 100-fold increased tumorigenic potential compared with non-tumorigenic cancer cells. The CD44+CD24+ESA+ pancreatic cancer cells showed the stem cell properties of self-renewal, the ability to produce differentiated progeny, and increased expression of the developmental signalling molecule, sonic hedgehog(54).

CD24 negative cells as cancer stem cells :

Prostatic Cancer :

By using flow cytometry, Hurt *et al.* isolated a population of CD44+ve and CD24-ve prostate cells and found that they display stem cell characteristics as well as gene expression patterns that predict overall survival in prostate cancer patients (31).

Breast carcinoma:

Research showed that, in most human breast cancers, only a minority subpopulation of the tumour clone, defined as (CD44+, CD24-/low) and representing 11%–35% of the total cancer cells, is endowed with the capacity to sustain tumour growth, when xeno-grafted in NODSCID mice (48).

In short CD24 is definitely linked to “**stemness**”, but whether its presence or its absence marks the stem cells is apparently different in different carcinomas.

Roles of CD24 in tumours:

There are more than 20 different types of solid and haematological malignancies shown till now to be related with CD24 and the list continues to grow. This small molecule has been linked to vital cellular events including altered cell proliferation, adhesion, invasion in vitro and tumour growth in vivo (33, 55-58). CD24 on tumour cells binds to P-selectin on endothelial cells and platelets and this interaction has been proposed significant for breast cancer cell metastasis (14, 59). Similarly, upregulation of CD24 has been shown to promote tumour cell invasion by reducing TFI-2 (tissue factor pathway inhibitor-2 (55).

Downregulation of CD24 has been shown to inhibit invasive growth, increased apoptosis and results in a better response to

chemotherapy in a gastric cancer cell line (60). Expression of CD24 has been linked to poor prognosis, recurrence (61) and reduced patient survival in pancreatic cancers(34) liver cancer, gastric cancer and cervical cancer(36, 62).

In non-small cell lung cancer, the CD24 expression is an independent marker for the overall survival of cancer patients(7). However, our group has shown that CD24 is not a prognostic factor in colorectal carcinoma(29).

CD24 as therapeutic option:

As described above evidence underpins the significance of CD24 in several human diseases including a long and growing list of tumours. Multiples studies have provided evidence on the prognostic and diagnostic role of CD24. There has been some progress in the design of novel treatment options targeting CD24 and some have found promising results(63).

In tumours :

Burkett's lymphoma is a B-cell neoplasm with a high expression of CD24. A study by Suzuki *et al.* showed that anti-CD24 monoclonal antibodies not only inhibit aggregation but also reduce the growth of these CD24 expressing Burkett's lymphoma cells. These antibodies lead to cross linkage of CD24 molecules and induction of apoptosis in a lipid raft dependant manner (39).

Up to 90% of colorectal carcinomas show increased expression of CD24, found as early as, at the adenoma stage and linked to prognosis in some studies (8). Similarly, many other gastrointestinal malignancies show over expression of CD24 such as pancreatic, gastric, oesophageal cancers etc. (60, 64). In 2008 Sagiv *et al.* targeted colorectal and pancreatic cancer cells using two anti CD24 techniques i-e monoclonal anti-CD24

antibody and siRNA. They found growth inhibition and less severe malignant phenotype as a result of targeting CD24 using the above mentioned techniques (63).

In 2011, a new and very interesting model to kill tumour cells with high CD24 expression was presented by Shapira *et al.* They conjugated a highly potent exotoxin (PE-38) with the CD24 antibody (SWA11) with the help of ZZ domain (modified Fc binding protein from *Staph. aureus*). They showed the effective and selective killing of human colorectal cancer cells in mice by this immuno-conjugate. This coupled strategy to kill the tumour cells was more potent than using the unarmed mAb alone(65).

Although these studies are quite promising, however, there are still few hurdles in translating these strategies into clinical trials. For example, the issue of immunogenicity posed by the murine components limits multiple cycle use of these treatments. Similarly, eventhough it is known that most adult cells do not express CD24 once differentiated, yet there are some normal cells including immune cells that do express CD24 (7). Hence, targeting may also adversely affect these cells. Currently, strategies to overcome these hurdles are under investigations.

In sepsis:

Besides a role in the development of tumours, another very significant and relatively newly identified role of CD24 is enabling dendritic cells to differentiate between Damage associated molecular patterns (DAMPs) and Pathogen associated molecular patterns (PAMPs). Chen and Yang Liu *et al.* (2009) have shown that CD24 and Siglec10 provides a negative feedback loop resulting in prevention of cytokine release when stimulation of TLR (Toll like receptors) takes place by DAMPs and not by PAMPs (21, 41).

The Paulson *et al.* (66) proposed that the sugars present on the CD24 molecule may be vital in mediating the above mentioned role and proposed the possibility of destruction of these sialic acid residues present extensively on CD24 by bacterial sialidases in the setting of sepsis. They showed that that sepsis was ameliorated when these sialidases were inhibited and this also required intact CD24-siglec axis as loss of CD24 or Siglecs both abrogated the effects of sialidases inhibitors in the treatment of sepsis (41, 66), **Figure 7**.

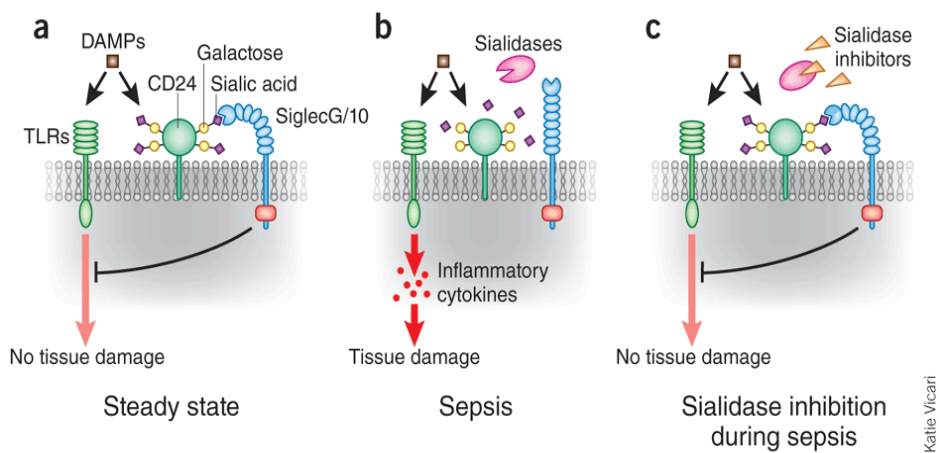


Figure 7: Sialidase inhibitors DAMP en sepsis.⁽⁶⁶⁾

(a) Normally, DAMPs attenuate pro-inflammatory TLR signaling by forming a ternary complex with sialylated CD24 and SiglecG/10. (b) During sepsis, bacterial sialidases cleave sialic acids on CD24, disrupting the CD24/SiglecG/10 inhibitory circuit and leading to enhanced cytokine production. (c) Sialidase inhibitors block the desialylation of CD24 that occurs during sepsis, preserving the Siglec inhibitory circuit and suppressing the inflammatory response.

Such studies are promising new strategies to combat sepsis and organ damage caused by drug toxicity by preserving the integrity of the CD24-Siglec axis (66, 67).

Current controversies about role of CD24:

Certain controversial aspects are found regarding the biology of CD24 in the current literature. These include features of stemness, prognostic role and effects on cellular proliferation and certain signalling outcomes. Some possible explanations to these can be tissue specific and site specific glycosylation of CD24 and hence diverse signalling outcomes.

Similarly, the location of CD24 can also be a potential reason and surface versus cytoplasmic or nuclear CD24 may have very different signalling outcomes. Yet another potential reason for discrepancies about CD24 was brought up by Kristiansen *et al.* and that is the difference of antibodies used to detect CD24 protein itself (68).

Their study compared the epitopes identified by three different CD24 antibodies i-e SN3b CD24, SWA-11, and ML-5. Both SWA-11 and ML-5 bind to the core protein of CD24 whereas mAb SN3b does not identify the CD24 protein core itself; rather it binds to a glycan structure that decorates the CD24 molecule. However, this glycan is not present on all forms of CD24 and, possibly, more importantly, can be present on other yet unidentified molecules (68).

This study was carried out using monoclonal antibody SWA11 for the detection of CD24 and it was a kind gift from Prof Peter Altevogt.

Study Aims

Study Aims:

Study Aims:

Increasing literature points towards the significance of CD24 in human pathologies ranging from autoimmune diseases to malignancies. There are more than thirty different types of tumours associated with CD24 and the list is still growing. CD24 has been linked to tumour pathogenesis, prognosis, and metastasis besides some promising therapeutic potential.

However, much less is known about its signalling partners, and exact mechanisms leading to these diverse roles.

The overall aim of this piece of work was to explore CD24 biology a bit further.

Specifically, in this study, we focussed on three aspects:

- CD24 has been shown to regulate the differential response of immune cells when exposed to Damage Associated Molecular Patterns (DAMPs) versus Pathogen Associated Molecular Patterns (PAMPs). As the tumours also show both the high CD24 expression levels and release of DAMPs by the necrotic cells. We intended to explore the possibility of similar modulatory role of CD24 in tumour cells when exposed to DAMPs. This was done using directional and non-directional cell motility and cell proliferation assays, after exposure to autologous DAMPs in colorectal cell lines with positive and negative expression of CD24.
- We also aimed at exploring signaling relationship between CD24 and some tumour related molecules including Cten, ILK and FAK by performing co-transfections. We also sought to figure out functional relevance between these molecules by carrying out functional assays.
- Glycosylation has been implicated as an important potential factor for CD24 associated cellular events. To

Study Aims

explore the significance of these glycosylation sites we attempted to mutate potential N-glycosylation sites in CD24 molecule using site-directed mutagenesis.

Chapter Two: Materials and Methods.

Cell Lines:

Our lab had twenty six well established colorectal cancer cell lines. These were obtained from Molecular and Population Genetics Laboratory, London Research Institute, Cancer Research, London, UK. These cell lines were originally from ATCC[®]™ (American Type Culture Collection), the premier global biological materials resource and standards organization.

The cell lines used in this study included SW620, HCT116, DLD1, RKO and SW480. As per regular protocol, all of these cell lines underwent regular checks for mycoplasma infection, as well as DNA fingerprinting in order to confirm the correct identity of the cell line against the most original stock of each particular cell line.

Moreover, the expression levels of CD24 in the above mentioned cell lines were analysed in the lab using real time PCR and the protein expression was verified by performing western blot for CD24 as well as by flow cytometry (**See Appendix iii**).

A brief description of cell lines used in the current study along with salient molecular features is described below:

SW620 (ATCC[®] CCL-227™):

- Organism: Homo sapiens, human
 - Tissue: colon
 - Source: lymph node
 - Disease: Dukes' type C, colorectal adenocarcinoma.
 - Morphology: epithelial
 - Growth Properties: adherent.
- Genes expressed:
carcinoembryonic antigen (CEA) 0.15 ng/10 exp6 cells/10 days; transforming growth factor alpha; keratin; matrilysin, myc +; myb +; ras +; fos +; sis +; p53 +; abl -; ros -; src -, blood type A; Rh+, The cells are negative for expression of CSAp (CSAp-) and colon

antigen 3, negative., The cells are positive for keratin by immunoperoxidase staining., The line is positive for expression of c-myc, K-ras, H-ras, N-ras, Myb, sis and fos oncogenes.

SW480 (ATCC® CCL228™):

- Organism: Homo sapiens, human
 - Tissue: colon
 - Disease: Dukes' type B, colorectal adenocarcinoma
 - Morphology: epithelial
 - Growth Properties: adherent
- Genes expressed:
 carcinoembryonic antigen (CEA) 0.7 ng/10 exp6 cells/10 days; keratin; transforming growth factor beta, myc +; myb + ; ras +; fos +; sis +; p53 +; abl -; ros -; src -, HLA A2, B8, B17; blood type A; Rh+, The cells are positive for keratin by immunoperoxidase staining., The line is positive for expression of c-myc, K-ras, H-ras, N-ras, myb, sis and fos oncogenes.

DLD1 (ATCC® CCL-221™):

- Organism: Homo sapiens, human
 - Tissue: colon
 - Disease: Dukes' type C, colorectal adenocarcinoma
 - Cell Type: epithelial
 - Morphology: epithelial
 - Growth Properties: adherent
- Genes expressed:
 carcinoembryonic antigen (CEA) 0.5 ng/10 exp6 cells/10 days; colon antigen 3; keratin, myc +; myb + ; ras +; fos +; sis +; p53 +; abl -; ros -; src -, blood type O, DLD-1 cells are positive for p53 antigen expression (the p53 antigen produced has a C -> T mutation resulting in Ser -> Phe at position 241)., The cells are positive for keratin by immunoperoxidase staining., The line is positive for expression of c-myc, K-ras, H-ras, N-ras, myb, sis and fos oncogenes.

HCT116 (ATCC® CCL-247™):

- Organism: Homo sapiens, human
- Tissue: colon
- Disease: colorectal carcinoma
- Morphology: epithelial
- Growth Properties: adherent

Genes expressed:

The cells are positive for keratin by immunoperoxidase staining. HCT 116 cells are positive for transforming growth factor beta 1 (TGF beta 1) and beta 2 (TGF beta 2) expression. Carcinoembryonic antigen (CEA) 1 ng per 10⁶ cells per 10 days.

RKO (ATCC® CRL-2577™):

- Organism: Homo sapiens, human
- Tissue: colon
- Disease: Carcinoma
- Morphology: epithelial

Growth Properties: adherent

Genes expressed:

RKO cells contain wild-type p53 but lack endogenous human thyroid receptor nuclear receptor (h-TRbeta1).

Table 1: Status of significant oncogenes in the cell lines used ⁽⁶⁹⁾.

GENES	SW620	SW480	DLD1	HCT116	RKO
KRAS	mutant	mutant	mutant	mutant	wild type
BRAF	wild type	wild type	wild type	wild type	mutant
PI3K	wild type	wild type	mutant	mutant	mutant
P53	mutant	mutant	mutant	wild type	wild type
NRAS	wild type				
CD24	positive	positive	positive	negative	negative
CTEN	positive	positive	positive	negative	negative

Cell cultures:

The cells were cultured in Dulbecco's Modified Eagle's Medium (DMEM) (GIBCO®, Invitrogen, UK) containing 10% FBS (Invitrogen, UK), 100 units/ml penicillin, and 100µg/ml streptomycin (Invitrogen, UK). Cultures were maintained in a 37°C incubator in a humidified atmosphere of 95% O₂ and 5%

CO₂. Cells were cultured ordinarily in T75 (75 cm²) culture treated flasks (Costar, UK) and were mostly adherent to the culture flask surface. For cell passaging, cells were allowed to grow to 90% confluence and then trypsinised in order to detach them from the surface of the tissue culture flask. The medium was removed from cells and the cells were washed twice with 5ml of PBS (Sigma, USA). Following this, 1ml of trypsin-EDTA was added to the cells, the flask was placed in the incubator at 37°C for 5min, after which, the cells could be seen to detach from the bottom of the flask. The cells were then re-suspended in 9mL of fresh medium, the FBS in the medium is important for inactivating the trypsin. The medium containing the cells was then plated into new flasks and the level of dilution of cell suspension to fresh plating medium was mostly kept at 1:10 dilution.

Transient forced expression of CD24 by transfection:

Transfection:

It is a robust technique that allows introduction of genetic material (DNA and double stranded RNA) of choice into the mammalian cells. It is a powerful technique used by the scientists to study the effects of genes of interest. This inserted DNA/ds RNA leads to expression, or production of proteins or altering the endogenous gene expression using the cellular machinery of the transfected mammalian cells. Transfection helps in studying functions of these genes and gene products. Currently a wide range of methodologies are commercially available for transfection using physical, chemical and biological approaches.

For successful transfection a nucleic acid, which carries a net negative charge under normal physiological conditions, must cross the cell membrane that also carries a net negative charge. A very popular approach in this regard is the use of Lipofectamine (chemical- transfection).

Lipofectamine 2000 is a cationic liposome based reagent and it delivers great transfection efficiency leading to high levels of transgene expression in a range of mammalian cell types besides having a simple protocol. Lipofectamine 2000 complexes with nucleic acid molecules, allowing them to overcome the electrostatic repulsion of the cell membrane and to be taken up by the cell (70, 71).

Stable versus transient transfection:

The method of transfection into a cell can be transient or stable and both techniques offer varying benefits to scientists. In transient transfection, the transfected material enters the cell but does not get integrated into the cellular genome. In this method the gene expression changes can be studied in a window of 8 to 96 hours post-transfection. This method is useful for short-term expression of genes or gene products, gene knockdown or small-scale protein production.

On the other hand, in stable transfection, plasmid DNA successfully incorporates into the cellular genome and gets passed on to the future generations of the transfected cells. This method is less commonly used because of its complexity and time consumption. In this technique the plasmid DNA is designed to contain a gene that expresses antibiotic resistance in addition to the gene of interest. Continued antibiotic treatment of the transfected cells for a long-term results in the expansion of only the stably-transfected cells, while non-transfected/transiently transfected cells die off due

to the lack of antibiotic resistance. Stable transfection is mainly used for protein production on a large scale, research on long-term genetic regulations, extended pharmacology research or gene therapy. However, once successful it is quite useful and avoids huge variability of expression levels as seen with each repetition of transient transfections (70).

Time course stability of CD24:

Regarding transient transfections, depending on the relative stability of the mRNA / protein expressed and the sensitivity of the assay system employed the expression profile can vary considerably. Hence it is important to optimise the transfection conditions as well as to know the time course stability of the protein under study. This is significant in order to correctly plan and interpret relevant experimental models. The expression plasmid CD24 - pcDNA3.1 was successfully constructed in our lab (**see Appendix ix**) and fully optimised to be used for transient forced expression of CD24 in cell lines having low or negative expression of CD24. In our lab settings peak CD24 expression levels were seen after 24 hours with significant protein levels maintained even after 72 hours post transfection (unpublished data). In current study we used the above time window (24-72 hours post transfection) for our experiments.

Methodology of transient transfection:

The expression construct (CD24 - pcDNA3.1) was used to express CD24 in the low CD24 expressor cell line HCT116. Transfection was performed according to the Lipofectamine®2000 (Invitrogen) instructions manual. Briefly, one day before transfection 5×10^5 cells were plated in 2 ml of growth medium (DMEM) with 10 % FBS in 6-well plates

(volumes are adjusted according to plate size used). On the second day, cells were transfected when confluence reached between 60 and 90 %. Cells were serum starved (by keeping in DMEM only without FBS for two hours) before transfection. A total of 4.0 µg/well of plasmid DNA or the control empty vector (pcDNA3.1) was diluted in 250 µl Opti-MEM® I -Serum-reduced medium (Invitrogen) and mixed gently. Lipofectamine® 2000 (Invitrogen) was gently mixed before use, and then 10 µl was diluted in 250 µl of Opti-MEM® I Medium and incubated for 5 minutes at room temperature. Subsequently, the diluted plasmid DNA was combined with the diluted Lipofectamine®2000, mixed gently and incubated for 20 minutes at room temperature. The complexes were lastly added to the cells containing 1.5 ml of fresh Opti-MEM® I -Serum - reduced medium and plates were rocked back and forth carefully and incubated at 37°C in 5% CO₂ incubator. Transfections were performed in triplicate. After 4-7 hours of transfection, the media was changed with fresh DMEM with 20% FBS and 1% P/S. After 24 hours the cells were either (1) harvested for protein extraction and western blot (2) used directly for the relevant functional assays.

Total RNA extraction:

The RNeasy Mini Kit (Qiagen, Crawley, UK.) was used to extract total RNA from cultured cells. Cells were trypsinised as described for passaging, and then cells were pelleted. Pellets were re-suspended in 5mL of the medium, and counted using an automated cell counter (Bio-Rad, TC20™ Automated Cell Counter Model #1450102). The cells were aliquoted to get a maximum of 1×10^7 cells per aliquot, washed twice with PBS, re-suspended in 1ml PBS, transferred to a 1.5ml tube and spun for 5 min at 300xg. The supernatant was discarded and the

pellet was lysed with either 350µl or 600µl of RLT lysis buffer according to the starting number of cells (< 5 X 10⁶ cells were lysed in 350 µl, from 5 X 10⁶ to 1 X 10⁷ were cells lysed in 600 µl). The cell suspension in the lysis buffer was further homogenised using QIAshredder™ spin columns (Qiagen, Crawley, UK) placed in a 2 ml collection tube, and centrifuged for 2 min at full speed. The lysate was then mixed with 70% ethanol and placed into a spin column with a silica membrane and centrifuged at 8000xg. for 15 sec. On-column DNase digestion was required for the elimination of genomic DNA contamination, to prepare the spin column, 350 µl Buffer RW1 was added to the RNeasy spin column and centrifuge for 15 seconds at 8000xg.

To perform DNA digestion 10 µl DNase I stock solution was added to 70 µl Buffer RDD, then the DNase I incubation mix (80 µl) was added directly to the RNeasy spin column membrane, and placed on the bench top (20–30°C) for 15 min. The membrane containing the RNA was washed once with 700 µl of RWI buffer, then twice with 500µl of RPE buffer (containing ethanol). After the last wash, the column was spun dry at 8000xg. to remove the remaining traces of ethanol from the membrane. The RNA was then eluted in 30 µl of RNase free-water.

RNA/DNA quantification and quality check:

To check the quantity and quality of the RNA, the spectrophotometer (NanoDrop™ 1000 Spectrophotometer, Thermo Scientific) was blanked with RNase free water. The absorbance at 260nm and 280nm was measured. The measure of A₂₆₀ gave the quantity of total RNA in µg. The ratio A₂₆₀/A₂₈₀ gave an estimation of the purity of the RNA (RNeasy mini Handbook, Qiagen, Crawley, UK). A ratio of ~1.8

is commonly accepted as “pure” for DNA, and the ratio of ~ 2.0 is generally accepted as “pure” for RNA. If the ratio is noticeably lower, in any case, it may point to the presence of protein, ethanol or other contaminants that absorb strongly at or near 280 nm.

Synthesis of complementary DNA from RNA:

In a 50 μ l reaction 400ng of random hexamers (Thermo Scientific AB gene Cat#12657375) were used (1 μ l per reaction). 5 μ g of RNA was diluted in dH₂O (RNase, DNase free water) for each sample to make a final volume of 21 μ l. Samples were incubated at 70°C for 10 minutes (This denatures the RNA prior to allowing the random hexamers to anneal to the template strand). Samples were placed on ice for 5 minutes then pulse centrifuged to collect samples. While samples are on the ice, a Master Mix was made as described in **Table 2**. Master Mix was then mixed by gentle pipetting and pulse centrifuge to collect contents. 29 μ l of Master Mix were added to each RNA sample (making a total volume of 50 μ l). These samples were incubated at 37°C for 1hr (This allows the Reverse Transcriptase enzyme (M-MLV Invitrogen cat#2802513) to synthesize the complementary DNA sequence to the template RNA strand from the added nucleotides). Finally, samples were incubated at 95°C for 10 minutes (This step will denature the enzyme, preventing it interacting in subsequent reactions). In order to exclude genomic DNA contamination, RT negative samples were made going through the same steps of reverse transcription except for adding the reverse transcriptase **Table 3**.

Without this enzymes, no cDNA is made, so when those samples are used for Q-PCR, if there is any amplification observed, it indicates the presence of genomic contamination in the RNA samples extracted.

Table 2: Master Mix made for the reverse transcription reaction.

Master Mix.		
	1 reaction (μl).	4 reactions (μl).
5x First-Strand Buffer	10	40
dNTP (10mM)	1.5	6
DTT(0.1M)	5	20
M-MLV-RT (200U/μl) enzyme (Invitrogen)	2	8
dH ₂ O	10.5	42

Table 3: Master mix made for the RT- negative reactions.

Master Mix.		
	1 reaction (μl).	4 reactions (μl).
5x First-Strand Buffer	10	40
dNTP (10mM)	1.5	6
DTT(0.1M)	5	20
dH ₂ O	12.5	50

Q-PCR:

In order to look for comparative mRNA levels of Cten after CD24 forced expression, the following primers were used (MWG-Biotech AG).

Table 4: Primers used for qPCR.

Gene of interest.	Primer Sequence.	Product size.	Annealing temperature.
HPRT. (NM_000194)	Forward Primer 5'AAATTCTTTGCTGACCTGCTG 3'	122	60°C
	Reverse Primer 5' TCCCCTGTTGACTGGTCATT 3'		
CD24. (NM_01323 0.2)	Forward Primer 5' ACCCACGCAGATTTATTCCA 3'	110	59°C
	Reverse Primer 5' CCTTGGTGGTGGCATTAGTT 3'		
Cten. (NM_032865)	Forward Primer 5' GCGTCTGCTCAGA ATCGAC 3'	110	56°C
	Reverse primer 5' GATGAGGAAGTGTCGGATGG 3'		

Set up of PCR reaction:

All experiments were carried out in triplicate and the values of amplification were normalized to the house keeping gene Homo sapiens Hypoxanthine phosphoribosyl transferase 1 (HPRT1) **Table 4.** The Brilliant SYBR® Green QPCR Master was purchased from Stratagene, UK. The final volume of each reaction was 10µl containing 5µl of 1X SYBR Green Master Mix (Stratagene, UK), 0.4 µl of each primer (final concentration: 250 nM), and 1µl of cDNA templates (2 ng/1 µl) **Table 5.** Cycling conditions for the reactions were 1 cycle of denaturation for 10 minutes at 95 °C followed by 40 cycles of denaturation (30 Seconds at 95°C), annealing (60 Seconds at a temperature specific for the primer in use) and extension (30 Seconds at 72°C) in the thermal cycler (Mx3005PTM, Stratagene). Finally, the reactions were left for 1 cycle for 120 seconds for the generation of a dissociation curve (divided as 1 minute denaturation at 95 °C, 30 seconds at 55 °C, and 30 seconds at 95°C). The data for Q-PCR were analysed by the MxPro-QPCR software version 3.20 using the standard curve method. For each QRT-PCR experiment, a standard curve had to be generated for each target gene. Standard curves were generated using 10 fold serial dilutions of neat cDNA. The controls for QPCR experiments were “No template control (NTC)” reactions containing all the reagents excluding the DNA template, and RT- negative control to

analyse the possibility of genomic DNA contamination during the step of cDNA synthesis.

Table 5: Master mix for qPCR .

Components.	X1 Reaction (10µl).	X 20 Reactions.
Master mix.	5 µl	100 µl
Forward primer.	0.4 µl	8µl
Reverse primer.	0.4 µl	8µl
Water (PCR clean).	3.2 µl	64µl
Template.	Added separately	1µl each

Western blot:

Protein extraction:

After aspiration of the media, the cells were washed with the appropriate volume of ice-cold 1X PBS according to the size of the flask or the plate in use. Cells were trypsinized and were transferred to a 1.5 ml eppendorf tube with media containing FBS. The tubes were centrifuged at maximum speed (200 x g) at 4 °C for 5 minutes and then washed twice with ice-cold 1X PBS. The cell pellets were afterwards treated with ice-cold RIPA buffer (RadioImmuno Precipitation Assay) (Thermoscientific, UK, Cat. NO. 89901) (25mMTris-HCl pH 7.6, 150 mM NaCl, 1% NP-40, 1% sodium deoxycholate, 0.1% SDS) with Halt Protease and Phosphatase Inhibitor

Cocktail, EDTA-free (100X) added as 1:100 concentration (Pierce, UK, Cat. NO. 78445). Tubes were incubated for 5 minutes on ice. The eppendorf tubes were centrifuged at maximum speed (17,000 x g) at 4°C in BIOFUGE fresco machine for 20 minutes. The supernatant was collected, aliquoted into 0.5ml tubes and store at -20°C.

Protein quantification:

For the purpose of equal loading in western blotting experiments, the concentration of total proteins in each of the cell lysates was quantified. The BCA Protein Assay Kit (Thermo Fisher Scientific Inc, Rockford, USA, Catalogue No.23225) was used according to the manufacturer's instructions using the microplate procedure (**see Appendix iv, Appendix v**). The Spectrophotometer was used to measure the absorbance at 550 nm. The standard curve was made to calculate the amount of proteins in each sample by comparing the absorbance of each sample with those of the standard curve (**see Appendix vi**).

SDS gel electrophoresis:

Using the Bio-Rad gel system, SDS PAGE (4 % and 12 % were prepared whenever needed according to the target protein size) running gel was prepared (**see Appendix vii**), using the Biorad gel system. The glass plates (0.75mm) were set up in a casting frame to produce a good seal after they

were properly cleaned with mild detergent and air-dried with 70% alcohol. A 10% SDS PAGE running gel was prepared and gently delivered into the plates up to a level that was 1cm below the wells so as to allow for a layer of stacking gel below the wells. After ensuring the resolving gel was set the prepared stacking gel was applied onto the resolving gel (**see Appendix vii**) and a 0.75 mm comb introduced carefully into the stacking gel. After polymerisation, the gel was transferred to the Biorad electrophoresis unit followed by the addition of 1x Tris-glycine buffer (0.25M Tris, 1.92M Glycine, 1% SDS by GENEFLOW) electrophoresis buffer to cover the base and the top of the gel. The comb was then carefully removed. 50 µg of each protein sample were added to a 4X SDS loading buffer containing 5% β-mercaptoethanol. The samples were boiled at 95°C for 5 minutes in a hotplate, subsequently, samples were transferred to ice for another 5 minutes after denaturation. After centrifuging for 1 minute at 17,000 x g, the samples were loaded into the wells and underwent electrophoresis for 60 minutes at 60 mA. A labelled size marker (rainbow marker) was used to measure the target protein size (Bio-Rad, UK). In the later part of the study, ready to use, pre-made SDS gels were also used for western blots (BIO-RAD Catalogue # 1611159, 4–20% Ready Gel® Tris-HCl Gel, 10 well, 50 µl).

Transfer to PVDF membranes:

The resolving gel was equilibrated in a transfer buffer (0.25M Tris, 1.92M Glycine and 20% methanol) for 5 minutes. A Hybond-P PVDF (Polyvinylidene fluoride) membrane (Amersham Bioscience, Buckinghamshire, UK) was used for protein transfer and all equilibrations were done according to the manufacturer's instructions. Following the formation of a transfer sandwich, the transfer of proteins was carried out using the semi-dry transfer unit (Bio-Rad, UK) at 0.8mA/cm² of membrane (64 mA for 2 gels).

Immuno-detection:

After transfer, the membranes were blocked with 5% non-fat dry milk/BSA in PBS/TBS containing 0.1% Tween20 for 1 hour at room temperature and then incubated overnight at 4°C on a roller with the relevant antibody diluted to the optimal concentration in the same solution used for blocking the membranes. For the features and clones of antibodies used in this study see **Table 6**.

For the purpose of checking the equality of loading, the monoclonal anti β -actin antibody (Sigma Aldrich, UK) was used at a dilution of 1:2000 against the ubiquitous β -actin protein. The blots were washed three times in PBS with 0.1% Tween20 (each washing for 5 mins) and then incubated for 1 hour at room temperature with a horseradish peroxidase-

linked secondary antibody. The secondary antibodies were from SIGMA; anti-mouse (A4416-SIGMA Aldrich, UK) or anti-rabbit (A6154-SIGMA Aldrich, UK); the secondary antibodies were diluted in the same solution used for blocking. The blots were washed once again after secondary antibody incubation three times (for 5 mins each) in PBS with 0.1% Tween20 and the last wash was with PBS only. The immuno-reactive proteins were visualized with Enhanced Chemiluminescence detection kit (Super-signal West Pico Chemiluminescent Substrate, Thermochemical, UK) and the ECL was kept on the blot for one to two minutes in dark and bands were visualised by exposure to X-ray film (Kodak UK).

Table 6 : Summary of antibodies used in the study.

Antibody.	Origin.	Band size.	Dilution Buffer.	Blocking. (1 hour room temp / overnight at 4°C).	Dilution.	Washing. Except the last wash after secondary ab incubation (TBS alone).	Species.	Secondary Ab type and dilution. (Both secondary antibodies raised in Goat). SIGMA ALDRICH 1:10000 (1 μ l:10ml).
E-cadherin.	Cell signalling. 24F10 # 31955	135 KD.	5% BSA in TBS with tween.	5% BSA in TBS with tween.	1:1000 10 μ L:10mL	TBS with tween.	Rabbit.	Anti rabbit IgG coupled with HRP, 5% ,BSA in TBS with tween 1 hour Room temperature (RT).
N-cadherin.	Abcam. Ab98952	100KD.	5% BSA in TBS with tween.	5% BSA in TBS with tween.	1:100 30 μ L:3mL	TBS with tween.	Mouse.	Anti mouse IgG coupled with HRP, 5% BSA in TBS with tween1 hour RT.
Snail(L70g2).	Cell signalling. 3895S	29KD.	5% BSA in TBS with tween.	5% BSA in TBS with tween.	1:1000 10 μ L:10mL	TBS with tween.	Mouse.	Anti mouse IgG coupled with HRP, 5% BSA in TBS with tween1 hour RT.
HSP90.	Abcam. [E296] (ab32568)	90KD.	5% BSA in TBS with tween.	5% BSA in TBS with tween.	1:100 30 μ L:3mL	PBS with tween.	Rabbit.	Anti rabbit IgG coupled with HRP, 5% BSA in TBS with tween1 hour RT.

Table 6 continued...

Antibody.	Origin.	Band size.	Dilution Buffer.	Blocking. (1 hour room temp / overnight at 4°C).	Dilution.	Washing. Except the last wash after secondary ab incubation (TBS alone).	Species.	Secondary Ab type and dilution. (Both secondary antibodies raised in Goat). SIGMA ALDRICH 1:10000 (1ul:10ml).
FAK.	Cell signalling. 3285	125KDa.	5% BSA in PBS with tween.	5% BSA in PBS with tween.	1:500 10µL:5 mL	PBS with tween.	Rabbit.	Anti Rabbit IgG coupled with HRP, 5%, BSA in PBS with tween1 hour RT.
ILK.	Cell signalling. 3862	50KDa.	5% BSA in PBS with tween.	5% BSA in PBS with tween.	1:500 10µL:5 mL	PBS with tween.	Rabbit.	Anti Rabbit IgG coupled with HRP, 5% BSA in PBS with tween1 hour RT.
Cten.	Sigma TNS4. CLONE 3B8 WHOO84951 M1-100ug	78KDa.	5% milk in PBS with tween.	5% milk in PBS with tween.	1:1000 10µL:10mL	PBS with tween.	Mouse.	Anti Mouse IgG coupled with HRP, 5% milk in PBS with tween 1 hour RT.

Table 6 continued.....

Antibody.	Origin.	Band size.	Dilution Buffer.	Blocking. (1 hour room temp / overnight at 4°C).	Dilution.	Washing. Except the last wash after secondary ab incubation (TBS alone).	Species.	Secondary Ab type and dilution. (Both secondary antibodies raised in Goat). SIGMA ALDRICH 1:10000 (1ul:10ml).
H3.	Cell signalling. 9715S	18KDa.	5% milk PBS with tween.	5% milk PBS with tween.	1:500 10µL:5 mL	PBS with tween.	Rabbit.	Anti Rabbit IgG coupled with HRP, 5% milk in PBS with tween 1 hour RT.
HMGB1.	Cell signalling. 3935	29KDa.	5% BSA in PBS with tween.	5% BSA in PBS with tween.	1:1000 10µL:10mL	PBS with tween.	Rabbit.	Anti Rabbit IgG coupled with HRP, 5% BSA in PBS with tween 1 hour RT.
β- actin.	SIGMA CLONE. Ac-15 A1978- 200ul 011M4812	43KDa.	5% milk in PBS with tween.	5% milk in PBS with tween.	1:2000 5µL:10mL	PBS with tween.	Mouse.	Anti Mouse IgG coupled with HRP, 5% milk in PBS with tween 1 hour RT.
SWA11 / CD24.	Gift from Peter Altevogt.	20-70 KDa.	3% milk PBS with tween.	3% milk PBS with tween	1:1 3mL:3mL	PBS with tween.	Mouse.	Anti Mouse IgG coupled with HRP, 5% milk in PBS with tween 1 hour RT.

Cell migration assays:

Trans-well migration assay:

The cellular migratory capacities were tested using the trans-well migration assay and the cellular wound healing assay. The trans-well migration assay uses a Boyden chamber, 24 Trans-well inserts (Costar, Corning, NY, USA) with 6.5 mm diameter and polycarbonate membrane of 8- μ m pore size. 600 μ l of DMEM supplemented with 20% FCS was added to the lower chamber. In the upper chamber, 5×10^4 to 2×10^5 cells (depending on the cell line type) were suspended in 100 μ l of DMEM with 10% FCS. Migration was assessed after 24 to 48 hours and single cells which had migrated through the membrane to the lower chamber were counted visually by an inverted microscope. Assays were performed in triplicate and on at least three different occasions. In order to reduce error, cells were counted by two observers at multiple occasions and found comparable counts by both.

Wound healing Assay:

Cell migration was also measured using a cell wounding assay performed in 6-well plates. Cells were grown to 90 % confluency and then serum-deprived for 24 hours in serum-free medium. A sterile 200 μ l pipette tip was used to create three separate parallel scratches and migration of the cells across the wound line was assessed after 24 hours. Photographs were taken just after wounding(T=0) and after

24 hrs, using a charge-coupled device (CCD) camera (Canon, Japan) attached to the inverted phase-contrast microscope (Zeiss, Germany) at a magnification of 40x. The position of each photograph was noted by the help of markings made at the under surface of the culture plates. Migration of cells across the wound line was assessed 24 hours after by using T Scratch software, this is freely available software and can be downloaded from.

<http://www.cse-lab.ethz.ch/software.html>

It reads the empty area in a picture and gives it as a percentage. The software enables a reliable and reproducible quantification of open areas (72). Assays were done in triplicate and repeated at least on three different settings.

Methylene blue proliferation assay:

For the purpose of comparing cell numbers between different experimental conditions, a time course proliferation assay was performed in 6-well plates and repeated in 24-well plates (Corning Incorporation, Coaster, UK). The number of cells seeded depended on the size of the plate in use thus, 1×10^4 cells were seeded in 24-well plates and 5×10^4 cells were seeded in 6-well plates. After relevant cell treatments, cell numbers were measured as follows: medium was aspirated and cells were washed with PBS once and fixed at room temperature for 30

minutes with absolute methanol (1ml per well for 6-well plates and 200 μ l per well for 24-well plates). Subsequently, cells were allowed to air dry for 5 minutes after tapping out of methanol. This was followed by staining with 1% methylene blue (1g methylene blue hydrate (Sigma, UK), and 100 ml distilled water) for 30 minutes at 37°C. Next, the methylene blue was aspirated and wells were thoroughly washed three times with distilled water. Finally, the stain was eluted from the cells using 0.1% HCL in ethanol (1 ml in each well in a 6-well plates and 200 μ l per well for 24-well plates), and then 100 μ l of the eluent of each well was transferred into 96 well plate, and absorbance was measured at a wave length of 570nm using a plate reader (Lab systems, UK). Each experiment was performed in triplicate and repeated in at least three independent experiments. The spectrophotometric absorbance of methylene blue was measured at specified time points (24 hours, 72 hours, and 5 days), the spectrophotometric reading is considered as reflective of cell number in each well.

Trypan blue exclusion assay for counting dead cells:

Trypan blue is a vital stain that is used to selectively stain dead cells with a blue colour. Since live cells are very selective in the compounds that pass through their membrane, in a viable cell, trypan blue is not absorbed, and hence, cell is not coloured. However, trypan blue does cross the membrane of dead cells. The assay is used to compare the number of dead cells after different treatment conditions in culture and for counting viable cells. The cell suspension (prepared by trypsinisation of cells) was diluted with trypan blue (sigma Aldrich, UK, cat. no. t8154) in a 1:4 dilution (100µl cell suspension added to 300 µl of trypan blue), the mix was incubated for 10 minutes at room temperature.

The haemocytometer was used to determine total cell counts and viable cell number (presumably cells floating in the medium are detached dead cells as CRC cell lines tested in our study are mostly adherent to culture plate surfaces). Each square of the haemocytometer, with cover-slip in place, represents a total volume of 0.1 mm³ and the cell concentration per ml is determined using the following calculations: cells per ml = the average count per square X dilution factor X 10⁴. Total number of cells = cells per ml X the original volume of sample from which cell sample was removed. Assays were performed in triplicate and repeated

on three separate occasions. Data were analysed using Graph Pad Prism 6 software available at: www.graphpad.com

Knock down of CD24:

The protocol described in the Lipofectamine®2000 manufacturer's instructions manual was used for siRNA (small interfering RNA) transfection into the relevant cells. Briefly, 2×10^5 cells were seeded in 2ml DMEM media with 10 % FBS and antibiotics (PS 1%) in 6-well plates (Corning) (volumes are adjusted according to plate size used). Cells were allowed to adhere for 24 hours prior to transfection. Cells were transfected when confluence reached between 40 and 60 % at the time of transfection. The medium was aspirated and cells were washed with PBS and 2ml Opti-MEM®I was added to the cells.

For each transfection sample, oligomer-Lipofectamine® 2000 complexes were prepared as follows: 100 pico-mol Stealth siRNA oligomer i-e (5 µl) for CD24 was diluted in 250 µl Opti-MEM® I Reduced Serum Medium (final concentration of siRNA when added to the cells is 50 nM), then mixed gently. 10µl (or the optimized volume according to the gene of interest) of Lipofectamine®2000 was added to 250µl Opti-MEM® I, mixed gently and incubated for 5 minutes at room temperature.

After 5 minutes, the diluted oligomer was combined with the diluted Lipofectamine[®]2000, mixed gently and then incubated for 20 minutes at room temperature. The oligomer-Lipofectamine[®]2000 complexes were added to each well containing cells and 250µl Opti- MEM[®] I (to make a final concentration of 50nm of the siRNA duplex), and mixed gently by rocking the plate back and forth. The media was changed after 4-6 hours by DMEM medium (with FBS 20 % and PS 1%), plates were incubated at 37°C in 5% CO₂ incubator. Forty eight hours later, transfected cells were either (1) harvested for protein extraction and western blot (2) used directly for the relevant functional assays.

The oligomers used in the study are listed in **Table 11**.

Statistical Analysis:

Statistical analysis was performed using the software GraphPad Prism version 6.00 for Windows (GraphPad Software, La Jolla California USA, www.graphpad.com). All data are presented as mean ± standard error of the mean (SEM). Statistical significance between groups was evaluated using an unpaired two-tailed Student's t-test and Two way ANOVA test. Mean differences were considered significant when was $P \leq 0.05$.

Chapter Three: DAMPs and CD24.

Introduction:

Cells can be damaged either by pathogens or by lethal /sub-lethal stimuli including physical stress, chemicals and thermal form of injury leading to innate immune system activation. It is known that the innate immune system recognises damaging stimuli by Pattern recognition receptors (PRRs). These include NOD like receptors (NLRs), Toll like receptors (TLRs), C-type lectin receptors (CLRs). These receptors interact with pathogens by detecting the conserved structural moieties present in the pathogens called Pathogen Associated Molecular Patterns (PAMPs). The exposure of cells to these PAMPs leads to a cascade of downstream events aiming at eradication and prevention of damage by the offending pathogen (73).

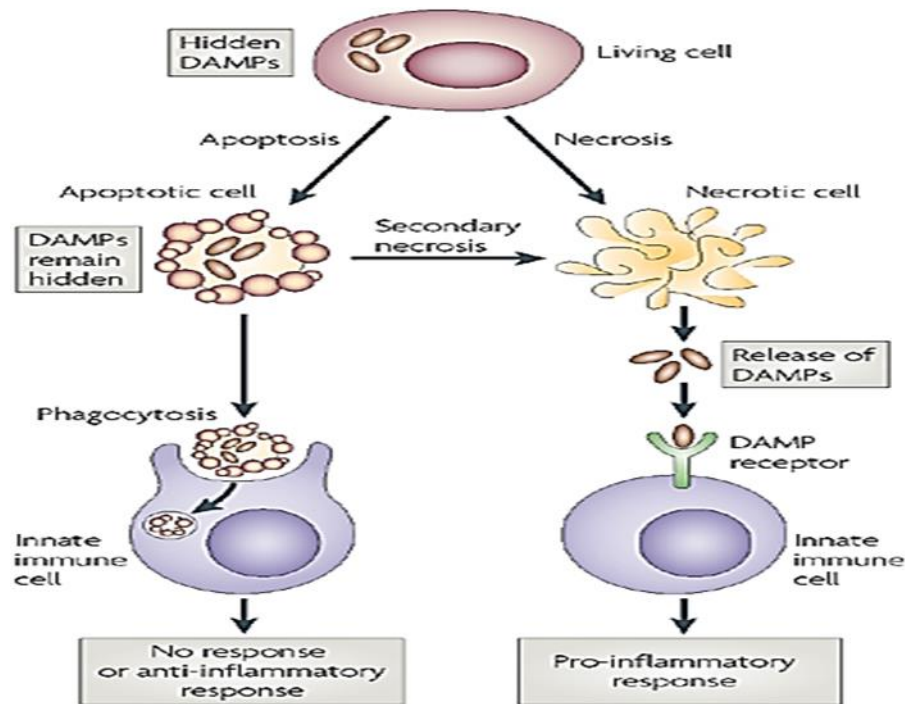
In contrast, cellular responses to damaging stimuli are not that clearly understood. The concept of "danger" was proposed about 25 years ago through observations that cellular damage results in disruption of the cellular membrane with release of endogenous molecules into the cellular microenvironment. The release of cellular contents together with damage induced degradation products from the extracellular matrix form what are known as Damage (or Danger) Associated Molecular Patterns (DAMPs) (21) **Figure 8.**

This is primarily the characteristic of necrotic cell death although now studies have shown that some apoptotic cells and phagocytes also release DAMPs (73).

The cell-derived DAMPs include cytoplasmic proteins (such as Heat Shock Protein (hsp90, and hsp70), nuclear proteins (such as high mobility group box 1(HMGB1), nucleic acids and metabolic products. They can be detected by adjacent living cells and may provide signals, which, for example, help to initiate or maintain an immune response (73, 74).

The mechanisms by which cells are able to detect DAMPs are unclear although a number of cell surface receptors have been described for specific DAMP molecules. Toll-Like Receptor (TLR) 2 and 4, as well as Receptor for Advanced Glycation End products (RAGE) have been reported as receptors for HMGB1(75, 7). It is interesting that both DAMPs and PAMPs can interact with Toll like receptors (TLRs) and NOD-like receptors (NLRs) but the downstream response appears to be very different (7).

How this differential response was mediated remained a mystery till quite recently. CD24 emerged as a molecule that has been observed to physically interact with important DAMPs including HMGB1, HSP90 and HSP70. Siglecs are also recently identified ligands of CD24 as shown by co immunoprecipitation experiments by Chen *et al.* (41).



Nature Reviews | Immunology

Figure 8: Release of DAMPs from necrotic cells to induce sterile inflammation .⁽⁷⁶⁾

They proposed a model where by TLR may be interacting with CD24 and members of the Siglec family of transmembrane proteins. In this model **DAMPs, CD24** and **Siglec** molecules (Siglec G in mice, Siglec 10 in humans) form a tri-molecular complex. CD24, through its interaction with Siglec, was proposed to inhibit the host response to tissue injury by modulating NF- κ B activation⁽⁷⁷⁾. The extensive glycosylation of CD24 molecules can be the explanation of CD24's ability to interact and form complexes with Siglecs and DAMPs (HMGB1 and HSPs).

These sites provide multiple binding sites that potentially can interact with multiple molecules simultaneously. This pathway imposed a significant negative feedback loop limiting inflammation and a high surge of cytokines when the cells are damaged by non-pathogenic stimuli. This was presented as a simple model by the same group as shown in the diagram below (21), **Figure 9**.

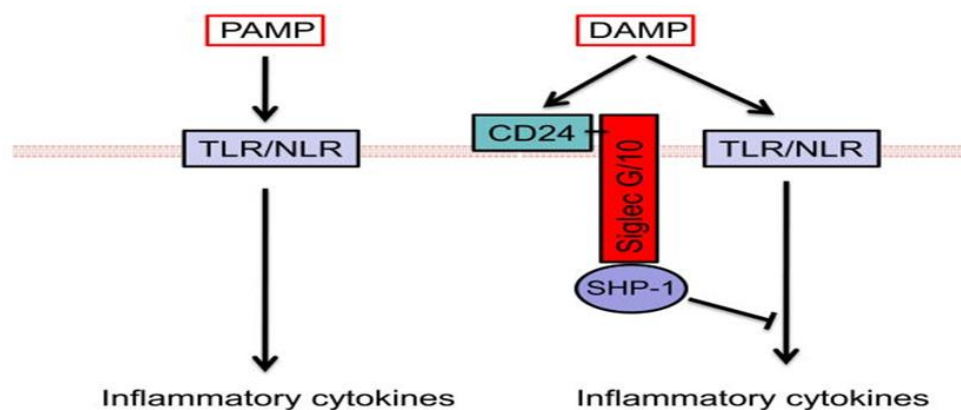


Figure 9: Simplified model of CD24/Siglec/DAMP interaction.

The model represents physiological pathway leading to a differential response of cells to PAMPs and DAMPs mediated by tri- molecular complex formed by CD24/ Siglec/DAMPs leading to SHP-1 activation(21).

To verify the hypothesis that CD24 plays a vital role in discriminating tissue response to DAMPs from PAMPs, Chen *et al.* induced damage in the mice liver cells by using the well-known hepatotoxic drug i-e acetaminophen. Acetaminophen (N-acetyl-p-aminophenol [APAP]), also termed paracetamol, is one of the most commonly used experimental models of inducing acute liver cell damage in mice (78). The model is

highly reproducible and causes dose-dependent hepatotoxicity that can be induced by even single dose of APAP. They treated CD24 ^{-/-} mice with sub lethal dose (10mg/mouse) of acetaminophen (APAP) and observed that a dose that was well tolerated by wild type mice resulted in significantly reduced survival of CD24 ^{-/-} mice compared to Wild type controls (death within 20 hours post treatment with APAP). They also detected significantly increased levels of inflammatory cytokines (including IL-6 and TNF α) and hepatic enzymes in CD24 deficient mice compared to Wild type group after APAP (Acetaminophen) treatment. These mice were rescued and showed decreased serum levels of cytokines and enzymes after treatment with HMGB1 blocking antibodies in the CD24 ^{-/-} group pointing towards HMGB1 to be the direct mediator of injury in the absence of CD24 (67).

How this inhibitory effect of CD24 on the HMGB1 was mediated was unclear, as CD24 has no known signal transduction mechanism. Siglecs were looked up in this regard by Chen *et al.* based on the evidences that these cell surface receptors belonging to immunoglobulin super-family can recognize sialic acid-containing proteins. Siglecs have been considered as negative regulators of the immune system by virtue of presence of one or more cytosolic immune receptor tyrosine-based inhibitory motifs (ITIMs). They found direct interaction between

CD24 and Siglec 10 in mice by co-immunoprecipitation and flow cytometric analyses and hence provided evidence that CD24 interacts directly with HMGB1 and Siglec molecules. Based on above findings they presented their **tri-molecular** model of **CD24-Siglecs- HMGB1** as a loop that discriminates cellular response to danger versus pathogens(41).

Very recently it has been proposed that pathogens lead to sepsis (there by causing excessive release of inflammatory cytokines and tissue damage) by breaking the above mentioned interaction. This is achieved by bacterial sialidases cleaving off CD24 sugar moieties. Inhibition of sialidases resulted in dampening of sepsis and is being explored as potential treatment option (66).

This further emphasises the significance of glycosylation of CD24 and exploring these sugar sites was one of the targets of our study and will be discussed in detail. Within the gastrointestinal tract, there are a number of non-infectious inflammatory conditions in which there is likely to be a release of DAMPs. Similarly, most solid malignancies are marked by necrosis and probable release of DAMPs in tumour and tissue microenvironment. Over the past decade, research has been undertaken to explore how this affects the adjacent cells and tissues.

Some studies have related these DAMPs to be important contributory factors in development of chronic diseases and even malignancies(79).

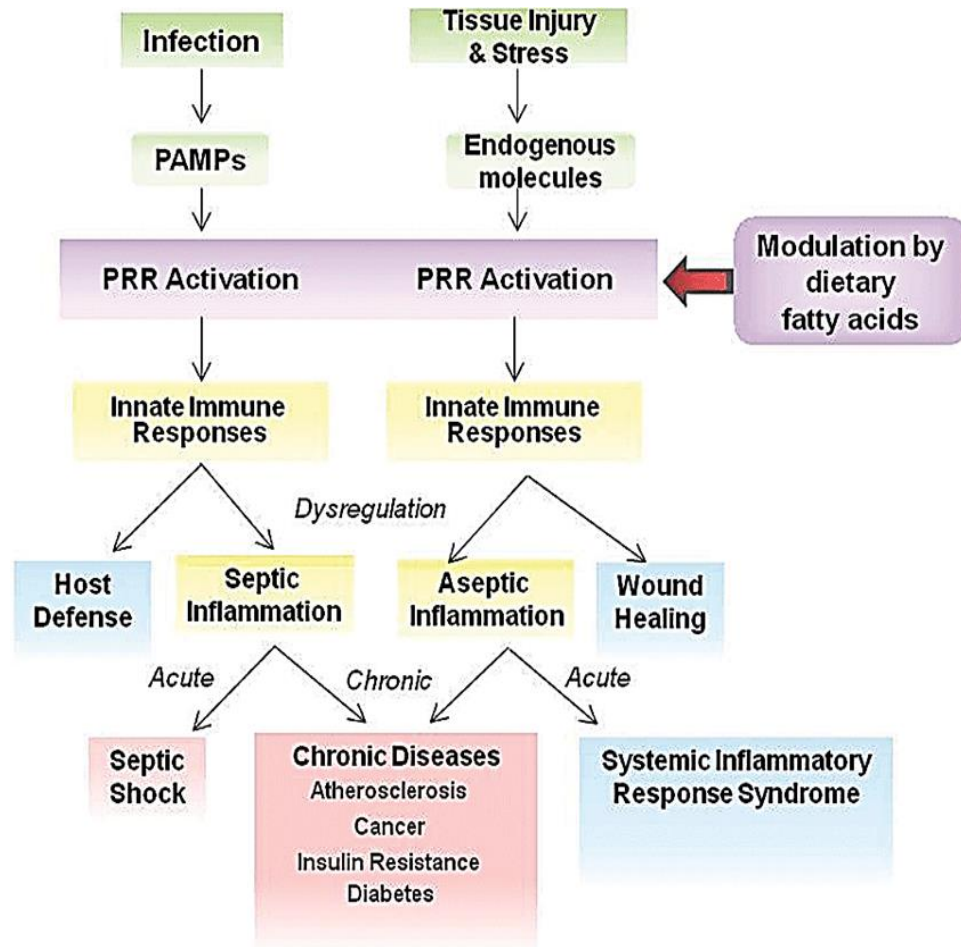


Figure 10: Flow diagram of potential outcomes of tissue injury⁽⁷⁹⁾.

The prototype DAMP presented in literature is HMGB1 (80). In 2004 Rovere-Querini *et al.* showed that the supernatants of necrotic cells lead to dendritic cell maturation via HMGB1(81). The presence of HMGB1 in necrotic cell pellets, as well as supernatant from Hela cells when damaged by repeated freeze

thaw cycles, was shown by western blot and this naturally released HMGB1 had comparable effects to recombinant HMGB1(81). In 2006 Yang De *et al.* proposed a chemotactic role of DAMPs on dendritic cells at the site of injury (82). It was later shown that effects of DAMPs were not limited to immune cells - rather it was seen in a setting of macrophage/enterocyte co-culture that necrotic macrophages (prepared by repeated freeze thaw) released DAMPs and these reduced enterocyte cell migration pointing towards the differential role of these substances on immune cells and epithelial cells (74). Another very recent study by Lotfi *et al.* demonstrated that necrotic material from both normal as well as tumour cells (prepared from necrotic cell lysates from HCT116, CaCo2 ,COLO as well as from platelets and mesenchymal stem cells) promotes proliferation and trafficking of human mesenchymal stem cells (MSCs) (80). These effects were neutralised when HMGB1 antibodies were used indicating it to be the common and major player released from these diverse cellular sources and quite interestingly the cellular response was similar irrespective of the source of DAMPs (80).

Whilst much of the work on responsiveness to DAMPs has focused on inflammatory and immune cells, it is possible that DAMPs may also be detected by intestinal epithelial cells. It has been shown that intestinal epithelial cells express Toll-like

receptors and RAGE and we have recently shown that expression of CD24 is up-regulated during active inflammation in epithelial cells in both Crohn's disease and Ulcerative Colitis (26, 44). These diseases are characterised by extensive tissue necrosis followed by tissue healing. For the latter to occur, epithelial cells must proliferate and migrate over damaged areas to restore epithelial continuity before re-modelling can begin. The above studies explored interactions between DAMPs released by immune cells acting on epithelial cells and vice versa but none of the studies tried to look up if dead epithelial cells can give messages to the remaining alive adjacent cells directly.

Given that CD24 is linked to cellular properties like migration and growth and is increased in the setting of colorectal cancers and inflammatory bowel disease (26), we hypothesised that autologous DAMPs may influence epithelial cell functions. If so, DAMPs could cause alteration of cell motility and proliferation since these would be important in the healing process. We therefore, sought to investigate firstly whether or not colorectal carcinoma cells (epithelial cells) show any response to autologous DAMPs. Secondly, if any of these effects were mediated through CD24.

Materials and methods:

Preparation of DAMPs:

Colorectal carcinoma cell lines (HCT116/RKO/SW620/SW480 and DLD1) were exposed to autologously derived DAMPs (i.e. derived from the same cell line) in order to prevent any possible activation due, for example, to cell line-specific growth factor production. DAMPs were prepared following the protocol by Lotfi *et al.* and in accordance with the standard method (8, 35, 37, 80, 83). Briefly, cells were grown to confluence, the tissue culture medium was aspirated and the cells were washed twice in Phosphate Buffered Saline (PBS, Sigma, USA). After this, 5ml of PBS was added to the cells which were then scraped off the flask with a scraper (Corning, UK). A single cell suspension was obtained by repeatedly pipetting the cells through a 10ml pipette tip. A total of 10^6 cells suspended in 1000 μ l of PBS were transferred into a 1.5ml eppendorf tube (Sigma Aldrich UK).

The cells underwent four freeze-thaw cycles (consisting of freezing in dry ice for 5-7 minutes and thawing in a water bath at 37°C for 5-7 minutes) in order to release the DAMPs from the cells. The tubes were centrifuged at 17,000 x g for 1 minute and the supernatant was collected in new tubes. The proteins in the supernatant were quantified, using the BCA Protein Assay Kit (Thermo Fisher Scientific Inc., Rockford, USA) in accordance

with the manufacturer's instructions. Western blots for HMGB1/ β -actin/ HSP90/ Histone 3 were performed on the supernatants as an indicator of cell lysis and for presence of DAMPs. Various concentrations of NCL (necrotic cell lysate) supernatant were tested in order to determine the optimal concentration for the DAMP stimulation experiments.

Wound Healing Assays:

Wound healing assays were performed in 6 well plates (Costa, UK). Cells were grown to confluence in full medium and then starved for 24 hours in serum free medium. A "wound" was created using a sterile 100 μ l pipette tip and the wells were supplemented with either autologously derived DAMPs to a final concentration of 0.08 μ g/ μ l of DAMPs or, for the controls, an equivalent volume of PBS. Photographs were taken using a charge-coupled device (CCD) camera (Canon) attached to the inverted phase-contrast microscope at a magnification of 40x. Migration of cells across the wound line was assessed 24 hours after wounding using T Scratch software (72). The experiments were repeated four times at different occasions with each condition in triplicate with three wounds in each well.

Transwell Migration Assays:

Transwell cell migration assay was performed using a Boyden chamber containing a polycarbonate filter with an 8 μ m pore

size (Costar, UK) as previously described (26). Prior to the addition of cells, the Boyden chambers were incubated in 600µl serum free DMEM for one hour at 37°C. This was removed and medium (600µl) supplemented with 20% FBS was added to the lower chamber. A total of 10^5 cells were added into the upper chamber in 200µl of medium supplemented with 10% FBS. In order to evaluate directional motility, medium in the lower chamber was supplemented with either autologously derived DAMPs to a final concentration of 0.08µg/µl of DAMPs or, for the controls, an equivalent volume of PBS.

Cell migration across the membrane was allowed to take place over a period of 8-12 hours depending on the cell line after which the chambers were removed. The plates were incubated for a further two hours to allow migrating cells to settle down to the bottom of the wells and cells which had migrated to the bottom wells were counted by direct microscopy. Cells were counted by two different experimenters for validation. The experiments were conducted in triplicate and repeated three times.

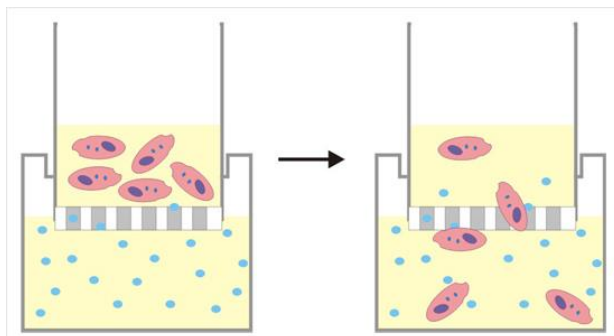


Figure 11: Trans well migration.

The Cells loaded in the upper chamber pass through the pores and are migrated to the bottom wells. These were counted by direct microscopy after allowing them to settle for two hours.

Proliferation Assay:

Presto-Blue® (PB) is a new, simple and extremely fast live assay. This assay is a commercially available, ready-to-use, water-soluble preparation. PrestoBlue® reagent contains a cell-permeant compound (**Resazurin**) that is blue in colour and virtually non-fluorescent in solution. When added to media, PrestoBlue® reagent is rapidly taken up by cells. The reducing environment within viable cells converts PrestoBlue® reagent to an intensely red-fluorescent dye (**Resorufin**). This change can be detected by measuring fluorescence or absorbance.

Conversion is proportional to the number of metabolically active cells and therefore can be measured quantitatively and hence can be used as a proliferation assay. **Resazurin**-based viability assays do not require cell lysis and hence, the same plates can be measured at different time points making is a very useful

assay to observe the effect of DAMPs on cellular proliferation over a course of 2-5 days. The experiment was performed according to the manufacturer's protocol (Thermo Fisher Scientific, UK, Cat # A-13261).

Briefly, cells were exposed to autologous DAMPs at a concentration of 0.08ug/ μ l in full media (DMEM+10% FBS) and control cells were treated with equal volume of PBS in full media. Cells were seeded at a density of 2×10^4 cells/well in a 24-well plate with each condition in triplicate.

Cell proliferation was determined by incubation with PrestoBlue® master mix at 1 : 10 dilution (i-e 2.7ml DMEM+ 300 μ l of presto blue reagent). A total of 400 μ l of this master mix was added to each well for 1 h at 37C° in the dark. 100 μ l was added to each well of a 96 well plate (hence in triplicate from each well of 24 well plate).

Three wells with master mix incubated with media but without the cells served as the "Blank". The fluorescence intensity of the Resazurin product (Resorufin) was measured using Fluostar Optima® (BMG LabTech, Germany) at 530 nm (excitation wavelength) and 590 nm (emission wavelength). After each reading excess, Prestoblu® master mix was aspirated from the wells and cells were re incubated with either full media or full media with DAMPs as described above. Readings were taken at 0, 24, 48 and 72 h using three gains (500, 1000, and 1500).

The experiment was performed on three different cell lines and repeated on two separate occasions, with each condition in triplicate.

Results:

It has already been shown by multiple studies that damage to cells by repeated freeze thaw cycles results in the breakdown of cell membranes. This leads to the formation of necrotic cell lysate (NCL) and it is generally taken as a natural source of DAMPs. As mentioned earlier, studies have shown HMGB1 to be abundant ubiquitous DAMP common to various cell lysates tested (from necrotic macrophages, platelets, mesenchymal stem cells and colorectal cancer cells such as from HCT116 and COLO) in addition to other DAMPs (80, 81). This approach is more helpful in our view, compared to some studies using only recombinant or purified single component, as this cellular lysate and the released contents are a closer reproduction of tissue microenvironment when the cells lysis occurs as a result of lethal tissue damage.

Hence, we prepared our DAMPs by the above mentioned protocol. We performed western blot analysis on these lysates to ensure complete rupture of membranes and presence of DAMPs in that supernatant. Four antibodies were used: HMGB1 is the prototype of DAMPs, present in the cell nucleus but acts as DAMP when released after cell lysis. HSP90 is also a specific DAMP itself present mostly in the cytoplasm, β -actin is a cytoplasmic protein and confirms the release of cytoplasmic contents, H3 is a nuclear protein and released only after

damage to nuclear membrane (hence all its accompanying contents). All antibodies were strongly positive **Figure 12**.

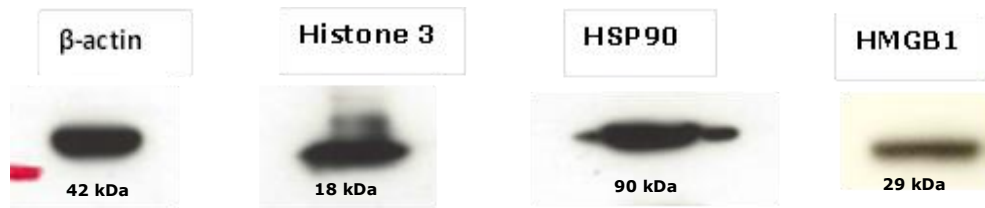


Figure 12 : Western blot showing DAMPs in supernatants (SW620).

To ensure complete lysis of cells and thereby the release of DAMPs western blots were performed on supernatants from SW620. β -actin, Histone 3 (H_3), Heat shock protein 90 (HSP90) and HMGB1 were immunoblotted.

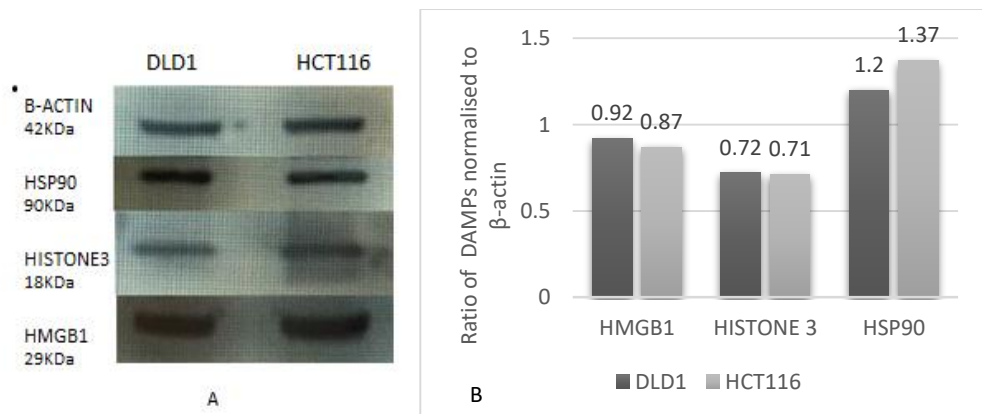


Figure 13: Western blot showing DAMPs in supernatants (DLD1 AND HCT116).

DAMPs western blots performed on supernatants from DLD1 and HCT116. β -actin, Histone 3 (H_3), Heat shock protein 90 (HSP90) and HMGB1 were immunoblotted (A). Densitometry bar graph (B).

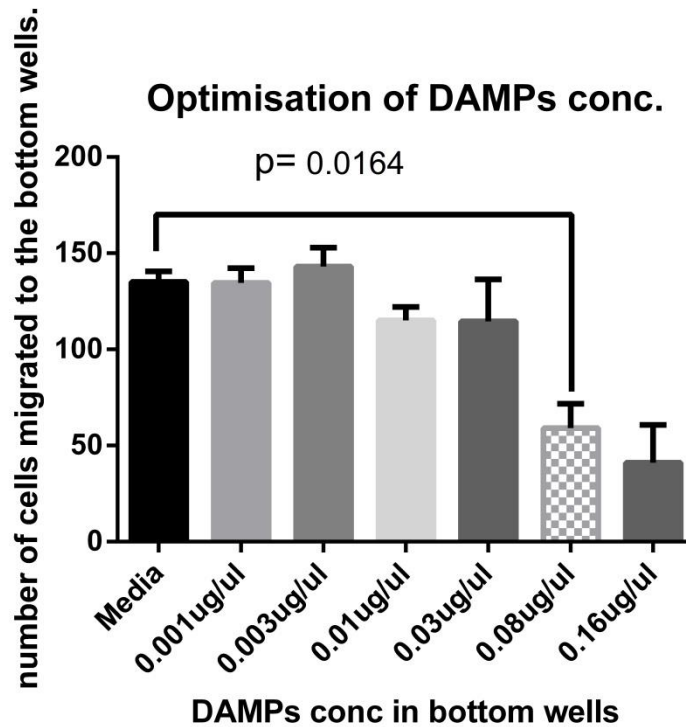


Figure 14: Optimisation of supernatant conc. for functional assays.

To know the optimum concentration of DAMPs (NCL) to be used in our functional assays, total protein conc. of the necrotic cell lysate was measured and taken as an indirect representation of amount of DAMPs in them. Various amounts ranging from 0.01 to 0.16 $\mu\text{g}/\mu\text{l}$ were tested in transwell migration assay using SW620. Significant effects were seen at a concentration of 0.08 $\mu\text{g}/\mu\text{l}$ or above. Student t-test was used to analyse the data and a p value of ≤ 0.05 was considered significant. Conc. (concentration).

We hypothesised that DAMPs may cause physiological changes in epithelial cells which can be related to cell motility and therefore, be relevant to both tissue healing (in the normal physiological context) and local tumour invasion (in the context of malignancy). We did not know the likely nature of this effect (increasing or decreasing motility) nor the “dosage” required. We tested SW620 cells in transwell migration assays in order to find the optimal concentration of lysate to be used in the next

experiments. To achieve that we compared the motility of cells through the transwell membrane when exposed to increasing concentration of DAMPs in the bottom wells compared to media. The lower chambers of the wells were supplemented with DAMPs (NCL) in a concentration ranging from 0.001 to 0.1 $\mu\text{g}/\mu\text{l}$. Compared to controls which were supplemented with PBS, a significant difference in motility was seen when cells were stimulated with DAMPs at a concentration of 0.08 $\mu\text{g}/\mu\text{l}$ and so we chose this concentration **Figure 14**.

DAMPs inhibit both directional and non-directional motility:

Our initial optimisation data showed that DAMPs were inhibiting cell motility in colorectal carcinoma cell lines (colonic epithelial cells). In order to confirm that this was not a cell line-specific effect, we tested an additional 3 cell lines. In order to analyse relevance of this effect to CD24, we selected two cell lines which had high expression of CD24 (DLD1 and SW620) and 2 cell lines which were negative for CD24 i.e. HCT116 and RKO. Analysis of CD24 expression levels has been done by our group previously analysing both mRNA and protein levels for CD24 in each cell line through qPCR, flow cytometry and western blots analyses (**see Appendix iii**). We also performed western blot to confirm CD24 expressions in these cell lines **Figure 15**.

Non directional cell motility was tested using wound healing assay and showed, in 3 out of 4 cell lines (RKO) tested, a significant inhibition of cell motility across the wound following exposure to DAMPs **Figure 16**. This effect was observed irrespective of CD24 expression in the cell lines, it indicated that CD24 may not be essential for a DAMPs response in colorectal cancer cell lines (colonic epithelial cells) **Figure 17**.

Many studies have shown that DAMPs can act as chemo-attractants for dendritic cells and thus we investigated whether they could modulate chemotaxis in epithelial cells. Transwell migration assays were performed with DAMPs added to the lower chamber. Compared to PBS controls, the presence of the DAMPs significantly inhibited cell migration across the membrane in three out of four tested (again RKO did not show a statistically significant difference) **Figure 18**. The reasoning for the lack of significant response in RKO cell line could be due to the difference in genetic mutations amongst them. RKO lacks mutant Kras and carries mutant Braf and opposite is true for rest of the three cell lines **Table 1**.

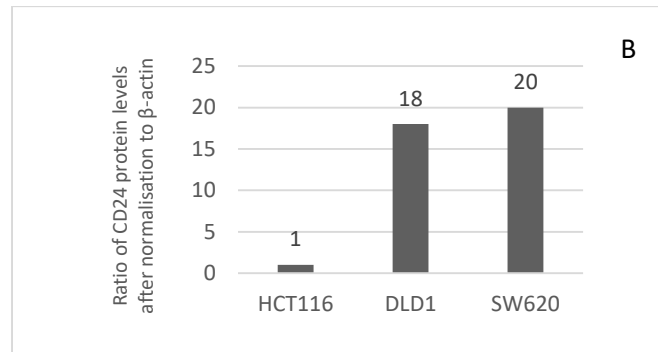
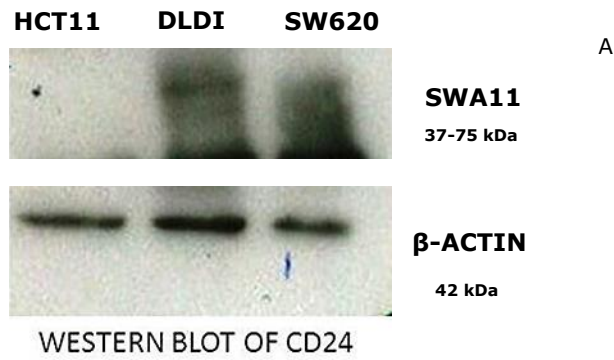


Figure 15: Western blots of cell lines showing CD24 expression levels.

CD24 protein levels were tested in lysates from HCT116/DLD1/SW620 cell lines by using SWA11 mAb. β-actin was loading control. HCT116 is negative whereas SW620 and DLD1 are strongly positive for CD24 (A). Densitometry bar graph (B).

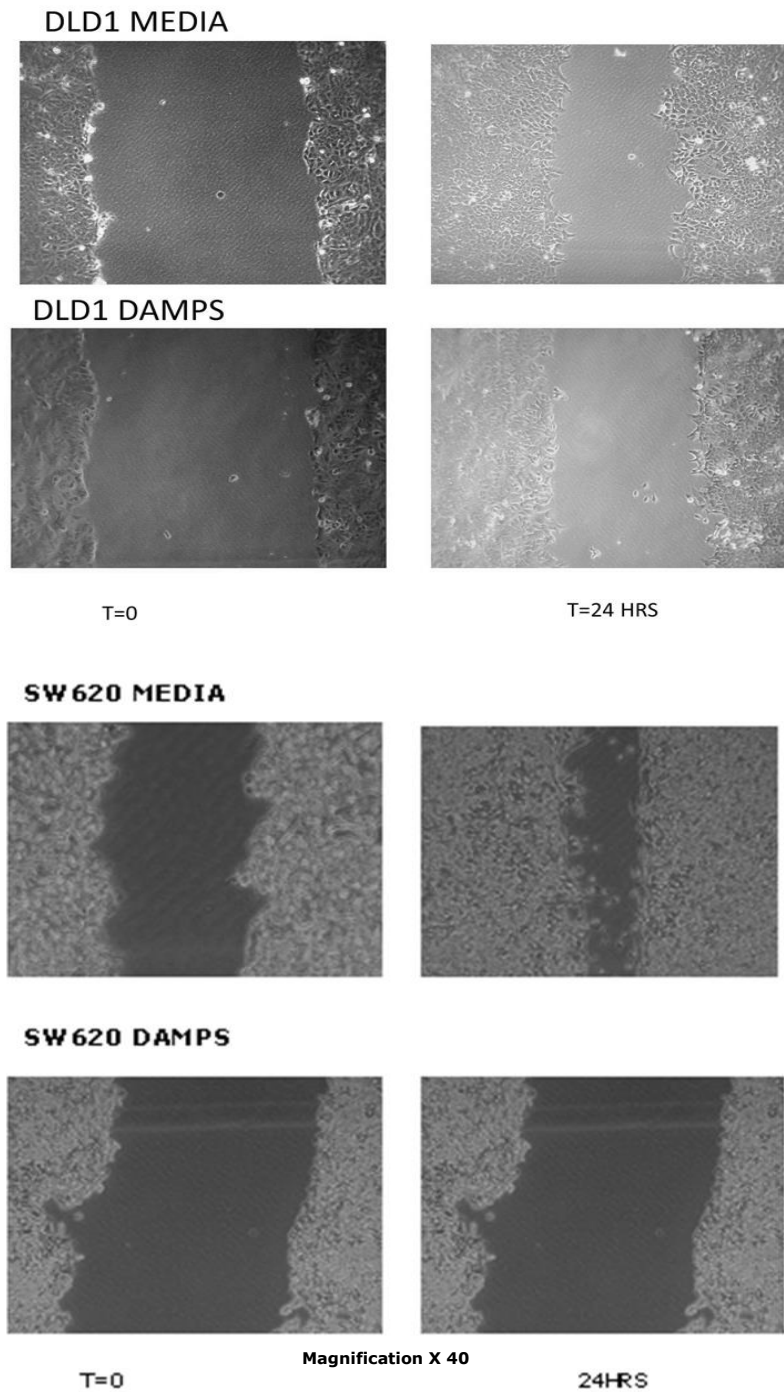


Figure 16: DAMPs reduced cell migration across the wound.

Representative images from colorectal carcinoma cell lines exposed to autologous DAMPs (0.08 $\mu\text{g}/\mu\text{l}$) or media alone. Photographs were taken for T=0hrs and then after 24 hrs at same the point for each condition (image magnification X 40). For each condition at least six sets of photographs were taken along the wound. Open wound area of the images was measured using T-scratch software(72). The experiment was repeated for each cell line in triplicate and on three different occasions.

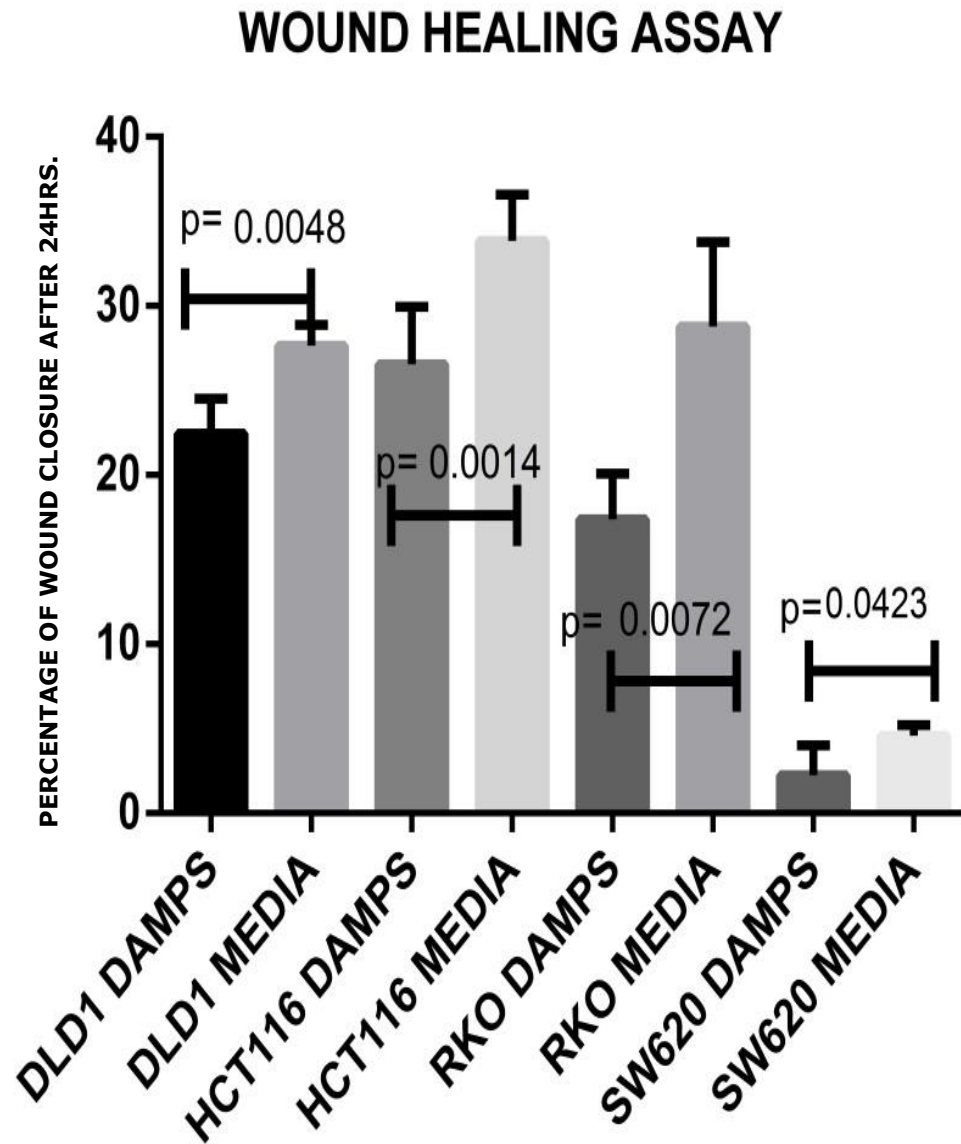


Figure 17: Wound healing assay in four colorectal cell lines.

Wound healing assay was performed and analysed using T-scratch software and the percentage of wound closure after 24hrs of exposure to autologous DAMPs was calculated and compared to media in four colorectal cell lines. All values were expressed as \pm SEM. DLD1 and SW620 are positive for CD24 and HCT116 and RKO are CD24 negative cell lines. These experiments were repeated thrice in triplicate at separate occasions. Student t-test was used to analyse the data and a p value of ≤ 0.05 was considered significant.

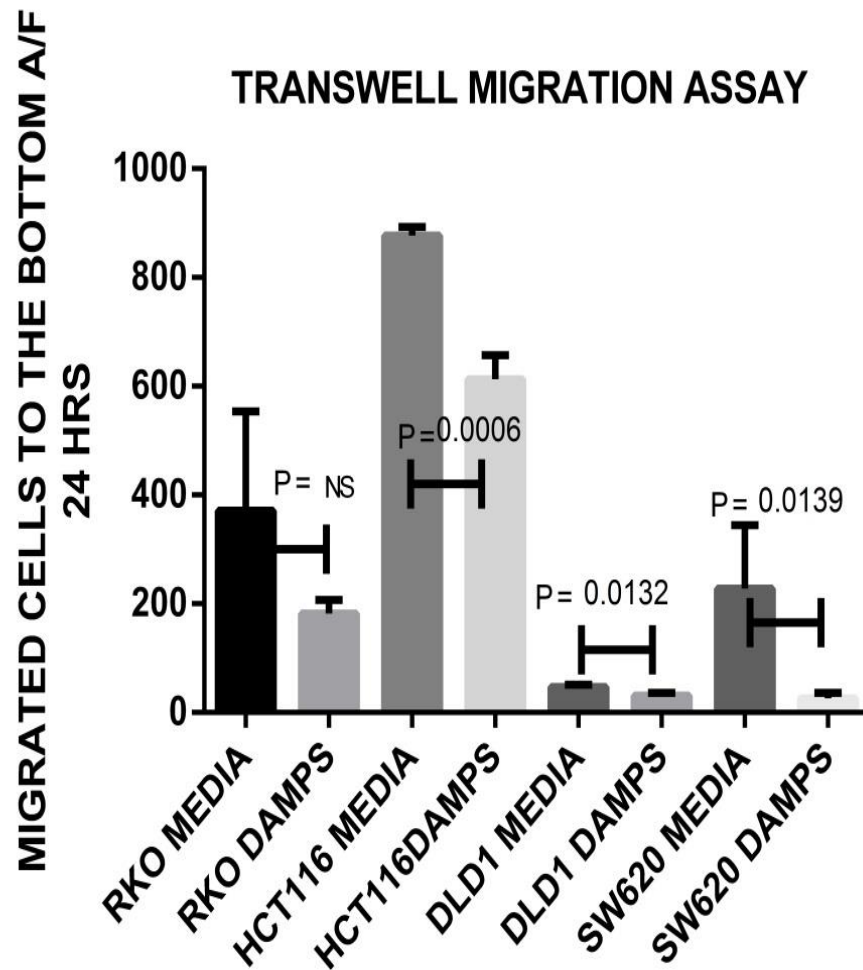


Figure 18: DAMPs inhibit directional motility as well in autologous cell lines.

We performed transwell migration assay with DAMPs in the bottom wells as stimulus and observed that less number of cells migrated to the bottom wells having DAMPs as compared to media in both CD24 positive and negative cell lines. The effect was statistically significant in 3 out of 4 cell lines. This effect was dose dependent with a minimum effective concentration of $0.08\mu\text{g}/\mu\text{l}$ of DAMPs as shown by the optimization experiments. Cells migrated to the bottom wells after 8- 24hrs were counted by direct microscopy. Results were analysed using Graph pad prism version 6. These experiments were repeated thrice in triplicate at separate occasions. Results expressed as mean \pm SEM and P-value of ≤ 0.05 were taken as significant. NS (not significant).

Mechanism of DAMPs inhibition of epithelial cell motility:

Next we tried to explore the possible mechanism leading to reduced cellular motility. In order to ascertain how DAMPs may be causing inhibition of cell motility, we tested SW620 by Western blot for expression of a panel of markers associated with Epithelial Mesenchymal Transition (EMT) including Snail, Cten, E-cadherin and N-cadherin. Exposure to DAMPs led to a clear reduction in Snail, Cten and N-cadherin protein levels. However, the levels of E-cadherin remained quite similar. β -actin was used as loading control **Figure 19**.

DAMPs act independently of CD24:

CD24 is a proposed DAMPs receptor in dendritic cells. Given our original observation of up-regulation of CD24 in epithelial cells in inflammatory bowel disease, we were prompted to investigate whether CD24 could also mediate the activity of DAMPs in non-immune cells. Our results on high and low expressing cell lines for CD24 suggested that CD24 was not essential to the DAMPs response. In order to ascertain whether there was some contribution to the DAMPs response by CD24, we repeated the experiments following modulation of levels of CD24 by forced expression and knockdown.

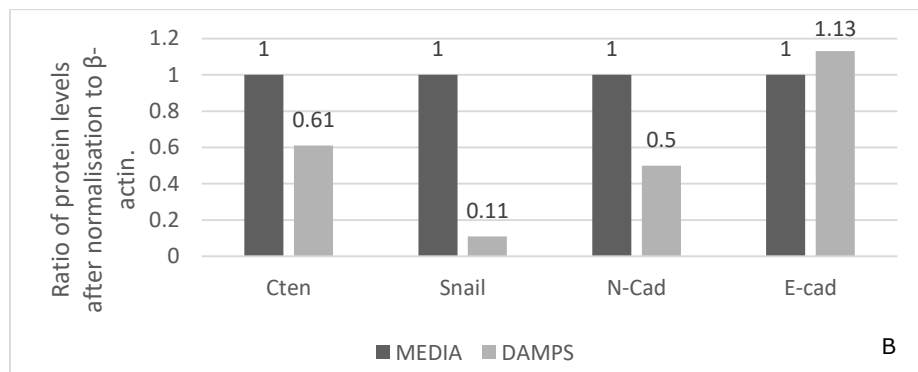
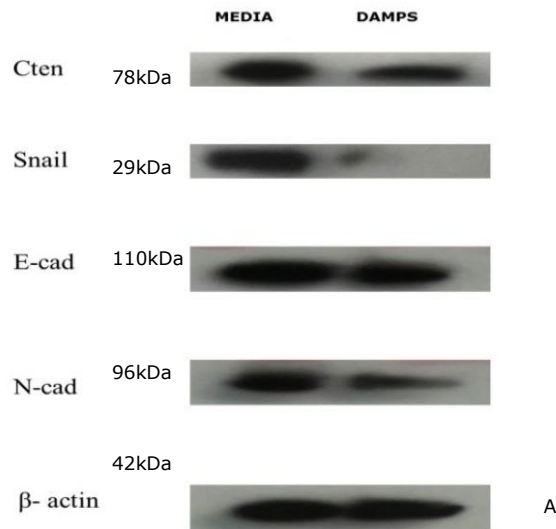


Figure 19: DAMPs decrease cell motility by inhibiting epithelial mesenchymal transition.

SW620 cells were exposed to DAMPs or media as a control for 24 hours and western blot was performed using a panel of motility markers including E-cadherin, N-cadherin, Cten and Snail, whereas β -actin was used as loading control (A). Densitometry bar graph (B). EMT (Epithelial mesenchymal transition).

CD24 was knocked down in SW620 and the transwell migration experiments were repeated. Comparison of the PBS controls showed that, in agreement with our previous published data,

knockdown of CD24 resulted in an inhibition of cell motility. Comparison of the DAMPs stimulated cells, however, showed that there was no significant difference between cells transfected with CD24 siRNA versus luciferase controls **Figure 20**. Thus, knockdown of CD24 could not rescue the inhibitory effects of DAMPs thereby suggesting again that CD24 was not modulating DAMPs response in colonic epithelial cells. The knock down was confirmed by western blot and gave typical but reduced smeary band in the knock down lane compared to scramble control **Figure 21**.

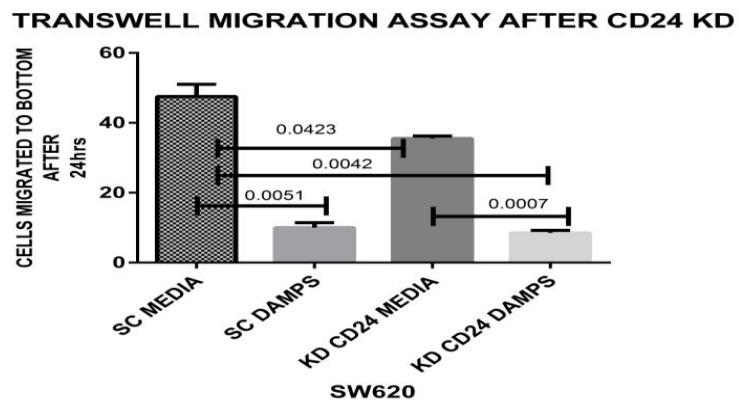


Figure 20: Inhibition of transwell migration by DAMPs is not mediated through CD24.

Transwell experiment was performed after 48 hours of knockdown of CD24 in SW620 using CD24 si RNA and cells were then exposed to 0.08 μ g/ μ l DAMPs in the bottom well and migration was compared with media. Although CD24 knockdown resulted in inhibition of cell migration but DAMPs were once again showing significant inhibition of migration in both CD24 presence and absence (SC DAMPS vs KD CD24 DAMPS). Hence indicating, inhibition was not mediated by CD24. Results shown here are the means \pm standard errors (SE) for three independent experiments. Data were analysed by Graph Pad prism6 using student t test and $P \leq 0.05$ as a significant p value. SC MEDIA (scramble control media), SC DAMPS (scramble control/luciferase SiRNA DAMPs), KD CD24 (Knock down CD24).

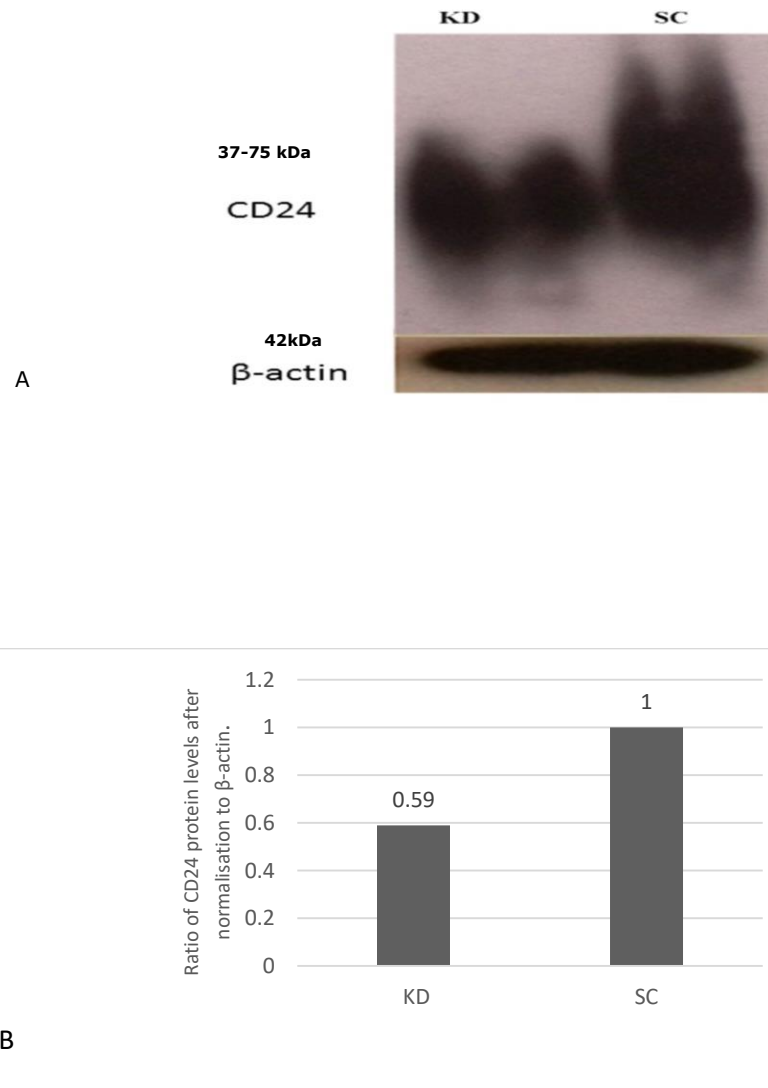
Knock Down of CD24 in SW620

Figure 21: Western blot showing CD24 knock down.

SW620 cells were transfected with either CD24 siRNA or Luciferase siRNA as control using Lipofectamine2000 reagent according to manufacturer guidelines. Cells were harvested for further transwell assay and immune blotting after 48 hours (A). Densitometry bar graph (B). SWA11Ab was used for CD24 and β -actin was loading control. KD (knock Down), SC (scramble control= Luciferase siRNA).

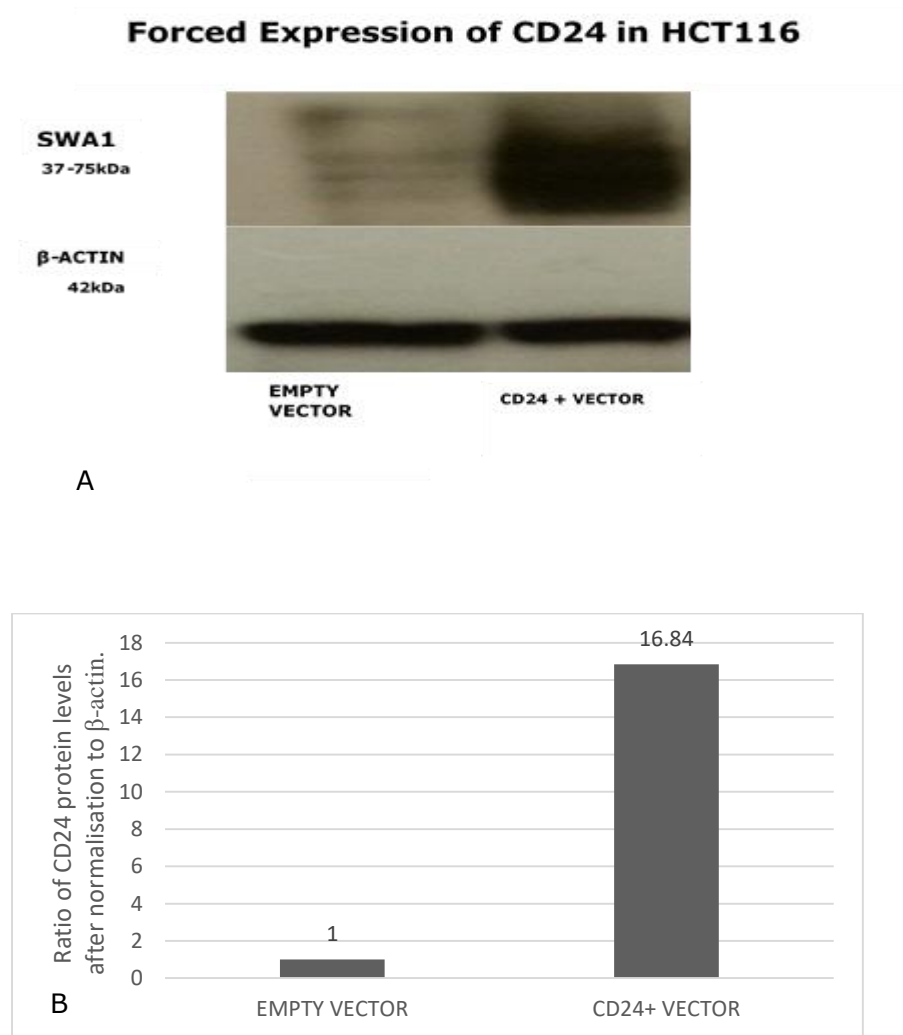


Figure 22: Forced expression of CD24 was confirmed by western blot.

HCT116 cells were transfected with the CD24 expression vector and upregulation of CD24 was confirmed by using SWA11 mAb for CD24 and β -actin was used as loading control (A). Densitometry bar graph (B).

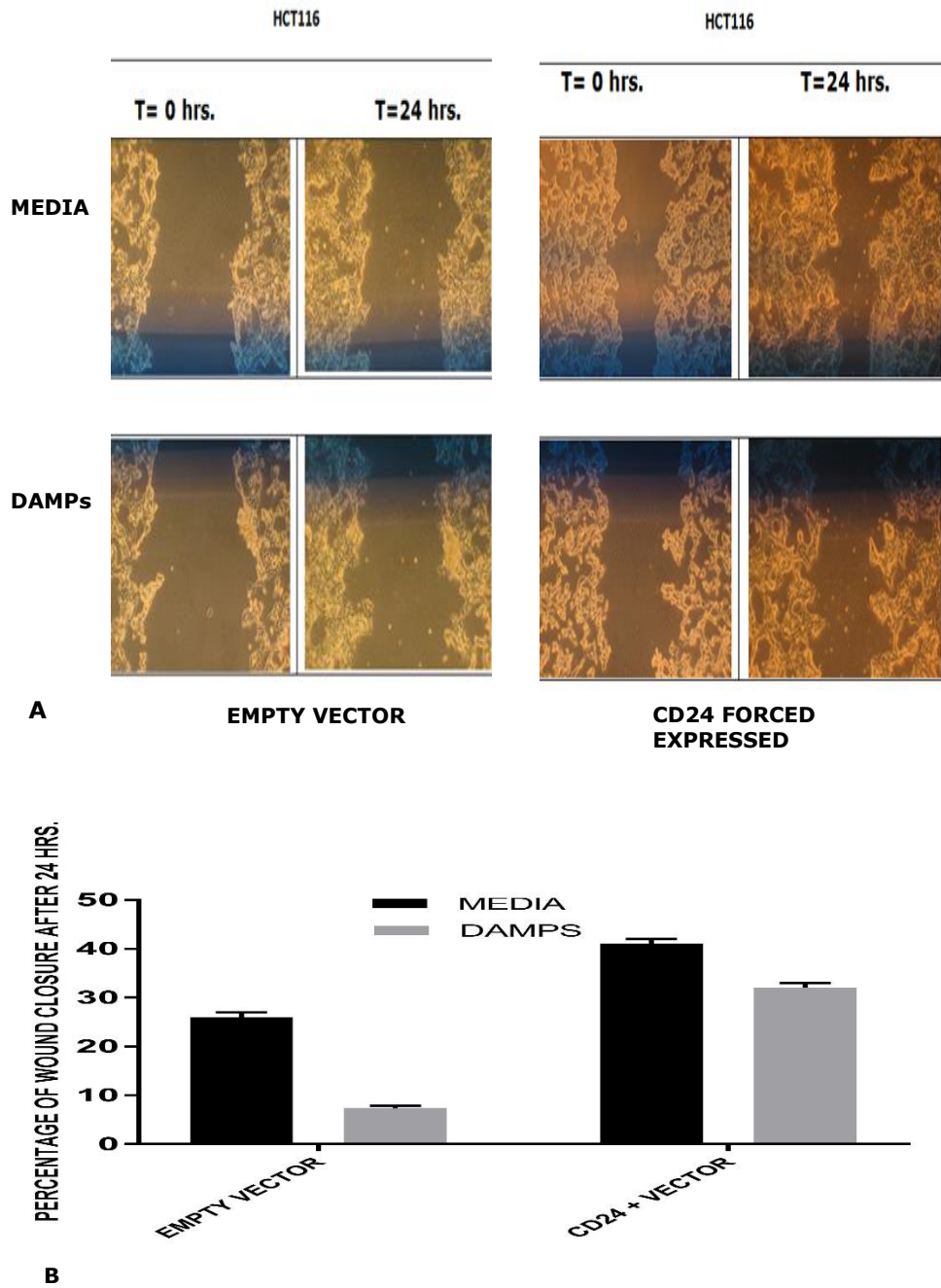


Figure 23: DAMPs inhibitory effect on motility appears independent of CD24.

To analyse the effect of CD24 on the response of DAMPs .Wound healing assay was repeated by exposing cells to DAMPs in HCT116 cells after forced expressed with CD24 and wound closure was compared to controls. (Image magnification X 40) (A).Graph showing inhibition of cell motility by DAMPs and rescue of cell motility with CD24 forced expression but less marked in the presence of DAMPs (B).

In accordance with the results of our previous experiments, it was observed that DAMPs were having inhibitory effects on motility. CD24 transfected cells showed rescue of migration with media, but less so in cells exposed to DAMPs **Figure 23**. These results, when taken together with knockdown experiments, suggest that the effect of DAMPs is to inhibit the motility of colorectal epithelial cells and this effect doesn't appear to be mediated through CD24.

DAMPs increase cell proliferation:

An increase in mitotic activity is commonly seen in inflamed tissue and, in addition to changes in cell motility, it is an important component of the healing response. We, therefore, investigated whether DAMPs could affect cell proliferation in SW620 / HCT116 and SW480. Stimulation of cells with DAMPs resulted in a significant increase in cell numbers. This was seen in both high and low expressers of CD24 **Figure 24**.

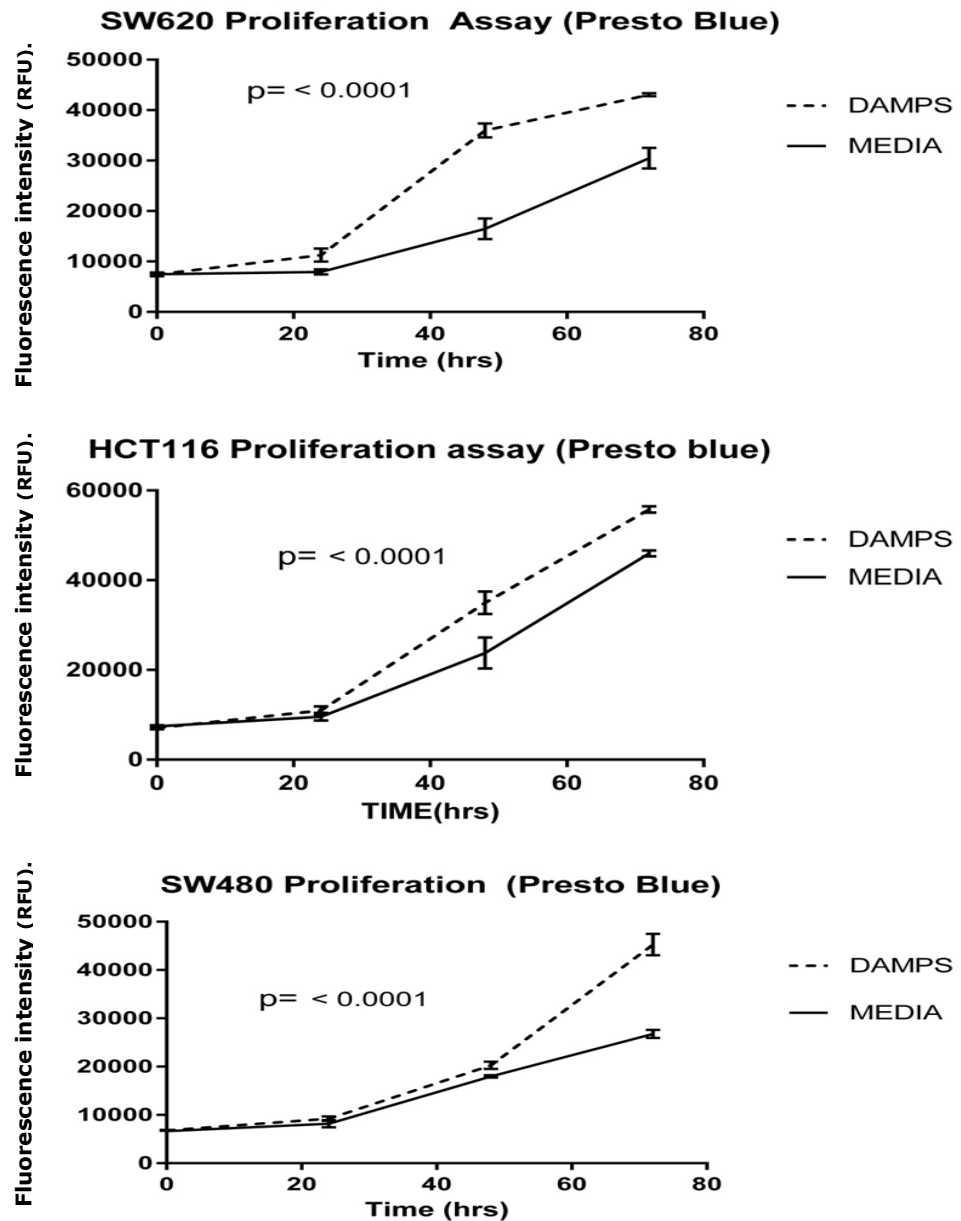


Figure 24: DAMPs induce significant increase in cellular proliferation.

Effects of DAMPs on cellular growth were assayed by Presto Blue method. Three cell lines (SW620/SW480/HCT116) were exposed to autologous DAMPs and cell proliferation was measured at $t=0$, 24, 48 and 72 hrs and compared with media alone. The fluorescence intensity was measured at 530 nm (excitation wavelength) and 590 nm (emission wavelength). There was a significant difference ($p \leq 0.001$) in proliferation between cells exposed to media versus DAMPs but regardless of CD24. The experiment was repeated and was performed in triplicate but showed same results. Data were analysed by Graph Pad prism6 using Two way ANOVA Test, comparing each time point.

Discussion:

There are many types of lethal pathological insult that can cause cell necrosis and spillage of cellular contents into the extracellular environment. In order for damaged tissue to be repaired, new cells must proliferate and migrate into the damaged area in order to replace the damaged tissues. It is not unreasonable therefore to conjecture that DAMPs may play a role in regulating the healing response. Whilst DAMPs have been studied in lymphoid and dendritic cells, the effect of DAMPs on epithelial cells has been relatively ignored.

Given solid tumours are marked by frequent necrosis and current research underscores the significance of tumour microenvironment in tumour progression and survival, some recent studies have explored the effects of DAMPs on mesenchymal stem cells and enterocytes. But none of the studies have explored if dying cancer cells could signal back to the autologous cancer cells.

In this study, therefore, we sought to examine the effect of DAMPs on autologous epithelial cell proliferation and motility. While most of the studies on DAMPs have used a single molecule as a representative of DAMPs (most commonly HMGB1), in our study, we used whole cell lysates as this is more reflective of the milieu found in tissue damage.

Both CD24 and DAMPs are believed to be increased in inflammatory bowel disease and the colorectal tumour microenvironment. We speculated firstly if DAMPs have any direct effect on epithelial cell proliferation and secondly if this effect is mediated through CD24 based on the fact both have been linked to cell proliferation in recent literature (56, 84, 85). Cell lines with different CD24 expression levels were tested for effects of DAMPs on cellular proliferation i.e. SW620 (high expresser of CD24), HCT116 (very low expresser) and SW480 (negative for CD24). We found that proliferation was significantly increased in all three cell lines using the Presto Blue proliferation assay. This assay allows measurement of cell proliferation over repeated time points in the same wells. And the proliferation shows a marked increase compared to untreated controls with increasing time **Figure 24.**

Pistoia *et al.* have also shown an increase in proliferation of mesenchymal stem cells (**MSCs**) by DAMPs and they proposed these MSCs in turn increase epithelial cell proliferation (84), whereas, we have found that DAMPs can directly stimulate cell proliferation as well. Our findings are quite similar to a very recent study by Kang *et al.* They also found increase in proliferation of pancreatic tumour cells by direct exposure to DAMPs (86).

However as our experiments showed increased cell proliferation in both high expressing and negative cell lines for CD24, it seems the effect is not mediated via this molecule and may quite be through RAGE or Toll like receptors.

Regarding effects of DAMPs on cell motility, intuitively we had expected DAMPs to stimulate cell motility. However our data, obtained in four different cell lines and using 2 different types of assays (i.e. transwell migration and wound healing assays), have unequivocally shown that, in fact, DAMPs inhibit epithelial cell motility. We have also shown that both general motility and chemotaxis are affected and that these effects are mediated through down-regulation of molecules such as Snail, N-cadherin and Cten whilst there was slight up-regulation of E-cadherin. These molecules are involved in epithelial–mesenchymal transition (EMT) and thus altered expression of these molecules raises the possibility of mesenchymal to epithelial transition (MET) as a consequence of DAMP activity. Our data are supported by procedure Dai *et al.* who showed that HMGB1 could inhibit cell motility and chemotaxis in enterocytes through TLR4 signalling which (which in turn led to increased focal adhesions (74).

Many studies of the effects of DAMPs in leucocytes have shown that they act as chemo-attractants and that they stimulate cell migration (39, 68, 86, 87). Thus, it would seem that DAMPs act

to attract inflammatory cells to a site of injury whilst repelling immigration of epithelial cells. It may be that, in the former case, the attraction of inflammatory cells helps to maintain the inflammatory reaction and limit the damaging stimulus. Inhibiting epithelial cell motility will delay healing but the DAMPs may be acting as signals which indicate that the context is not yet correct for healing to occur.

We also found that the inhibitory effect of DAMPs on colonic epithelial cells was independent of CD24. Migration in cells not expressing CD24 was inhibited and knock down of CD24 in SW620 (which expresses high levels of CD24) did not prevent the inhibition of motility. Thus, CD24 does not appear to modulate cellular response to DAMPs in these cells in direct contrast to immune cells in which CD24 is thought to inhibit TLR activity and suppress inflammation. We reasoned that in contrast to the experiments of by Chen *et al.* (41) we were trying to explore the epithelial cells (colorectal carcinoma cell lines) which may have quite different glycosylation patterns and surface expression of molecules as compared to immune cells and hence different interactions and signalling outcomes. It may be possible that epithelial CD24 does not interact with DAMPs and the results of Chen *et al.* may be specific to immune cells. Another reason for this lack of modulation could be the absence of Siglecs in epithelial cells as DAMPs may only

interact with CD24 by forming a tri-molecular complex as shown in immune cells (88).

The reasons for our observation of high expression of CD24 in the epithelial cells in active inflammatory bowel disease remain uncertain. CD24 has been proposed to have a number of other functions such as maintenance of stemness (89) and it may be that these are the reasons for up-regulation.

In summary, we have shown that DAMPs can inhibit the motility of colonic epithelial cells possibly through the process of MET. They also affect proliferation in these cells and their activity is independent of CD24 expression. Further work is needed in order to identify the specific receptors for DAMPs in colonic epithelial cells and more sophisticated in vitro models are necessary to interrogate the relationship between the epithelium, inflammatory cells and substances in the tissue microenvironment.

Chapter Four: CD24 Signalling Partners.

Introduction:

Given its unique structure, characteristic localisation and absence of any transmembrane domain for direct signalling, CD24 is very intriguing to researchers. Little is known about the mechanisms and signalling partners of this tiny molecule.

Studies by Altevogt *et al.*, Baumann *et al.* and Sagiv *et al.* have given some insight on potential signalling mechanisms and have attempted to explore possible therapeutic strategies (8, 35, 63, 68, 90).

Signalling Partners of CD24:

In order to understand how this molecule works it is important to consider its structure, how it possibly affects nearby molecules, what are the molecules present in the vicinity and if any links between these can be found. Regarding CD24 we already know that it is heavily glycosylated and some of its interactions with its ligands are mediated via these sugars. In addition it has also been revealed that CD24 is present at specialised membrane areas called lipid rafts (also called Detergent resistant membranes DRM or Glycolipid enriched membranes GEM). These lipid rafts have special assemblies of molecules called focal adhesions. Molecular trafficking is shown to be tightly regulated at these sites with potentially significant

effects on cellular events through unknown mechanisms (33). CD24 is a major component present in the lipid rafts and recent research has presented the notion that some of the functions attributed to this molecule may be linked to its presence at these docking sites. It is proposed that functions might be orchestrated by affecting molecules present at focal adhesions (33). Here we briefly discuss some of the relevant structures and molecules that might help in understanding the signalling biology of CD24.

Lipid Rafts:

Over the last three decades, research has unveiled diversity amongst different parts of cellular membranes. Plasma membranes are now considered to be areas of dynamic assemblies of lipids and cholesterol and also harbour specialised docking sites called lipid rafts (rich in cholesterol and sphingolipids) (91). This diversity and special assemblies suggest that membrane structure could be an important contributor to cell function and pathophysiology. The involvement of these domains in diverse cellular functions (e.g. growth factor signalling and membrane trafficking) and disease processes - including cancer, autoimmunity, and Alzheimer's disease - has confirmed this potential and prompted an increased research in this area (91). CD24 being a GPI linked protein, is also shown

in recent research to be a significant contributor to trafficking across these.

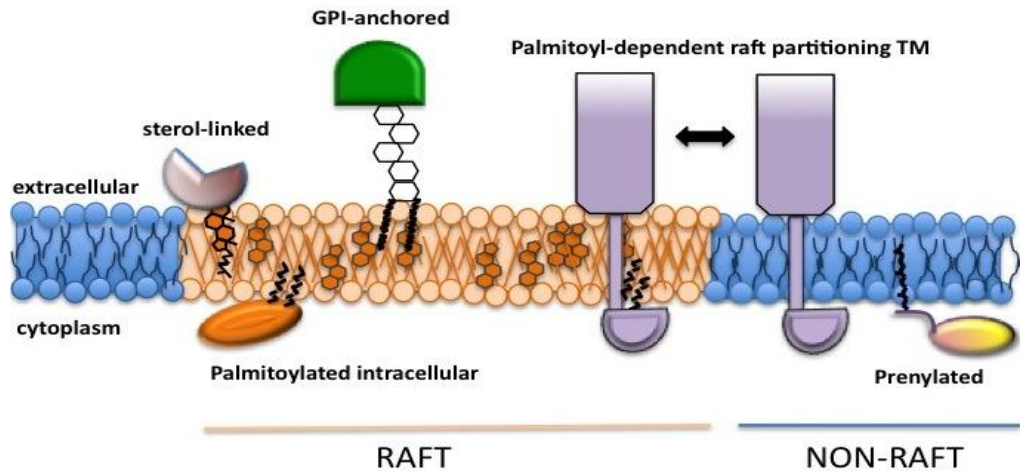


Figure 25: Schematic cartoon of lipid rafts showing GPI anchored proteins.⁽⁹¹⁾

CD24 is proposed to be “gate keeper” of these lipid raft domains. Studies have shown trafficking of certain significant signalling molecules in and out of these lipid rafts to be monitored by CD24. These include $\beta 1$ integrins (83) and CXCR in breast cancer (23, 92).

Focal Adhesions:

Focal adhesions were first identified in electron microscopic studies of cultured fibroblasts (93). These are specialised areas in the cell membranes that appear as focal plaques, dense spots or focal contacts seen on the ventral surfaces of the attached cells (93). Focal adhesions are large multiprotein complexes and they provide a structural connection between the actin

cytoskeleton inside the cell and the ECM (extra cellular matrix) components such as fibronectin and vimentin. This connection is via a family of specialised transmembrane receptors that are essential for the formation of focal adhesions and are known as Integrins (94).

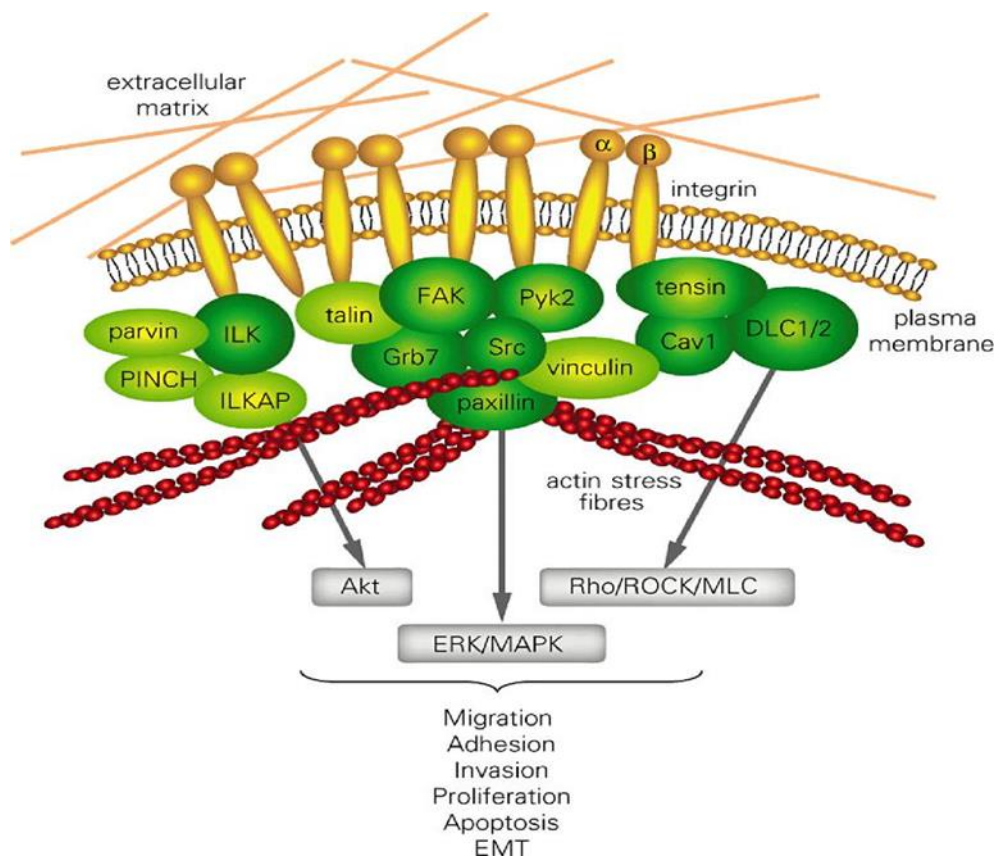


Figure 26: Schematic diagram illustrating a focal adhesion complex.

Focal adhesions provide the transmembrane link between the extracellular matrix (ECM) and the actin cytoskeleton. Integrins are transmembrane heterodimeric receptors composed of α and β subunits. The extracellular domain of integrins interacts with the ECM while the cytoplasmic tail binds to cytoskeletal proteins. Focal adhesions are formed by diverse molecules. Tightly ordered recruitment of focal adhesion components, assembly and disassembly of focal contacts take place during cellular motility and adhesion (95).

Studies have revealed that these Focal adhesions also modulate numerous critical cellular events, besides just providing anchorage, including signal transduction for mediating vital cellular events (96). In order to mediate a diverse range of signalling functions, focal adhesions have a special assembly of signalling molecules, including different protein kinases, phosphatases, their substrates, and various adapter proteins(93).

Quite interestingly, focal adhesions are formed at specific membrane domains called lipid rafts also occupied by CD24. As mentioned earlier, studies have indicated a role of CD24 in bringing Integrins to these lipid rafts (83). In this section of the study we will be focussing on a few more molecules associated with these focal adhesions. The aim will be to explore if CD24 mediates its role via any of these especially Cten, FAK and ILK.

Integrins:

One significant group of proteins, that are essential for maintaining the integrity of focal adhesions, are called Integrins. These are transmembrane receptors and structurally consist of obligate heterodimers. There are about 18 different types of α -subunits and 8 types of β subunits and lead to a range of receptor heterodimers that are thought to be associated with diverse and specific biological roles (97).

Integrins lack any intrinsic kinase activity. However, they have an assemblage of almost 50 proteins linked to their cytoplasmic tails including talin, paxillin, vinculin and alpha-actinin and these, in turn, interact with the actin cytoskeleton within the cell (97).

CD24 expression is shown to support rapid cell spreading and strongly induces cell motility. Using a doxycycline-inducible system to express CD24, Baumann *et al.* found that CD24 expression activates $\alpha 3\beta 1$ and $\alpha 4\beta 1$ integrins and thereby stimulates cell adhesion to fibronectin, collagens I/IV and laminins (33).

C-src:

In non-malignant cells, c-src kinase activity is tightly regulated. However many tumours are found to exhibit enhanced c-src kinase and this over expression is related to a poor prognosis. The kinase activity of c-src is known to play a significant role in the formation of focal adhesions and is shown to be through the phosphorylation of proteins such as FAK and paxillin (33).

Very recently Baumann *et al.*, has shown a significant molecular link of CD24, focal adhesion complex and intact lipid rafts in breast cancer cells. CD24-increased c-src kinase activity that led to increased formation of focal adhesion complexes, enhanced phosphorylation of FAK and paxillin. Thereby

presenting that c-src is a CD24-activated mediator that promotes integrin-mediated adhesion and invasion and this was dependent on intact lipid rafts (33).

Cten/TSN4:

C-terminal tensin-like (Cten) is a member of the tensin gene family but lacks the N-terminus actin-binding domain. Its role in tumours is not very clear as yet and both anti-tumour and pro-tumour roles have been attributed to this molecule and these roles may well be tissue specific (98).

The Cten gene translates for a complex protein which has multiple domains capable of interacting with several molecules which in turn play important roles in cell signalling. Significant domains of Cten include the Phospho-tyrosine binding domain (PTB) and Src homology domain (SH2). These domains help Cten to bind with the cytoplasmic tails of β integrin at focal adhesions and also with the proteins containing phosphorylated tyrosine residues like Focal adhesion Kinase (FAK), ILK, p130Cas and P13 kinase (99).

In colorectal cancer (CRC), up-regulation of Cten levels has been observed. Our group has found that increased expression of Cten results in increased cell migration (98). They also observed that the effect of Cten on cell migration and invasion was via modulation of downstream targets including down-

regulation of E-cadherin and induction of epithelial to mesenchymal transition (EMT) (98).

Not much is known about the regulation of Cten and our lab has already proposed EGFR_Kras-Cten signalling to be one of the pathways mediating this molecule. However this may not be the only loop regulating Cten (100). Many features indicated towards a potential link between Cten and CD24. Both Cten and CD24 are associated with increased cellular motility, invasiveness and adhesion. Akin to CD24, Cten is also upregulated early in the adenoma carcinoma sequence. Moreover, downstream targets for both molecules appear to be similar. As mentioned above, Altevogt *et al.* showed CD24 to be regulating c-src and FAK as well as STAT3 (101). Comparable effects by CD24 on STAT3 were observed by Lee *et al.* indicating STAT3 was activated by CD24 via NANOG (102). On the other hand a recent study by Barbieri *et al.* has proposed STAT3 to be upregulating Cten and mediating increased tumour migration and invasiveness (102, 103). Once again pointing towards a potential signalling link between CD24 and Cten.

FAK:

FAK (Focal adhesion kinase) is a 125 kDa non-receptor and non-membrane associated protein tyrosine kinase (PTK) discovered in the 1990s. It interacts with the cytoplasmic tails of Integrins

as well as other members of the focal adhesion protein complex such as paxillin (104-106). It is believed to be involved in many critical cellular events including adhesion, migration, proliferation and survival. It has been shown that FAK is over-expressed in invasive and metastatic colon tumours at both the protein and the mRNA levels (107). The expression and phosphorylation of FAK have been shown to correlate with more invasive tumour phenotype by virtue of inducing epithelial to mesenchymal transformation. In addition, some studies have linked FAK and the response of tumour cells to chemotherapy (108). Studies have also shown regulation of FAK by CD24. Baumann *et al.* have shown very recently (2011) that although the total FAK protein levels remain the same after upregulation of CD24, phospho-FAK is increased along with augmented c-src kinase activity in breast cancer cells (33). We explored this relationship between CD24 and FAK to see if CD24 mediated cell motility was linked to FAK, by creating experimental conditions with high CD24 and simultaneously knocking down FAK protein.

ILK:

Integrin linked kinase (ILK) was discovered in 1996 and as the name suggests it is linked to the cytoplasmic tail of $\beta 1$ and $\beta 3$ integrins. Quite similar to FAK, the presence of ILK at focal

adhesions allows it to play an essential role in the transduction of many biochemical signals that are triggered by cell-ECM interactions. These signals modulate diverse biological events, including cell survival, differentiation, proliferation, migration, invasion and angiogenesis (109-111).

It has been found that the C-terminal domain of ILK also interacts with actin-binding adaptor proteins, such as paxillin and parvins, which interact directly with the actin network, allowing ILK to bridge the effects of growth factors and extra cellular matrix (ECM) through growth factor receptors and transmembrane integrins to the actin cytoskeleton. This helps to regulate cytoskeletal re-organisation and cell migration processes (94).

It has been found that ILK expression correlates significantly with tumour invasion, grade and stage, in colorectal carcinomas and many other malignancies, suggesting a role in tumour progression. It has also been described that ILK expression correlates with stimulation of the Akt pathway, down-regulation of E-cadherin and activation of β -catenin in human colon cancer (112-114). We explored this molecule regarding mediating CD24 associated motility.

Material and methods:

Co-transfections :

In order to assess the downstream signalling partners of CD24, we employed a system of simultaneous co-transfection of a CD24 expression vector together with a siRNA targeted to the gene of interest. This would be done in a cell line which is a low-expressor of CD24 and would be followed by analysis of cell motility. In theory, forced expression of CD24 will induce cell motility and, if the gene of interest was important in mediating this function, then knockdown of that gene with siRNA should result in loss of cell motility. We tested Cten, ILK and FAK as potential mediators of CD24-induced cell motility. Changes in protein levels were confirmed by western blots. Appropriate internal controls were used in each experiment.

Briefly, 2×10^5 cells were seeded in 2ml DMEM media with 10 % FBS and antibiotics (PS 1%) in 6-well plates. Cells were allowed to adhere for 24 hours prior to transfection. Cells were transfected when confluence reaches between 50-60 % at the time of transfection. The medium was aspirated and cells were washed with PBS and 1.5ml Opti- MEM®I was added to the cells one hour before transfection. For each co-transfection sample, oligomer-Lipofectamine® 2000 complexes were prepared as per manufacturer guidelines (tabulated below). 100 pico-mol siRNA

oligomer for knock down and 4.0µg/well pcDNA 3.1CD24 plasmid (**see Appendix iii**) for forced expression were diluted simultaneously in 250µl Opti-MEM® I Reduced Serum Medium and mixed gently. 8.5µl (up to 15ul for some genes) of Lipofectamine® 2000 was added to 250µl Opti- MEM® I, mixed gently and incubated for 5 minutes at room temperature. After 5 minutes, the diluted oligomer/plasmid mixture was combined with the diluted Lipofectamine® 2000, mixed gently and then incubated for 20 minutes at room temperature. The oligomer/plasmid-Lipofectamine® 2000 complexes were then added to each well containing cells and Opti- MEM® I (to make a final concentration of 50nm of the siRNA duplex), and mixed gently by rocking the plate back and forth. The media was changed after 7 hours by 2ml of DMEM medium (with FBS 20 % and PS 1%), plates were incubated at 37°C in 5% CO₂ incubator. siRNA Luciferase and pcDNA3.1 plasmid were used as controls for co transfection. Forty eight hours later, transfected cells were

- (1) harvested for protein extraction and western blot.
- (2) used directly for the relevant functional assays.

Table 7: Timings of Media Changes during co-transfections.

Media changes during co transfections		
1	Seeding the cells.	Full media (10% FBS in DMEM with 1%pencillin and streptomycin).
2	1hour before transfection.	Opti-MEM® I.
3	4-7 hours after transfection.	Full media prepared with 20% FBS.

Table 8: scaling concentrations for transfection components

Culture vessel	Vol. of plating media	Vol. of dilution media	DNA	Lipofectamine® 2000	siRNA
96 Well	100µl	2 x 25µl	0.2µg	0.5µl	
24 Well	500µl	2 x 50µl	0.8µg	2.0µl	
12 Well	1ml	2 x 100µl	1.6µg	4.0µl	
6 Well	2ml	2 x 250µl	4.0µg	10µl	100pmol
60 mm	5ml	2 x 0.5ml	8.0µg	20µl	
10 cm	15ml	2 x 1.5ml	24µg	60µl	

Calculations for Forced expression and Knock down:

Manufacturer's recommendation for DNA in a 6 well plate is 4 μg / well of the plasmid.

- a. pcDNA3.1 (Empty Vector).
- b. pcDNA3.1-CD24 (Vector for CD24).

Manufacturer's recommendation for siRNA in a 6well plate is 100pmol / well.

- c. si RNA luciferase 1ul/well.
- d. siRNA cten 10 μl /well.
- e. siRNA ILK 10 μl /well.
- f. siRNA FAK 7.5 μl /well.
- g. siRNA CD24 5 μl /well.

Table 9: Plate set up for co transfections using CD24 and Cten.

Control well	CD24 F/E	CD24 F/E WITH Cten KD	Cten KD
pcDNA3.1empty vector + siRNA luciferase	pcDNA3.1CD24 + siRNA luciferase	siRNA Cten + pcDNA3.1CD24	siRNA Cten + pcDNA3.1Empty vector

Table 10: Plate set up for co transfections using CD24 and FAK/ILK.

Control well	CD24 F/E	CD24 F/E WITH ILK KD	CD24 F/E WITH FAK KD
pcDNA3.1empty vector + siRNA luciferase	pcDNA3.1CD24 + siRNA luciferase	siRNA ILK + pcDNA3.1CD24	siRNA FAK + pcDNA3.1CD24

Table 11: Sequence of siRNAs used in co transfections and knock down.**Cten NM032865**

L AAGAGUAACUGUACCACGAGACCCG

R UUCUCAUUGACAUGGUGCUCUGGGC

ILK NM004517.2

L UUCUCCGUGUUGUCCAGCCACAGGC

R GCCUGUGGCUGGACAACACGGGAGAA

FAK NM005607

L GAUGUUGGUUUAAGCGAU

R AUCGCUUUAACCAACAUC

CD24 NM013230

L ACCACGCUUAGUUAUGACCUACGAA

R UUCGUAGGUCAUAACUAAGCGUGGU

Universal non targeting siRNA

L CAGUGUAGUAGUCGUUUC

(Luciferase specific)

R GAAACGACUACUACACUG

Co-Immunoprecipitation:

SW620 Cells from confluent flasks were trypsinized by adding 2ml of Trypsin /EDTA for 5minutes to each flask, re-suspended in 8 mL of Dulbecco's modified Eagle medium (DMEM) with 10% foetal bovine serum (FBS) and 1% penicillin/streptomycin (P/S).The suspension was centrifuged at 17,000xg. at room temperature for 5 minutes . The resulting cell pellet was washed with 1 mL phosphate-buffered saline (PBS) and the suspension was centrifuged at 17,000xg. at room temperature for 5 minutes.

PBS was aspirated and the pellet was treated with ice-cold lysis buffer (100 μ L RIPA buffer and 1 μ L Halt™ Protease & Phosphatase Inhibitor Cocktail (100x), Thermo Scientific) for 15 minutes. It was then centrifuged at maximum speed (17,000xg.) at 4 °C in BIOFUGE fresco machine. The supernatant (WCE= whole cell extract), was collected in eppendorf tubes and stored at -20°C.

Preclearing of cell lysates was done by adding 20 μ l of suspended Protein A/G-agarose beads (Calbiochem) and Incubating at 4°C for 30 minutes followed by centrifugation at 8000xg. for 5 min at 4°C to remove the beads with non-specifically bound proteins. Calculated by protein assay, 1mg of protein per IP was incubated with 2ul of CD24 antibody at 4 °C overnight.

The GFP antibody (iso-type control) and 10% sample input were used as negative and positive controls respectively. Then 20 μ l of protein A/G beads were added to the negative controls and sample tubes only and incubated for 2 h at 4°C. Beads were precipitated by centrifugation at 8000xg. for 5 min at 4°C and washed 3 times with lysis buffer or PBS (less stringent). Laemmli buffer was added and beads were heated at 90°C for three minutes and then spun for 1 minute at full speed (17,000xg).

After elution, the immunoprecipitates were run on SDS- PAGE gel (Bio-Rad Catalogue # 1611159, 4–20% Ready Gel® Tris-HCl Gel, 10 well, 50 μ l) and transferred to PVDF membrane by semi-dry technique (8volts for 1hour). The membrane was then western blotted using primary antibodies against Cten (1:1000 and also tried 1:500) and SWA11 for CD24. The secondary antibody was a horseradish peroxidase-linked secondary antibody (Sigma Aldrich) anti-mouse IgG raised in goat. As a loading control β -actin (1: 2000) was used (**see Table 6**).

The co-immuno-precipitated proteins were visualized with Enhanced Chemi-luminescence detection kit (Super signal West Pico Chemiluminescent Substrate, ThermoScientific, UK) and exposure to X-ray film (Kodak UK). To assess if the increased Cten after upregulation of CD24 was due to augmented Cten transcription. A qPCR was also performed on the cDNA,

extracted 48 hrs after transfection with CD24 expression vector in HCT116 cell line (Chapter 2: Materials and methods).

Cyclohexamide assay (CHX assay):

Cyclohexamide (CHX) is an inhibitor of protein biosynthesis in eukaryotic organisms. Cycloheximide interferes with the translocation step in protein synthesis (movement of two tRNA molecules and mRNA in relation to the ribosome) Treating cells with Cyclo-hexamide in a time-course experiment followed by Western blotting of the cell lysates for the protein of interest can give clues about its half-life. This is a helpful tool as it removes the new protein formation. And the decrease in protein levels with each passing time point indicates degradation. The difference in the protein levels amongst CD24 transfected +CHX and control groups (transfected but no CHX) will be compared and if CD24 functions by reducing degradation of Cten, leading to improved Cten levels after transfection, it will be unaffected by CHX addition over the time points, whereas if increased Cten levels were due to increased production, the CHX treated wells will show lesser amount of protein compared to the non CHX group. Hence using CHX assay and qPCR we tried to explore whether it is increased production or reduced degradation of Cten by CD24 that leads to increased Cten levels.

After 48 hours of forced expression with a CD24 expression vector, (according to protocol mentioned in materials and methods) Cells were divided into two groups and one group was exposed, to 100µg/ml cyclohexamide (from Sigma) for three time points 0, 8, 16 hours. Cell pellets were harvested at each time point and frozen for western blot confirmation later using both from cyclohexamide (CHX) exposed and media exposed control group. Western blots were performed SWA11 and Cten antibodies as per mentioned protocol in materials and methods chapter.

Results:

CD24 levels were modulated by either by ectopic expression of CD24 in cell lines with low CD24 expression (HCT116, RKO) or gene knockdown by RNA interference in cell lines with high CD24 expression (SW620,DLD1, GP2D).

Western blotting was used as a way to check the transfection efficiency and to confirm expression of the protein. The right size protein band ranging from 25kDa to 75kDa as well as having characteristic smeary pattern was detected using SWA11 antibody (detects the protein backbone of CD24) in all cell lines used.

Verification of CD24 expression by plasmid vector:

Upregulation of CD24 protein expression was confirmed by western blot, 48 hours post transfection of CD24 - pcDNA3.1. expression plasmid into HCT116 cells (using Lipofectamine 2000[®] based forced expression technique as described earlier in the material and methods chapter (**Figure 27**)).

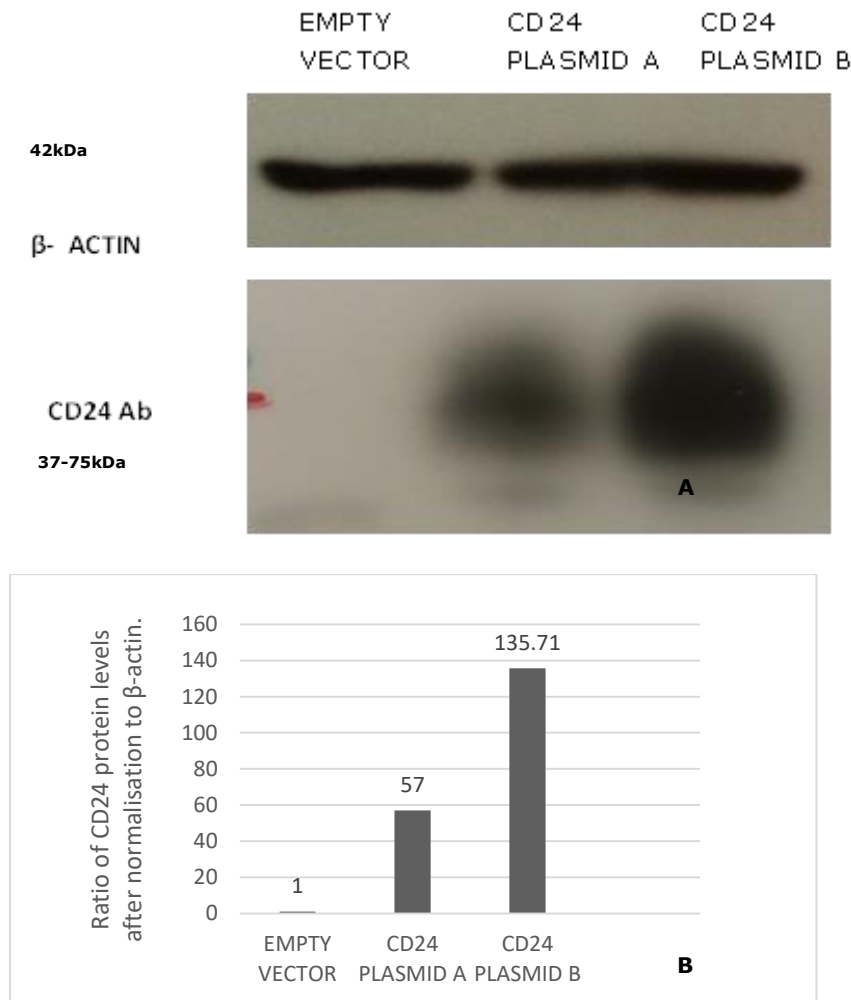


Figure 27: Selection of CD24 expression vector.

In order to assess the efficacy of our CD24 expression vector (CD24-pcDNA3.1), transfection was performed in HCT116 cell line. PcDNA3.1 Empty vector (annotated as Empty Vector) was used as vector control. Western blot was performed using Anti-CD24 antibody clone SWA 11. The house keeping protein β-actin was used as protein loading control. Both CD24 plasmids used (A, B) gave typical smeary pattern characteristic of CD24 protein ranging 25kDa to 75kDa (A). For further transfections and co-transfections CD24 plasmid B was used as it lead to better expression under similar conditions compared to plasmid A, although both lead to increased CD24 expression compared to empty vector. Densitometry bar graph (B).

The level of ectopic CD24 expression after transient transfection in HCT116 cells was compared to endogenous CD24 expression in SW620 cells by western blot analysis. We found a strong expression of CD24 after transfection that was similar to endogenously expressing cells. Upregulation of CD24 resulted in increased Cten protein **Figure 28**.

To further validate this regulation of Cten by CD24, SW620 (high expressor of CD24) cells were used. CD24 was knocked down using siRNA for CD24 and Luciferase as negative control according to the protocol explained earlier for knock down of CD24 (Chapter 2:Materials and Methods). Protein levels were compared after 48 hours of transfection using western blots. And it was observed that knock down of CD24 protein resulted in concurrent reduction of Cten protein levels **Figure 29**.

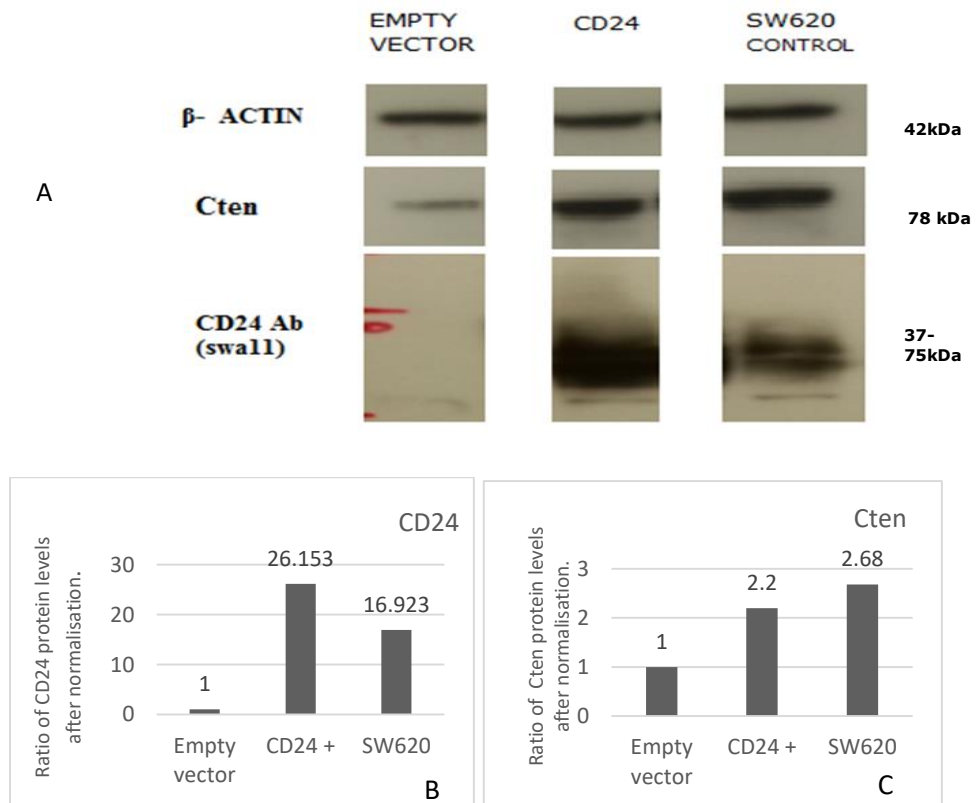


Figure 28: CD24 causes upregulation of Cten.

HCT116 was transfected with CD24 expression vector and levels of CD24 and Cten proteins were compared to empty vector (negative control) and SW620 (positive control) by western blot. CD24 forced expression resulted in increased protein levels of both CD24 and Cten compared to negative control (A). β -actin was used as protein loading control. Densitometry bar graph for CD24 protein levels (B). Densitometry bar graph for Cten protein levels (C).

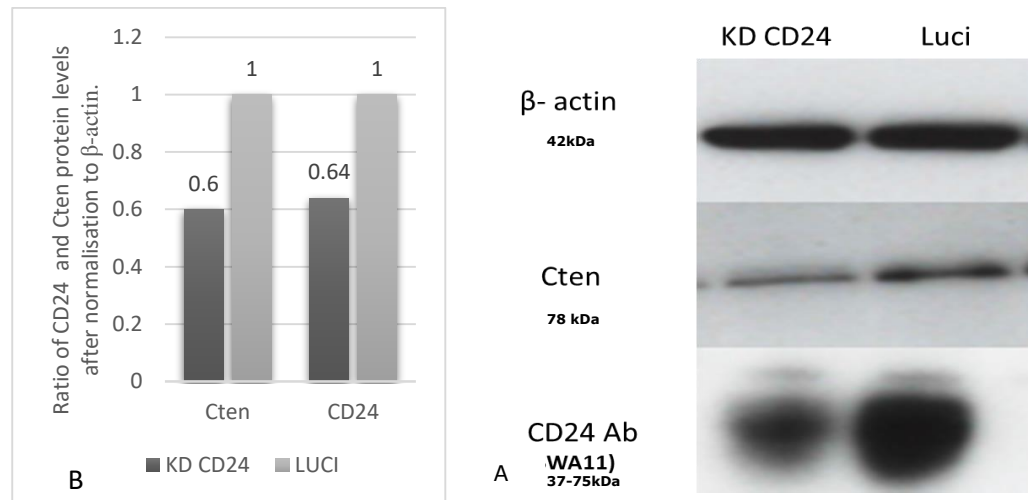


Figure 29: Knock down of CD24 causes down regulation of Cten.

In SW620 cell line CD24 was knocked down using siRNA for CD24. The expression levels of CD24 and Cten proteins in knock down wells (KD CD24) were compared to Luciferase control (Luci) 48 hours post transfection by western blot (A). β -actin was used as protein loading control. Knock down of CD24 protein resulted in decreased Cten protein levels. Densitometry bar graph for Cten and CD24 protein levels (B).

CD24 does not physically interact with Cten:

As CD24 is present in the lipid rafts and interacts with some proteins present at focal adhesions. Finding direct effects on Cten levels by up or down regulation of CD24 led us to analyse if these two molecules come in physical contact with each other as well.

In order to explore protein- protein interactions one very popular technique is co-immunoprecipitation. This experiment is performed under non-denaturing conditions. Therefore, it's a valuable tool to explore the protein interactions in near physiological conditions by virtue of keeping the post

translational modifications and conformation of proteins undisturbed by avoiding denaturation. In this technique the known protein (antigen) is termed the bait protein and the protein that it interacts with is called the prey protein.

To investigate this possibility we performed co-immunoprecipitation technique using Cten and CD24 in SW620 cell line. Input lane was used positive control for CD24. GFP (Green fluorescent protein) immunoglobulin was used as intrinsic isotype control to rule out non-specific binding of the beads. IP Cten followed by the western blot with Cten was positive control for Cten.



Figure 30: Investigation of physical interaction between CD24 and Cten proteins.

CD24 and Cten were co-immunoprecipitated from SW620 lysate. Input lane was the lysate alone (positive control). IP GFP lane was lysate with GFP Ig for isotype control (negative control). IP Cten lane was the lysate with beads and Cten Ab to pull out Cten and its attached proteins. Western blot were performed on the lysates after IP Cten using CD24 (SWA11) and showed no CD24 protein being pulled out. Western blot with Cten Ab shows Cten protein (positive control).

The presence of CD24 in the input lane indicates the presence of CD24 in the lysate, and absence of a band in IP GFP excludes nonspecific binding by the beads and antibodies, and absence of bands in IP Cten lane indicates that Cten does not IP with CD24. Whereas the presence of band in the Cten IP lane with western blot using Cten antibody indicate that the IP and the

antibodies both have worked **Figure 30**. Our lab (another PhD candidate) also performed reverse Co-IP using CD24 and Cten, however, she also could not find these two being pulled down together in reverse co-IP.

However, this still does not rule out the presence of a signalling relationship between these two molecules. As there are certain limitations of co-IP technique itself that should also be kept in mind before making any final conclusions from co-IP results about protein-protein interactions.

These limitations include.

- The affinity of the individual antibodies also varies greatly depending upon a range of factors including concentrations of proteins in lysates, avidity of epitopes, stringency of buffers etc. and may also account for absent bands besides the prey protein being pulled down with the bait protein. Using suitable controls and optimising these variables, as well as reverse co-IP helps overcome some of these limitations.
- Transient interaction between proteins may not be detected. Similarly the signals of low-affinity of protein interactions might not be detected.
- The result of co-IP could not determine whether the interaction is direct or indirect, since the possibility of involvement of additional proteins could not be ruled out.

This might be the case in CD24 and Cten interactions as well. As the signalling may be mediated through intermediate signalling partners such as c-src or STAT3 given few studies indicating that (101).

CD24 appears to signal through Cten and this is functionally relevant:

To further explore the possibility of a functional relationship between CD24 and Cten (as both appear to be mediating similar cellular properties in literature), we decided to create an experimental condition whereby CD24 was forcibly expressed in a negative cell line and Cten was simultaneously knock down. Cells were subjected to transwell motility assay 48 hours post co-transfections as described in methodology and harvested for western blot analysis.

Transwell migration after co-transfection of CD24+ / Cten-

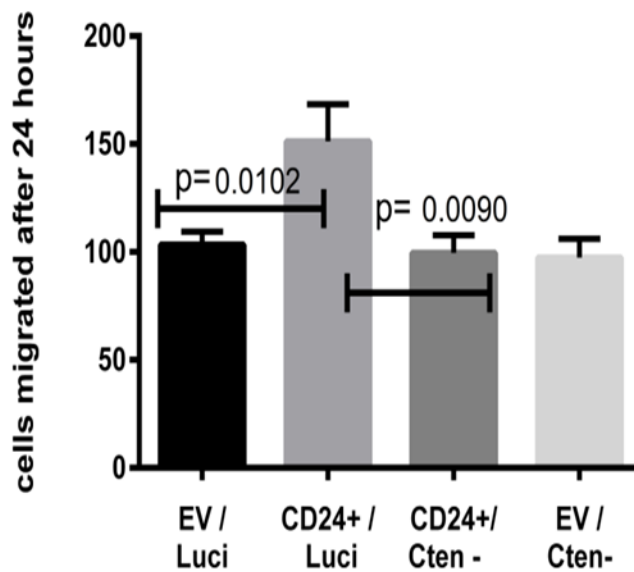


Figure 31: Transwell migration assay after co transfection with CD24 and Cten.

Transwell migration was done 48hours after the co-transfection in HCT116 and cells migrated to the bottom well were counted by direct microscopy after 24 hours. There was significant increase in cell migration as compared to empty vector and Luciferase control(EV/ Luciferase) with CD24 overexpression (Luci /CD24+). However this migration was significantly reduced by the simultaneous knockdown of Cten besides CD24 over expression(-Cten/CD24+). Similar reduction was observed with Cten knock down alone. The experiment was done in triplicate and analysed by Graph Pad prism using student T test and taking $p \leq 0.05$ as significant.

This experiment validated our previous findings of increased cell motility caused by ectopic CD24 and indicated that Cten Knock down abrogated the effects of CD24 on cell motility in colorectal cancer cell line raising the possibility that CD24 might be signalling through Cten as hypothesised.

Lysates from the above co-transfections were also subjected to western blots to confirm transfection efficiency and show changes in Cten and FAK levels. The data showed upregulation of Cten with ectopic expression of CD24. These experiments supported our hypothesis that CD24 signals through Cten and

there exists a functional relationship between CD24 and Cten as well. Indicating CD24 is upstream of Cten.

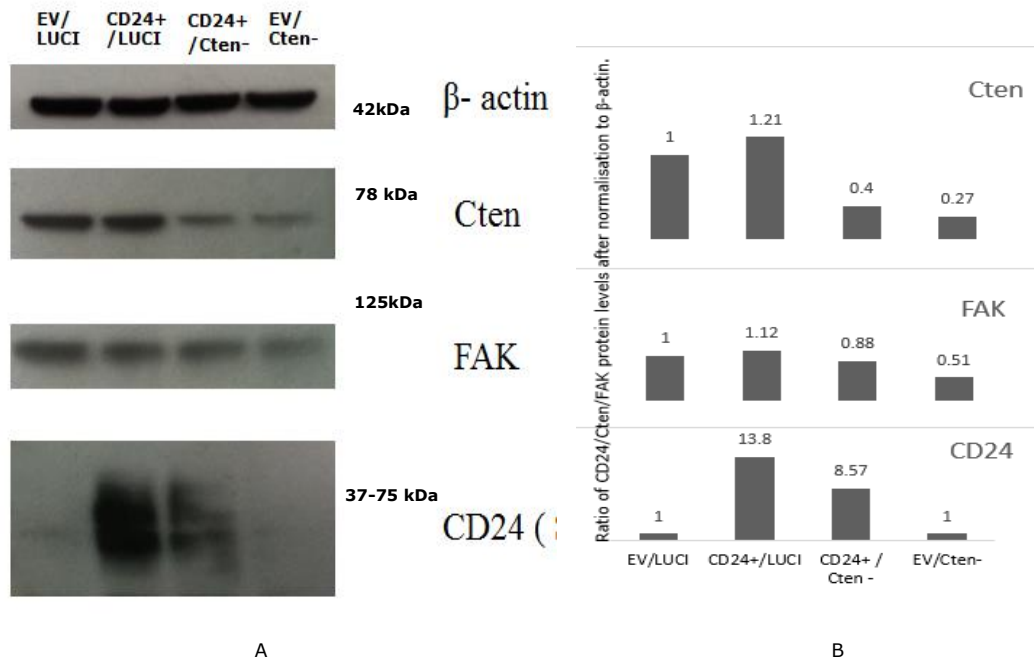


Figure 32: Western blot for co transfections.

Western blots represented in the first lane was lysate from cell co-transfected with PcDNA3.1 empty vector and Luciferase siRNA duplexes (EV/Luci) serving as control with no endogenous CD24. Next lane was transfected with CD24-PcDNA3.1 expression vector and Luciferase siRNA duplexes (CD24+/Luci) and shows increased CD24 and concurrent increase in Cten levels induced by CD24 but FAK levels appeared similar. Next set comprised of ectopic expression CD24-PcDNA3.1 and simultaneous Knock down of Cten using Cten specific siRNA and it shows reduced Cten levels as well as decreased FAK protein levels besides ectopic CD24 expression. And final set of co-transfection involved PcDNA3.1 empty vector and Cten specific siRNA (EV/-Cten). Confirming again that reduced FAK was associated with knock down of Cten and not with CD24 expression(A). Densitometry bar graph (B).

These western blots also revealed that, in agreement with other studies, total FAK protein levels remained similar after CD24 over expression. However, it appears that the down regulation of Cten by knock down reduced FAK protein, as published by our lab previously (115). These changes point towards the possibility that there may be indirect regulation of these kinases (FAK) by CD24 through Cten. Another possibility is that CD24

might not be increasing the total amount of FAK protein but augmenting its activity by increasing its phosphorylation as indicated by a study on breast cancer cells by Baumann *et al.* (33).

Results of qPCR and CHX- assay:

Our forced expression and knock down data with CD24 and Cten suggested changes of the two proteins in concordance i-e CD24 down regulation leads to reduced Cten protein levels and vice versa. The next question was what is the mechanism behind this regulation? Whether it is at transcriptional level i-e CD24 leads to increased mRNA levels for Cten, thereby increased Cten protein or this occurs at a post transcriptional level. The answer to the first possibility could be found using qPCR on the cDNA from the cells with forced expression of CD24. If the qPCR showed increased nucleic acid levels for Cten, in addition to CD24, the mechanism operating would be increased transcription of Cten.

The regulation of Cten by CD24 may well occur at a post transcriptional level i-e by increasing the half-life of Cten protein. To explore this possibility we used cyclohexamide assay on the cells with CD24 forced expression. This will stop the synthesis of new protein by the cellular machinery and hence if the protein levels of Cten still come up higher than the controls;

this will indicate that it's not the increased production but reduced degradation of Cten by CD24. If this turns to be the case it will need further exploration whether CD24 mediates this effect by increased Cten stabilisation or reduced degradation by proteasomes.

Unfortunately, the results of the qPCR analysis showed very close Ct values amongst controls with amplification even in the NTC wells. This indicated a contamination of the components of reaction mixture making the results unreliable. This required a fresh repeat of the experiment. As regards the CHX assay, as both of the proteins tested i-e CD24 and Cten were unknown for their half-life, it was found that the selected time points weren't correct, as both the proteins, did not show any significant degradation even after 24 hours. The experiment needed a re plan as well regarding time points to be tested. Unfortunately, because of personal health and serious family issues, the study was disrupted and these experiments could not be repeated.

CD24 mediates increased cell motility via FAK and ILK:

Our data above show that CD24 is a positive regulator of Cten. In addition, the data (combined with previous data from our lab) show that Cten positively regulates ILK and FAK. We therefore, hypothesized that ILK and FAK may be common

downstream targets of CD24 and that CD24 mediated increase in cell motility is mediated through ILK and FAK.

To explore this possible link we used co-transfection techniques to forcibly express CD24 and simultaneously knock down either ILK or FAK. This would create a condition whereby CD24 was present but ILK/FAK were depleted. These co-transfections were carried out in the RKO and HCT116 cell lines as both having very low expression of CD24 endogenously. The transfected cells were subjected to transwell cell migration assay to assess the effects on cell motility after 24- 48 hours post transfection. We tested whether there was any functional relevance between CD24.

The cell line HCT116 was co-transfected with ILK-specific small interfering RNA and CD24-PcDNA3.1 expression vector (denoted as CD24+/ILK-) and the number of cells migrating to the bottom of the wells were counted after 24 hours and compared with control wells (CD24+/LUCI).

It was observed that compared with cells co-transfected with control small interfering RNA (Luciferase= LUCI) and PcDNA3.1-Empty vector (EV) wells (in which neither CD24 nor ILK were altered) there was significant increase ($p=0.04$) in transwell cell motility in cells transfected with CD24 expression vector and control small siRNA Luciferase (CD24 +/LUCI), hence having

increased CD24 expression but no change to ILK) which was in accordance with previous findings.

However, the knockdown of ILK resulted in abrogation of the effect of CD24 on cell migration (denoted as CD24+/ILK-). This was similar to our previous findings with Cten and it further strengthens the existence of signalling and functional relationship between CD24, Cten and ILK. **(Figure 33).**

Transwell migration after co-transfection of CD24+/ ILK-

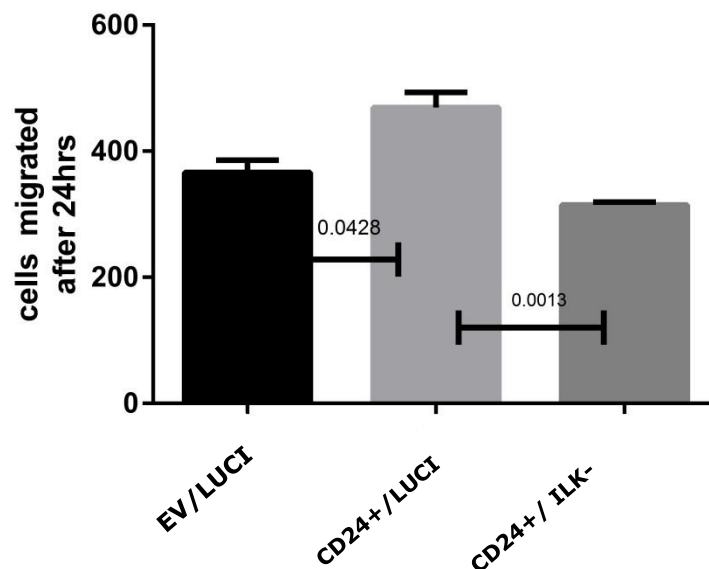


Figure 33: CD24 increases motility via ILK.

Transwell migration was done 48 hours after the co-transfection in HCT116 and cells migrated to the bottom well were counted after 24 hours. There was a significant increase in cell migration as compared to empty vector and Luciferase control (EV/LUCI) with CD24 overexpression (CD24+/LUCI). However, this migration was significantly reduced by the knockdown of ILK besides CD24 over expression (CD24+/ILK-). LUCI = Luciferase control. The p-value of ≤ 0.05 was taken as significant.

We next extended our investigation to be tested on another important signalling kinase namely Focal adhesion kinase. As this has also shown to promote cell migration and linked to play the main role in cancer metastasis either by phosphorylation and association with *Src* or interaction with *PI3K* and the adaptor molecule Grb7 as proposed by Zhao and Guan (116). As FAK is linked to integrins and *src* as well by many recent studies mediating cancer cell migration and adhesion (117). Unpublished data from our lab also found that CD24 affects the phosphorylation of FAK. We tested if there exists a functional association between the two molecules.

Transwell migration after cotransfection of CD24+ / ILK- / FAK-

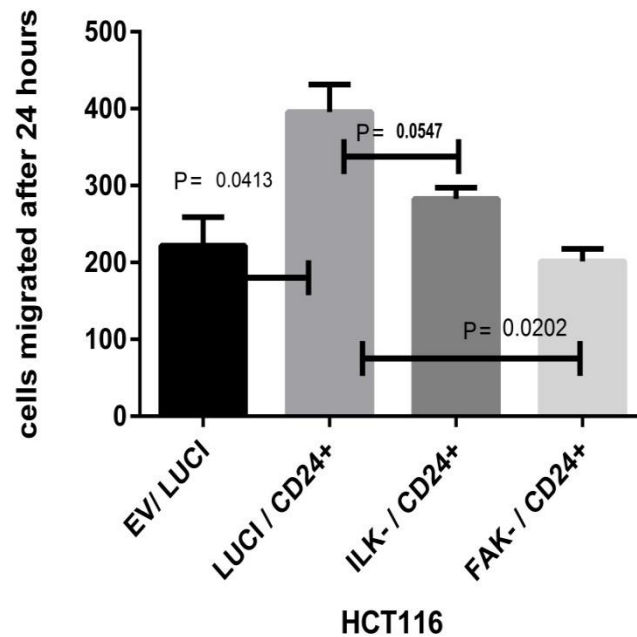


Figure 34: CD24 mediates cell motility via FAK and ILK in HCT116.

Transwell migration was done 48 hours after the co-transfection in HCT116 and cells migrated to the bottom well were counted after 24 hours. There was a significant increase ($p=0.04$) in cell migration as compared to empty vector and Scramble control (EV/LUCI) with CD24 overexpression (LUCI/CD24+). However, this migration was significantly reduced by the simultaneous knockdown of both ILK and FAK besides CD24 over expression. The experiment was done in triplicate and analysed by Graph Pad prism using student T test and taking ≤ 0.05 as significant p value. LUCI= Luciferase control siRNA. EV= Empty vector control.

Transwell migration after co-transfection of CD24+/ ILK-/ FAK-

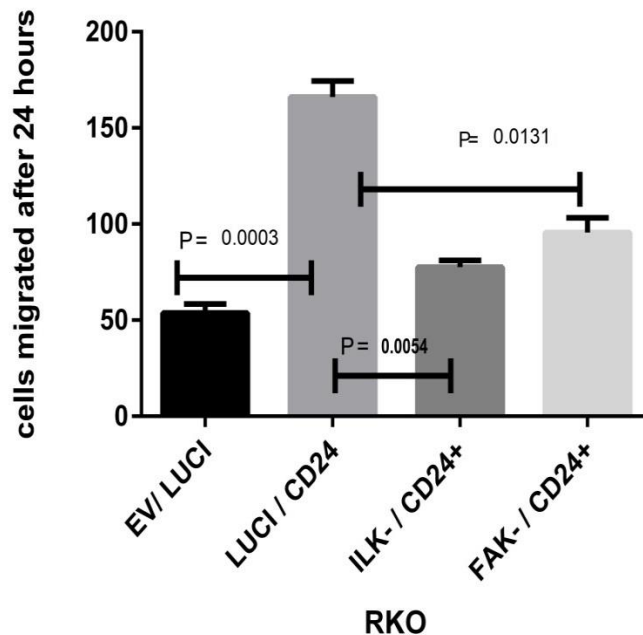


Figure 35: CD24 has a functional relationship with FAK and ILK in RKO.

Transwell migration was done 48 hours after the co-transfection in RKO and cells migrated to the bottom well were counted after 24 hours. There was a significant increase in cell migration as compared to empty vector and Luciferase control (EV/LUCI) with CD24 overexpression (LUCI/CD24+). However, this migration was significantly reduced by the simultaneous knockdown of ILK besides CD24 over expression (-ILK/CD24+). A similar reduction was observed with FAK knock down (FAK-/CD24+). The experiment was done in triplicate and analysed by Graph Pad prism using student T test and taking ≤ 0.05 as significant p value.

Co-transfections were performed as described above but including knock down of FAK and we tested these in two cell lines as shown in **Figure 34** and **Figure 35**. This was interesting to find that both FAK and ILK knockdown led to abrogation of increased cell motility by CD24, raising the possibility of a common downstream pathway from CD24 involving Cten, FAK and ILK.

Discussion:

The interaction of cells with the extracellular matrix regulates many physiological and pathological outcomes. These interactions are accompanied by the recruitment of multiple cytoskeletal and regulatory proteins to focal adhesions involved in coordinating integrin mediated signal transduction associated with cell motility, gene expression and cell proliferation(118).

It has been shown that CD24 promotes cell motility in a β 1 integrin-dependent manner and it is dependent on intact lipid rafts. It was observed in a study that blocking of β 1 integrin interaction significantly reduced the migration of the CD24-transfectants while it had no effect on the motility of the CD24-negative control cells (83).

It was also further proposed by studies that CD24 leads to activation of c-scr (33) and STAT3(101). Quite interestingly, evidence emerged for Cten to be also activated by STAT3 and c-src besides activation by EGFR and Braf-Kras pathway (103). Cten was also linked to Wnt signalling pathway (119) that has a been shown to be the regulator of CD24 by our group (unpublished data).

The presence of Cten at focal adhesions in association with integrins and focal adhesion kinases. And having similar downstream effects on cellular characteristics lead us to explore if CD24 has regulatory effects on Cten. And whether or not,

CD24 was mediating its effects on motility via Cten. Our experiments testing this hypothesis endorsed direct regulatory effect of CD24 on Cten and it has been observed in our lab that both molecules go hand in hand in cell lines i-e the cell lines with high expression of CD24 also had high Cten (DLD1 and SW620) levels and vice versa (HCT116 and RKO).

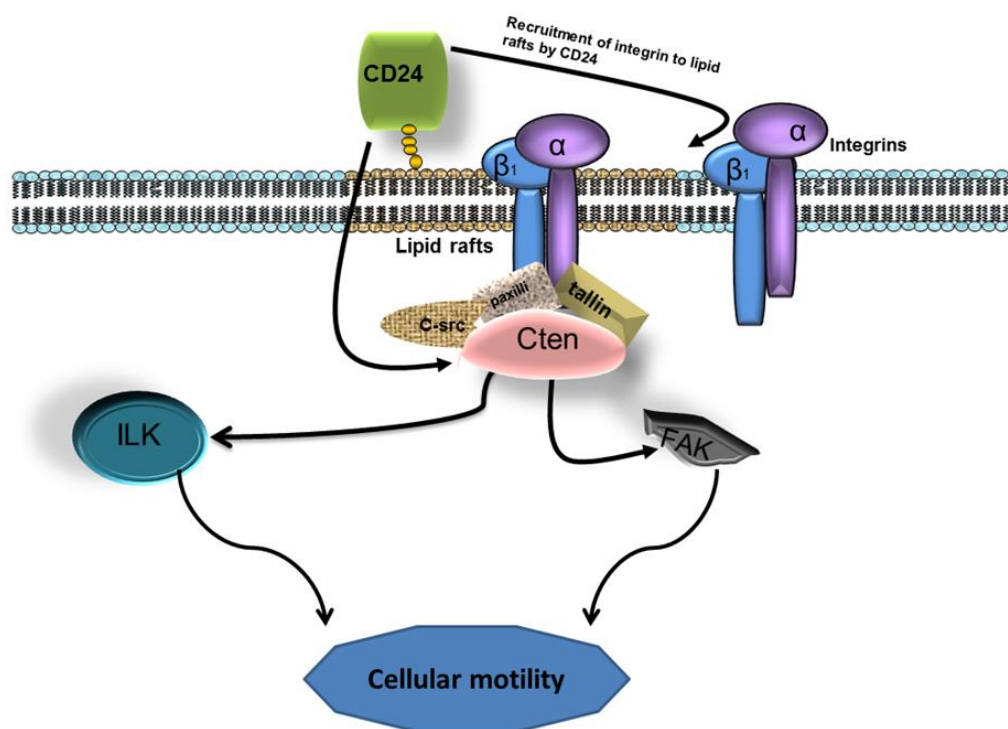


Figure 36: Schematic diagram for proposed link between CD24 and Cten/ILK and FAK.

Cell motility and migration play an important role in tumour growth and metastatic spread and overexpression of FAK seem to enhance cell migration, whereas lack of FAK expression reduces cell migration (108). Our lab already showed Cten to be mediating cellular motility via ILK and down regulation of E-

cadherin (99). This study further extends that CD24 is upstream of Cten and motility is mediated both by FAK and ILK. Whether there exists a switch between ILK and FAK remains to be elucidated.

Based on the experiments performed above and the published information in previous studies including by Baumann *et al.* (33). We propose here, that it appears that CD24 localises β -integrins to lipid rafts, also leads to phosphorylation of c-src and STAT3 (101) that in turn leads to increased Cten levels. This causes activation and phosphorylation of FAK and ILK (33, 99) resulting in increased cellular motility as observed by our transwell migration assay **Figure 36**.

Although this may not be the only signalling loop between these molecules as cellular machinery does harbour multiple interacting loops with overlaps. However, the evidence provided by the above experiments regarding CD24 and Cten regulation and the functional relationships between CD24, and FAK/ILK may also be significant contributors to the biology of these molecules.

Despite the fact that the above co transfections did show clear trends, were performed in triplicate and repeated to produce similar results by another colleague for their project, yet the absence of supporting western blots undermine the strength of our arguments and is acknowledged as a limitation. An

equipment used for western blots was working sub-optimally, resulting in the lysates from the above transfections being wasted. This part of the project was then moved on to the next PhD student due to time constraint, he also found similar results with supportive western blots not only in colorectal but as well as in pancreatic cell lines (unpublished data).

Nevertheless, the above data indicates that CD24 does not increase FAK protein levels, there is a possibility that CD24 might enhance its function by increasing FAK phosphorylation as indicated in breast cancer cell lines (33) and should be sought further.

Chapter Five: Mutating N-glycosylation sites of CD24.

Introduction:

N-Glycosylation of Proteins:

Proteins undergo a wide variety of modifications after their synthesis and that is vital for the immense diversity in their structure and function found in cellular biology. One of the most common modifications is the addition of N-glycans (the sugars, which get attached to the proteins using the Nitrogen atom, present in the **amide group** of amino acids) to the newly synthesized proteins through a process called N-glycosylation. (120).

N-glycosylation is a post- translational biochemical event in which a glycan (sugar moiety) is attached to a **Nitrogen** atom present in the amide part of the **Asparagine** amino acid. This process occurs within the endoplasmic reticulum and Golgi apparatus.

Steps of glycosylation:

O-glycosylation is also a stepwise process in which monosaccharides are first attached to the **Oxygen** atom present in the hydroxyl group of **serine** and **threonine** residues. The monosaccharides are then added to the growing oligosaccharide chain during the later stages of protein synthesis in **Golgi**(121).

The addition of O-sugars is thus, quite different from addition of GPI anchor and N-glycans to proteins, as both N-sugars and GPI anchor get attached to protein in pre-assembled form. **N-glycans** (with GlcNAc β -Asn bond), are transferred in a **pre-assembled** dolichol-linked sugar chain to protein after partial enzymatic trimming and is further extended by the addition of monosaccharides (121).

These modifications of the N-glycan in the ER comprise sequential removal of glucose and α -1,2-mannosyl residues to produce oligomannose type glycans **Figure 37**.

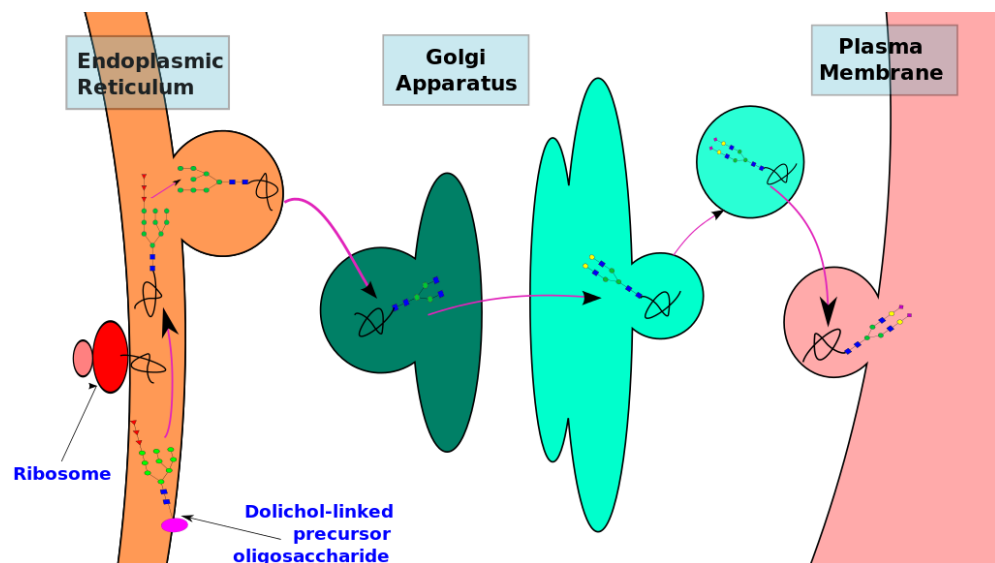


Figure 37: Steps of protein N-glycosylation⁽¹²²⁾.

Proteins synthesised in the endoplasmic reticulum are N-glycosylated by attachment of pre-synthesized Dolichol-linked sugar chain. And this chain is further modified and elongated in Golgi apparatus for further maturation.

Factors affecting N-glycosylation :

The N-glycosylation process uses the **nitrogen atom** of **asparagine** amino acid residues for attachment of sugars. The asparagine must be present in a specific Tri-peptide sequence

also called a **sequon**. The motif for N-glycosylation is **Asn-X-S/T** where S is serine and T is threonine, whereas X is any other amino acid. Studies have shown a differential influence of **X** on N-glycosylation(123). For example, proline at position X appears to be an inhibitor of N-glycosylation whereas, threonine containing sequons are more prevalent sites of N-glycosylation as compared to serine sequons. Structural factors such as primary/secondary/ tertiary structure of a protein as well as position and adjacent sequence may also affect the glycosylation of consensus sequence. Hence, proteins having **Asn-X-S/T motifs** have potential N-glycosylation sites that may have variable glycosylation or might not be glycosylated at all (123-125).

Yet another important level of regulation is by the enzymes involved in the glycosylation steps. Glycosyl hydrolases (GHs), glycosyl transferases (GTs) and nucleotide sugar transporters make up the 'hardware' of the pathway. These occur in the Golgi apparatus and are responsible for converting simple glycans like oligomannose, into a hybrid- and complex-type oligosaccharides. These glycan transforming enzymes can fluctuate amid different species, tissues and cell types and produce variable N-glycan structures. Making glycosylation a very dynamic process (126, 127). These GHs and GTs even have different substrate specificities and act sequentially. It is

also seen that these enzymes physically compete for the sugar substrate and hence this can be one additional reason of dissimilarity in glycosylation of same the protein amongst different tissues (127). Studies have linked dysregulation of these enzymes to important human diseases including oral cancer (120, 128).

Functional Significance of N-Glycosylation:

Protein glycosylation is seen in all eukaryotic cells. N-glycosylation of proteins is very significant and in some cases essential for cell viability. A multitude of enzymes are involved in this process and genes for these enzymes are fairly conserved amongst species. N-glycosylation is thought to help in important physiological processes such as folding of proteins, maintaining their stability, conformation, and localization to cellular and subcellular sites (124, 128, 129). There is growing evidence about the link between N-glycosylation regulating genes and cellular growth, proliferation and various aspects of the cell cycle (130). In addition, there are studies linking site specific N-glycans on proteins such as immunoglobulins and their function (127). However, this aspect of N-glycosylation has not been tested experimentally for most glycoproteins including CD24.

Cancers and N- Glycosylation:

All mammalian cells are decorated with a variety of sugar moieties **Figure 38** and it has been observed that changes in the cellular properties also affect these sugars. Neoplastic transformation is also found to alter the glycosylation pattern of tumour cells. Based on these observations certain carbohydrate structures have emerged as helpful tumour markers. Examples include MUC1/2, CEA, Ca19-9 etc. These glycoproteins are also being used as adjuvants in tumour diagnosis and for monitoring prognosis i-e MUC1/2 CEA etc. (131-133).

A very recent study by Valeras *et al.* 2014 linked disturbed N-glycosylation of proteins like E-cadherin as a pathogenetic factor of oral cancer. They proposed that dysregulation of DPAGT1 (an enzyme involved in N-glycosylation of proteins including E-cadherin) leads to changes in intercellular interactions and cytoskeletal dynamics (120).

Another study in 2015 by Sethi *et al.* did a comparison of the N-glycome from colorectal carcinoma tissue and adjacent non tumour tissue and found N-glycoproteins signatures specific to colorectal tumours and also associated with tumour stage (134). Similarly, Kapiro *et al.* found differences in the N-glycome of colorectal adenomas and carcinomas and even found differences in glycosylation pattern between stage I, II

and III tumours (135). Current research is investigating potential ways of utilising these specific glycomic patterns in designing less invasive diagnostic tools and therapeutic possibilities in tumours expressing them and a few studies have already shown some promising results (63, 136, 137).

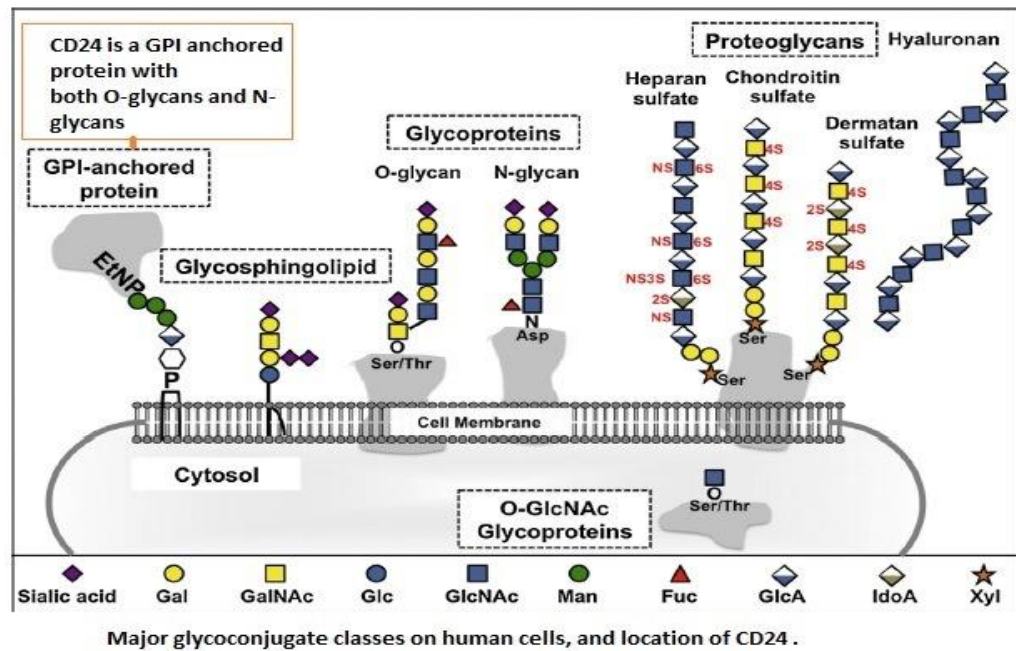


Figure 38: CD24 and common sugars on the human cell surface .Modified image (136).

A figure representing major classes of sugars displayed on the cell surface. The CD24 molecule is heavily glycosylated with O and N-sugars and it is attached to the cell membrane via another glycol-conjugate i-e GPI- anchor.

Post translational modification of CD24:

CD24 was initially thought to be a haematological differentiation marker and only expressed on immune cells and embryonic tissue. Over the past 35 years, evidence continues to mount regarding the association of CD24 with a variety of benign and

malignant diseases (7). CD24 gene polymorphisms have been linked to risk of developing and in certain cases progression of autoimmune diseases including Multiple sclerosis, SLE, autoimmune thyroid disease, Giant cell arteritis etc. (44, 46). It was also found to be related with haematological malignancies but the list of tumours with an aberrant high expression of CD24 is growing larger with each passing year, having more than 22 solid malignancies being directly linked to this small molecule (62, 88, 138, 139). Most of these studies have shown a direct prognostic relevance of CD24 expression. While other studies showing the role of CD24 in tumour progression, growth, metastasis and even to be a marker of cancer stem cells (15, 37, 49, 51, 54, 90, 140).

Over the past 30 years, most of the studies have focussed on the diagnostic and prognostic roles of CD24 but much less is still known about its exact biology, mechanism of action and signalling pathways. Poncet *et al.* analysed CD24 expression from developing human brain cells and in variety of neuronal tumours and found that expression of CD24 was transcriptionally regulated and RT-PCR showed the same transcript from various sources including haemopoietic, developing brain and tumour brain tissue. However, they found regulation at a post-transcriptional level as well. This was indicated by Western blot analysis of CD24, revealing

differential CD24 isoforms. These forms vary with tissue site (hematopoietic versus nervous), differentiation status and reflected variations in the extent of glycosylation, that is quite the case, with N-glycosylated proteins as described above (141).

CD24 is quite interesting in the sense that more than half of its weight is because of extensive glycosylation making it similar to mucins (9). It is attached to the cell surface with the help of a GPI anchor. CD24 molecule has only 31 amino-acids in mature protein but 16 potential O glycosylation sites and two potential N-glycosylation sites (25), **Figure 38**. This results in a range of molecular weights of this protein, from as low as 25KDa to as high as 70KDa. This also gives a typical smeary pattern quite characteristic of this protein on the western blot (68). The process of CD24 glycosylation takes place in the endoplasmic reticulum and continues in Golgi apparatus and finally the fully glycosylated molecule is transported to the cell surface attached to an outer leaf of plasma membrane via GPI anchor **Figure 39**.

Only a few studies have tried to explore the glycosylation aspect of CD24. One study by Ohl *et al.* compared N-glycans from mouse brain and human cell lines and found few similarities (10). In 2009 Bleckmann *et al.* used MALDI (matrix- assisted laser-desorption ionization) and ESI (electrospray ionization ion

trap) mass spectrometry analysis of the N-linked glycans of CD24 (142). They found highly heterogeneous glycans, expressing distinct carbohydrate epitopes like 3-linked sialic acid, Le^x or blood group H antigens, bi-ecting N-acetylglucosamine residues and N-acetylactosamine repeats as well as high-mannose and hybrid type species (142). The same group also did an analysis of O glycans present in murine CD24 and found important epitopes such as 3-linked sialic acid, disialyl motifs, Le^x, sialyl-Le^x or HNK-1 units. Some of these sugar epitopes have been linked to quite significant cellular properties including cell-cell interaction, adhesion, migration etc. in the current glycobiology literature (126, 143). These studies hint towards the notion that variability of CD24 glycosylation patterns could be a factor responsible for the broad spectrum of roles linked to this molecule (10, 144). To support this concept there are few examples onboard i-e this has been shown that sialyl Le^x carbohydrate is essential for the CD24-mediated rolling of tumour cells on P-selectin (7, 59). Similarly, the interaction of CD24 with L1 depends on the presence of specific glycosylation pattern (α - 2,3- linked sialic acid residues) and this interaction modulates neurite outgrowth (142). On the same note, Edwin Motari *et al.* in 2009 analysed in detail both N and O -sugars of recombinant CD24, the

glycoprotein's oligosaccharides were released by chemical and enzymatic methods before their analysis by MALDI-TOF-MS. They found Neu5Ac α -2,3/6Gal β -1,3GalNAc (sialyl-tumor antigen, sT), a cancer-associated carbohydrate, to be the most abundant sugar linked with CD24. They suggested the possibility that CD24 might be the major font of this sugar epitope displayed commonly in cancers (145). This part of the study aimed at exploring the functional significance of N-glycosylation sites present in CD24.

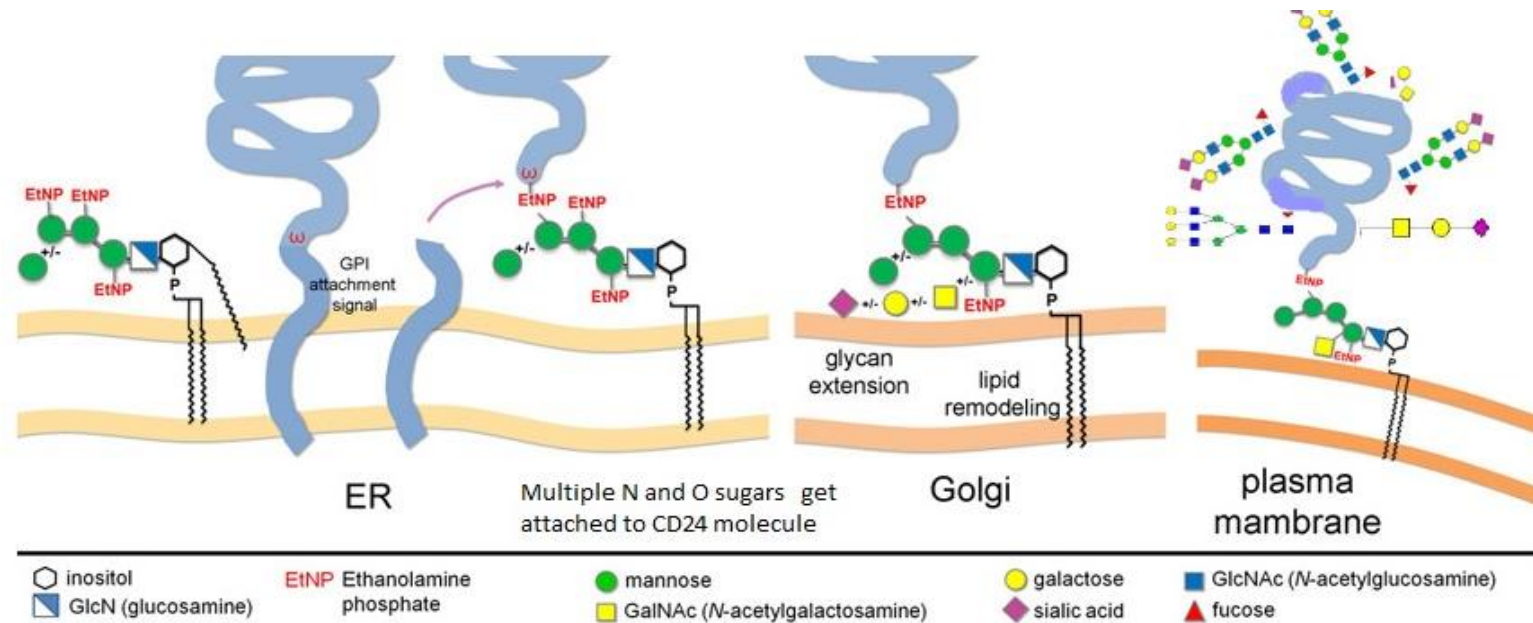


Figure 39 : GPI anchorage and glycosylation of CD24. (146)

The illustration shows main events in the maturation of CD24, a GPI-anchored protein. Acquiring GPI anchor in the ER, a process during which a signal sequence is cleaved (at a consensus omega residue) and the GPI anchor is attached via a terminal ethanolamine phosphate to the C-terminal of CD24. The protein is heavily glycosylated and modified with both O and N- glycans and the process completes in Golgi, finally localizing the mature CD24 glycoprotein to the plasma membrane (146).

Study hypothesis:

N-sugars play a significant role in mediating the biological role of CD24.

Materials and methods:

The ever-increasing quality of DNA proof-reading polymerases has facilitated numerous PCR-based approaches for mutating wild type DNA sequences. Several different approaches for site-directed mutagenesis (SDM) have been suggested and successfully established although all vary regarding primer designs and characteristics, templates used, steps needed and enzymes used etc. Their success rates depend on multiple factors in each case.

N-Glycosylation experiment plan:

The motif for N-glycosylation is **Asn-X-Ser/Thr**, where X is any amino acid except Pro, Asp or Glu (38). We decided to replace **asparagine (Asn)** of CD24 with **glutamine (Gln)**. Reasoning for selection of glutamine included the following:

- Asparagine and glutamine both are polar amino acids.
- Both are derived from acidic amino-acids (aspartic acid and Glutamic acid) having negatively charged side chains.
- Both are structurally very similar, the only difference being presence of one extra methyl group in glutamine.
- By replacing asparagine with glutamine, the N-glycosylation site will be disabled at that specific point. However, O-glycosylation sites will not be affected by

these mutations as glutamine does not bind to O-glycans (123, 147, 148).

So our aim was to mutate N-glycosylation sites of CD24 using site directed mutagenesis technique. The steps were as follows:

Step 1: Identification of potential N-glycosylation sites.

Step 2: Mutating **Asparagine (N)** with **Glutamine (Q)** using Site directed mutagenesis technique (by designing mutated primers).

ACC (Asn) -----> CAA (coding for glutamine) Gln.

AAT (Asn) -----> CAA (coding for glutamine) Gln.

Step 3: Running PCR using these mutant primers to induce mutation of N-36 and N-52 sites along with appropriate controls.

Step 4: Gel extraction and purification of PCR product.

Step 5: Dpn1 digestion of mutant PCR product to remove parental template DNA.

Step 6: Ligation of mutant PCR product.

Step 7: Transformation into E.coli for mutant plasmids to grow.

Step 8: Mini-prep and Nano-drop to obtain mutant plasmids.

Step 9: Confirmation of presence of only required mutation by Gene sequencing analysis.

Step 10: Transfection of desired mutants into cell lines to assess the effects caused by these N-glycosylation mutant sites by performing functional studies and western blot analysis **Figure 40.**

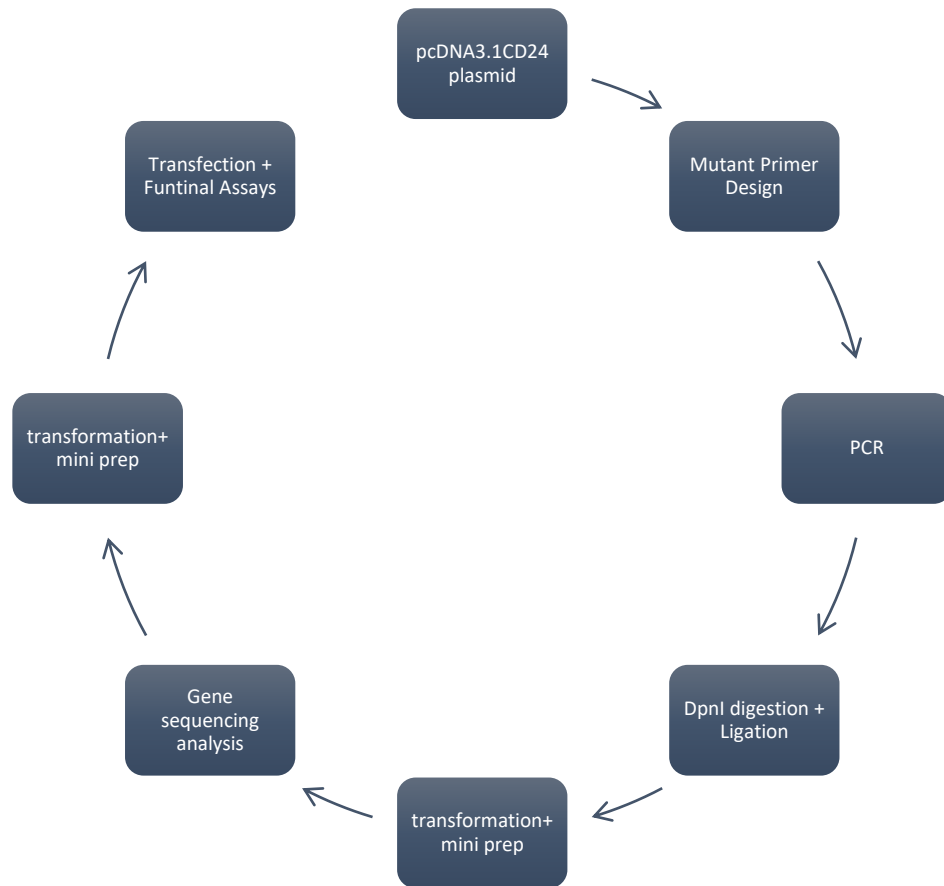


Figure 40: Flow diagram showing the experimental plan for site directed mutagenesis.

CD24 Signal Peptide:

CAGG ATG GGC AGA GCA ATG GTG GCC AGG CTC GGG CTG
 GGG CTG CTG CTG CTG GCA CTG CTC CTA CCC ACG CAG
 ATT TAT TCC AGT GAA ACA ACA ACT GGA ACT TCA AGT **AAC**
 TCC TCC CAG AGT ACT TCC **AAC** TCT GGG TTG GCC CCA **AAT**
 CCA ACT **AAT** GCC ACC ACC AAG GCG GCT GGT GGT GCC CTG CAG
 TCA ACA GCC AGT CTC TTC GTG GTC TCA CTC TCT CTT CTG CAT
 CTC TAC TCT TAA

Consensus Sequence for N- glycosylation site:

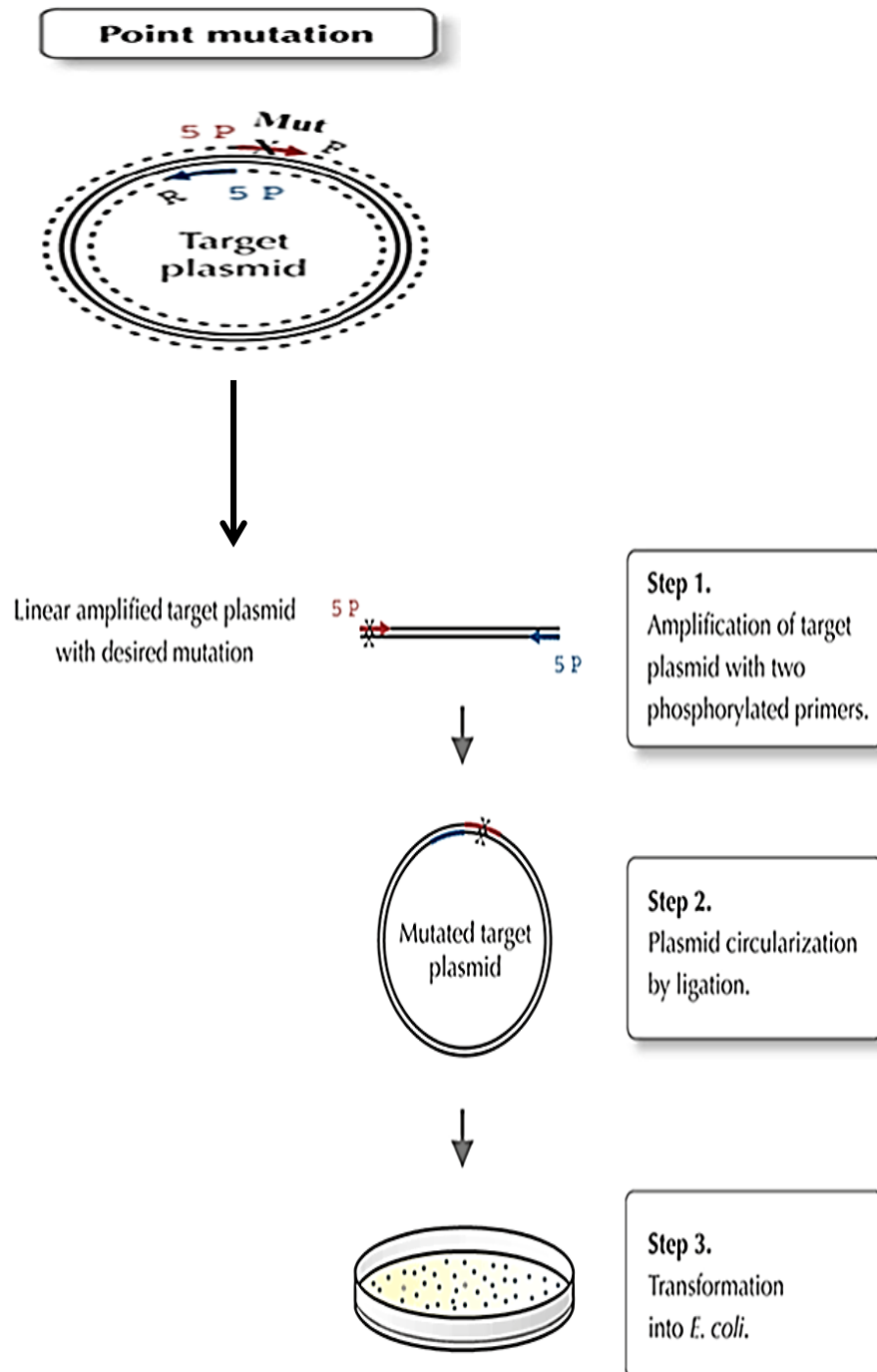
The motif for N-glycosylation is **Asn-X-Ser/Thr**, where **X** is any amino acid except Pro, Asp or Glu (38).

Table 12: Codons and the corresponding amino-acid sequence for CD24 mature peptide.

<i>ATG</i>	<i>GGC</i>	<i>AGA</i>	<i>GCA</i>	<i>ATG</i>	<i>GTG</i>	<i>GCC</i>	<i>AGG</i>	<i>CTC</i>	<i>GGG</i>	<i>CTG</i>	<i>GGG</i>
<i>Methionine</i>	<i>Glycine</i>	<i>Arginine</i>	<i>Alanine</i>	<i>Methionine</i>	<i>valine</i>	<i>Alanine</i>	<i>Arginine</i>	<i>Leucine</i>	<i>Glycine</i>	<i>Leucine</i>	<i>Glycine</i>
<i>CTG</i>	<i>CTG</i>	<i>CTG</i>	<i>CTG</i>	<i>GCA</i>	<i>CTG</i>	<i>CTC</i>	<i>CTA</i>	<i>CCC</i>	<i>ACG</i>	<i>CAG</i>	<i>ATT</i>
<i>Leucine</i>	<i>Leucine</i>	<i>Leucine</i>	<i>Leucine</i>	<i>Alanine</i>	<i>Leucine</i>	<i>Leucine</i>	<i>Leucine</i>	<i>Proline</i>	<i>Threonine</i>	<i>Glutamine</i>	<i>Isolucine</i>
<i>TAT</i>	<i>TCC</i>	<i>AGT</i>	<i>GAA</i>	<i>ACA</i>	<i>ACA</i>	<i>ACT</i>	<i>GGA</i>	<i>ACT</i>	<i>TCA</i>	<i>AGT</i>	<i>AAC*36</i>
<i>Tyrosine</i>	<i>Serine</i>	<i>Serine</i>	<i>Glutamic acid</i>	<i>Threonine</i>	<i>Threonine</i>	<i>Threonine</i>	<i>Glycine</i>	<i>Threonine</i>	<i>Serine</i>	<i>Serine</i>	<i>Asparagine</i>
<i>TCC</i>	<i>TCC</i>	<i>CAG</i>	<i>AGT</i>	<i>ACT</i>	<i>TCC</i>	<i>AAC</i>	<i>TCT</i>	<i>GGG</i>	<i>TTG</i>	<i>GCC</i>	<i>CCA</i>
<i>Serine</i>	<i>Serine</i>	<i>Glutamine</i>	<i>Serine</i>	<i>Threonine</i>	<i>Serine</i>	<i>Asparagine</i>	<i>serine</i>	<i>Glycine</i>	<i>Luecine</i>	<i>Alanine</i>	<i>Proline</i>
<i>AAT</i>	<i>CCA</i>	<i>ACT</i>	<i>AAT*52</i>	<i>GCC</i>	<i>ACC</i>	<i>ACC</i>	<i>AAG</i>	<i>GCG</i>	<i>GCT</i>	<i>GGT</i>	<i>GGT</i>
<i>Asparagine</i>	<i>Proline</i>	<i>Threonine</i>	<i>Asparagine</i>	<i>Alanine</i>	<i>Threonine</i>	<i>Threonine</i>	<i>Lysine</i>	<i>Alanine</i>	<i>Alanine</i>	<i>Glycine</i>	<i>Glycine</i>
<i>GCC</i>	<i>CTG</i>	<i>CAG</i>	<i>TCA</i>	<i>ACA</i>	<i>GCC</i>	<i>AGT</i>	<i>CTC</i>	<i>TTC</i>	<i>GTG</i>	<i>GTC</i>	<i>TCA</i>
<i>Alanine</i>	<i>Leucine</i>	<i>Glutamine</i>	<i>Serine</i>	<i>Threonine</i>	<i>Alanine</i>	<i>Serine</i>	<i>Leucine</i>	<i>phenylalanine</i>	<i>Valine</i>	<i>Valine</i>	<i>Serine</i>
<i>CTC</i>	<i>TCT</i>	<i>CTT</i>	<i>CTG</i>	<i>CAT</i>	<i>CTC</i>	<i>TAC</i>	<i>TCT</i>				
<i>Leucine</i>	<i>Serine</i>	<i>Leucine</i>	<i>Leucine</i>	<i>Histidine</i>	<i>Leucine</i>	<i>Tyrosine</i>	<i>Serine</i>				

Site-directed mutagenesis is a technique that creates a mutation at a defined site. Changes to sequence can be made using PCR by simply including the desired change in the PCR primers. The identification and construction of new commercial polymerases and advances in oligonucleotide synthesis have dramatically increased its efficiency. The protocol is briefly shown in the flow chart **Figure 41**.

Figure 41: Site directed mutagenesis flow chart:



Primer specifications for Site directed mutagenesis:

Manual Primers:

Our both mutant primer sets were designed manually keeping the following considerations. The forward and Reverse primers were back to back to each other in both cases. Following considerations were kept while designing these primers.

- Only forward primer contained the mutation (AAC/AAT→CAA).
- The mutant codon was kept in the middle of the forward primer with 12-15 bases on each side of the mutant codon to anneal with the template strand.
- GC content was between 35–65%.
- Melting temperature (T_m) between 55–65°C.
- The T_m difference between primers was limited to 2–3°C. The primer with the lower T_m dictated the annealing temperature used in the reaction.
- To avoid dimerization of primers sequences were checked for sequence homology between themselves.

We tried our best to follow as many steps we could to ensure good primer design but due to the constraints site-directed mutagenesis imposes on the location of the primers, meeting all of these parameters is not always possible.

Phusion Site-Directed Mutagenesis Kit # F-541 was used for our mutagenesis experiments with an additional step of DpnI digestion to remove template DNA.

Controls of mutagenesis:

Effective controls are an integral component of any mutagenesis experiment. The controls listed below were used to confirm each step in the process of making a site-specific mutation.

PCR controls:

Positive control— PCR containing a Template plasmid and wild type CD24 primers that would yield a wild type product was used as our positive control.

Negative controls—We used one PCR with no template DNA to be used in transformation reaction, as a back ground template control. No amplification product should be detectable. If a product is amplified, one of the reagents is contaminated and must be replaced.

We also used one PCR mix, with all of the PCR components, except polymerase. This will not produce any product and will only indicate the colonies produced by the template plasmid during transformation step.

Ligation controls:

Negative control—was a reaction containing the positive control from the PCR product and deficient in ligase. Once transformed, this reaction will offer a clue of how much background was present in the experimental reaction.

DpnI Digestion Controls:

Negative control—undigested, supercoiled plasmid and no DpnI enzyme. This reaction will not digest the template plasmid and hence the colonies will be both from template plasmid and newly synthesized products of PCR.

Transformation controls:

The following were transformed into competent cells in parallel to the experimental sample:

- PCR product positive control—Amplify the original plasmid using primers that do not introduce mutations to verify the experimental conditions will produce the expected product
- Ligation positive and negative control—The positive ligation control should have 5–100 times more colonies than the negative ligation control.
- DpnI positive and negative Control—the ratio of the number of colonies from the DpnI positive and negative control indicates the efficiency of the digestion. The negative control should have 5–100 times more colonies than the positive control.

Table 13: Primers used in our site directed mutagenesis experiments.

Gene of interest.	Primer Sequence. (All primers were purchased from Eurofins MWG-Biotech AG).	Annealing Temp.
CD24 wild type primers.	Forward primer 5'CACCATGGGCAGAGCAATGGTGG 3'	57 °C
	Reverse primer 5'TTAAGAGTAGAGATGCAGAAGAG 3'	57 °C
CD24 N-36 mutant primers. (manually designed)	Forward Primer 5" ACT TCA AGT CAATCC TCC CAG 3" (first)	Did not work
	5'ACT TCA AGT CAA TCC TCC CAG AGT ACT3'(redesigned)	63 °C
	Reverse Primer 5' TCC AGT TGT TGT TTC ACT GGA 3'	63 °C
CD24 N-52 mutant.	Forward Primer 5'AAT CCA ACT CAA GCC ACC ACC 3'	63 °C
	Reverse Primer 5' TGG GGC CAA CCC AGA GTT GGA3'	63 °C
T7.	Forward Primer 5' TAA-TAC-GAC-TCA-CTA-TAG-GG 3'	50 °C
BGH.	Reverse Primer 5' TAGAAGGCACAGTCGAGG 3'	54.8 °C
CD24 N-36 mutant. (SDM assist)	Forward Primer#15 5'CTTCAAGTCAGTCCTCCCAGAGT 3'	59 °C
	Reverse Primer#40 5' TGGGAGGACTGACTTGAAGTTCC 3'	62 °C
CD24 N-52 mutant (SDM assist)	Forward Primer#15 5` ATCCA ACTCAAGCCACCACCAAG 3`	65 °C
	Reverse Primer#40 5'GTGGTGGCTTGAGTTGGATTGG3'	65 °C

Primer phosphorylation step:

In order to phosphorylate the primers Thermo Scientific T4-Poly nucleotide Kinase (catalogue#EK0031) was used. And 250pmol of the oligonucleotide were mixed with 5 μ L of 10X reaction buffer A for T4 Polynucleotide Kinase and 5 μ L of 10 mM ATP. In the end 2 μ L T4 Polynucleotide Kinase 10 U/ μ L was added and finally water was added to make up a final volume of 50 μ L the reaction mix was incubated at 37°C for 30 minutes. T4 Polynucleotide Kinase was heat inactivated at 75°C for 10 minutes.

PCR reaction :

Mutant primers for CD24 N glycosylation sites 36 and 52 were designed manually. The amplification primer pairs shown in **Table 13** were purchased from (Eurofins MWG-Biotech AG) and subsequently diluted to a working concentration of 100pmol/ μ L. PcDNA3.1 CD24 plasmid DNA was used as our template. Above mentioned manually designed mutant primer sets were used, in a 50 μ l PCR reaction using the Phusion Hot Start II High-Fidelity DNA Polymerase (Thermo Scientific Cat. # F549L).

Table 14 shows the PCR reaction components. The Phusion Hot Start II DNA Polymerase-mediated PCR amplification reaction was performed in thermal cycler (Perkin Elmer GeneAmp PCR system 2400), and allowed to run for 37 cycles with the following cyclic conditions, one cycle of 98°C for 2

minutes (initial denaturation), followed by 35 cycle of 98°C for 1 minute (denaturation), 63°C for 30 seconds for both primer sets (annealing), 72°C for 2 minutes (extension). The final cycle was at 72°C for 10 minutes (final extension). PCR products were analysed using a 2% agarose gel to check for a single discrete band suitable for further steps. All PCR reagents, unless otherwise specified, were purchased from Roche Pharmaceuticals.

Table 14: Components and concentrations of mutagenesis reaction.

Component.	50 μ L X 1 reaction.	Final conc.
Nuclease free H ₂ O	add to 50 μ L	
5X Phusion HF Buffer	* 10 μ L	1X
10 mM dNTPs	1 μ L	200 μ M each
Forward primer**	2 μ L	250nM
Reverse primer**	2 μ L	250nM
Phusion Hot StartII DNA Polymerase II (2 U/ μ L)	0.5 μ L	0.02 U/ μ L
Template (DNA (pcDNA3.1CD24plasmid) 1ng/ μ L)	X 1 μ L	

Choice of polymerase:

The use of high-fidelity polymerases is preferred over Taq polymerase or other lower fidelity polymerases. High-fidelity polymerases decrease the number of PCR-induced errors such

as point mutations. Also, while using Oligonucleotide-directed Internal Mutagenesis technique it is essential to use a non-strand-displacing polymerase such as Phusion® (Thermo Fisher, New England Biolabs), and to avoid strand-displacing polymerases (149, 150). These two considerations were kept in mind while choosing Phusion hotstart II DNA polymerase for our mutagenesis project.

Gel extraction of PCR products:

Electrophoresed DNA was visualised under ultraviolet light and appropriate bands (5.7kb) were excised from the gel using a clean scalpel. The PCR product was then isolated from agarose gel using the QIAquick Gel Extraction system (QIAGEN, UK), following the manufacturer's standard protocol. After weighing, the excised gel fragments containing the band of interest were dissolved in 3x volumes of Buffer QG (supplied with the Kit), then incubated at 50°C for 10 minutes. After the gel slice had been dissolved completely, 1x gel volume of isopropanol (Sigma, USA) was added and mixed with the samples which were then washed with 750µl of Buffer PE (supplied with the Kit) to remove all traces of agarose and finally the DNA was eluted with 30µl of elution buffer.

Purification of PCR product:

The gel extracted PCR products was purified using QIAquick PCR Purification Kit (Qiagen) cat # 28104 according to the manufacturer's manual. In brief, one volume of PCR sample was added to 5 volumes of buffer PBI and mixed, then added to the QIA quick column and centrifuged for 60 seconds. The column was washed by adding 750 μ L of buffer PE and centrifuged for 60 seconds. DNA was eluted into a clean micro-centrifuge tube using 50 μ L of elution buffer.

DpnI Digestion step:

Add 1 μ L of DpnI restriction endonuclease (Roche cat#10742970001) to the reaction mixture to remove the original plasmid DNA. Incubate at 37°C for 30 mins.

Table 15: Components and concentrations of Digestion reaction.

Digestion Reaction.	50 μL reaction.
Restriction Endonuclease DpnI enzyme 10U/ μ L	1 μ L
10X Sure Cut buffer A(with Kit)	5 μ L
PCR product	3 μ L (1.5ug DNA)
Nuclease free Water	41 μ L

Ligation step :

To circularize the amplicon we used T4 DNA ligase (Invitrogen cat# 15224-07) and the reaction was carried out overnight at 4 °C. Heat inactivation of T4 DNA ligase enzyme was done next morning for **10** mins at **65 °C**.

Table 16: Components and concentrations of Ligation reaction.

Ligation.	10uL reaction	50uL reaction.
5 X T ₄ ligase buffer	0.5 µL	2.5 µL
T ₄ DNA ligase enzyme 100U/µL	2 µL	10 µL
PCR product	3 µL (1.5ug DNA)	3 µL
Nuclease free Water	4.5 µL	34.5

Transformation of CD24 mutants:

The mutant constructs from above reactions were transformed using NEB 5-alpha Competent *E. coli* (High Efficiency Cat# C2987P). Briefly, 10µl of above reactions were added into a vial of NEB 5-alpha Competent *E. coli* (50µl) and mixed gently, the reaction was then incubated on ice for 30 minutes, the contents of the vial were heat-shocked for 30 seconds at 42°C without shaking and were immediately transferred to ice for 5 minutes. 900µl of S.O.C. medium (Invitrogen, Cat# 15544-034) at room temperature were

added. The tube was tightly closed and shaken horizontally at 37°C for 1 hour. Tubes were spun at maximum speed for 1 minute to form a pellet and 800µl of supernatant was discarded, pellet was re-suspended in the remaining SOC medium (**see Appendix viiAppendix x**) and 50µl from each transformation reaction was spread on a LB (Luria broth) agar plate containing the appropriate selection of antibiotic to allow propagation of bacteria containing the plasmid (i.e. 100µg/ml ampicillin) and incubated overnight at 37°C. Plates with no polymerase control, undigested and un-ligated PCR products and cells alone were used as controls.

Analysing Mutants for presence of required Mutations:

24 hours after incubation on the LB agar plates, colonies were observed picked and cultured overnight in 5 ml of LB containing 100µg/ml ampicillin. The plasmid DNA was isolated from the 10 samples using the GenElute™ Plasmid Miniprep Kit (Sigma Aldrich). In brief, 5 ml of an overnight recombinant, E. coli culture were pelleted by centrifugation at 17,000xg. for 1 minute. The supernatant was discarded, and the pellet was completely re-suspended with 200µl of the re-suspension solution which is supplied with the kit. The contents were vortexed and pipetted up and down to thoroughly re-suspend the cells until homogeneous. The re-

suspended cells were lysed by adding 200 μ l of the lysis solution, and the contents were immediately mixed by gentle inversion (6–8 times) until the mixture became clear and viscous. Subsequently, the neutralization/binding solution was added to the precipitate and the cell debris was pelleted by centrifuging at 17,000xg. for 10 minutes. Column preparation solution was then added to each mini-prep column and centrifuged at 17,000xg. for 1 minute. The lysate from the cells was added to a GenElute Miniprep Binding Column and centrifuged at 17,000xg. for 1 minute. After discarding the flow-through, a 750 μ l of wash solution was added to the column and centrifuged at 17,000xg. for 1 minute. The flow-through was discarded and samples were centrifuged at maximum speed for 2 minutes. Finally, the plasmid DNA was eluted by adding 50 μ l of DNAase-RNAase free water to the column and centrifuged at 17,000xg. for 1 minute. The quantity and purity of the eluted plasmid were checked by using NanoDrop ND-1000 Spectrophotometer. A ratio of 1.8 – 2.0 was considered an indication of relative purity.

To confirm the presence of required mutations in N36 and N52 plasmids, 9 samples from each mutant plasmid DNA were sent to direct sequencing reaction. The T7 (forward) and BGH (Reverse) Vector primers were used for the sequencing.

The sequencing results were analysed using the Chromaslite software freely available at the web site http://www.technelysium.com.au/chromas_lite.html.

And Mega6 alignment software also freely available at <http://www.megasoftware.net/>

HRM technique for identification of mutants:

We also tried to detect the presence of mutant PCR products in our PCR reaction by using HRM (High Resolution Melting) that detects the presence of amplicons with different melting temperatures. As our mutant primers were not in 100% homology with the template they were expected to melt quicker than the parental DNA template similarly the hybrid products having one parental strand and one mutant strand will melt quicker compared to both wild type strands and hence giving different melting curves.

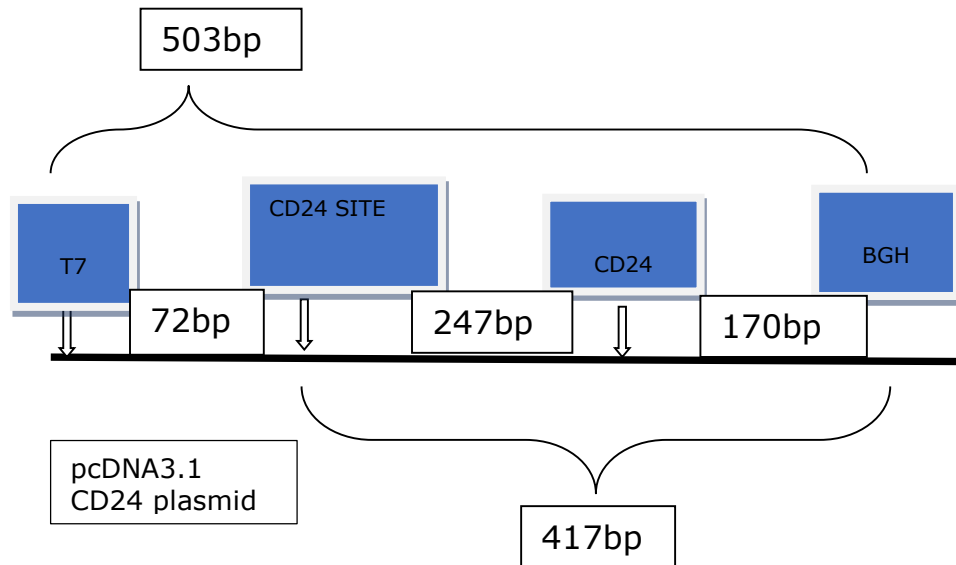


Figure 42: Diagram indicating expected product sizes using T7 and BGH primers.

Table 17 : HRM Reaction components.

Components for HRM using B7 and BGH primers 20 µl.		
	X1	X25
Hot shot master mix.	10	250
Template (mutant plasmids from mini preps).	1 µl to each	
T7 primer 250nM.	0.5 µl	12.5
BGH primer 250nM.	0.5 µl	12.5
Water.	6	150
Lc green.	2	50

HRM analysis:

As HRM best detects the products that are between 300-500bp we decided to use T7pand BGH primers and the expected product size was 503bp **Figure 42.**

The PCR reaction was in a final volume of 20 µl, which contained 1xHotShot master mix, 1 primer pair with each primer at 250 nM final concentration, 1x LC Green PLUS (Idaho Technology) and water to complete the total volume. The PCR products were transferred to Light Cycler capillaries (20 ml) (Roche).

The products were melted in the HR-1 HRM instrument (Idaho Technology) at a rate of 0.38C/s, with a starting temperature of 68C, a final temperature of 98C and fluorescence data acquisition at 70-85C°. The data had to be analysed using the HR-1 analysis tool custom software, and both derivative plots and difference plots would be generated after normalising and temperature shifting. The derivative and difference plots had to be visually inspected in order to separate out the mutants from the wild-type samples using a threshold of 4% difference in fluorescence.

Designing of new mutant primers using SDM assist software:

As our primers were manually designed and did not give us the required mutants even on repeat PCR and sequencing. We decided to redesign the primers using the specific software available for free to design the site directed mutagenesis primers. This software gave much precision and visual description of changes that are being introduced and allows the characteristics of the resultant primers to be automatically generated in a tabulated form (**Figure 43**). The features will be described in a bit detail under discussion section.

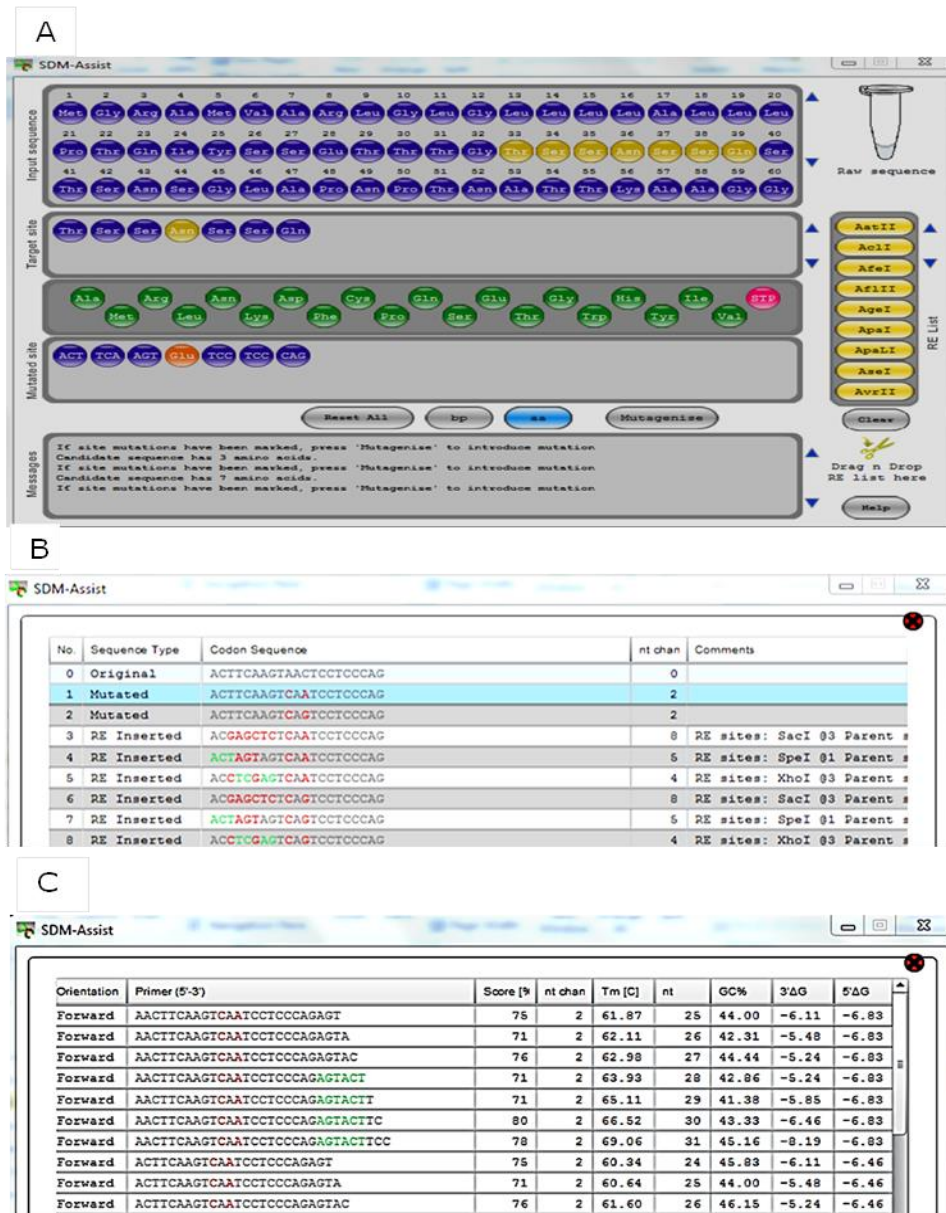


Figure 43: Screenshots of SDM-Assist while creating primers.

(A) Dragging and dropping of glutamine onto the Asparagine residues at position 36 leads to the formation of the target sequence and Pressing the “**Mutagenise**” button opens a new window (B) that includes all possible nucleotide sequences derived from replacement of Asparagine to glutamine. The table highlights the mutated nucleotides in red and resulting palindromes which create a restriction site in green. (C) The user has to choose one of the mutated sequences and presses the button “**primerise**” to get a list of potential primers and in our case we used #1 “CAA” mutation sequence to generate our primers and it gives list of possible primer sets with useful thermodynamic information both for forward and reverse possible primer sets.

Results:

The Mutant primers for CD24 N glycosylation site 36 and 52 were designed manually as described above and were purchased from (Eurofins MWG-Biotech AG). They were subsequently diluted to a working concentration of 100pmol/ μ l. The primers were phosphorylated before use.

And a temperature gradient PCR was run using a range of temperature 50C $^{\circ}$ to 70C $^{\circ}$.

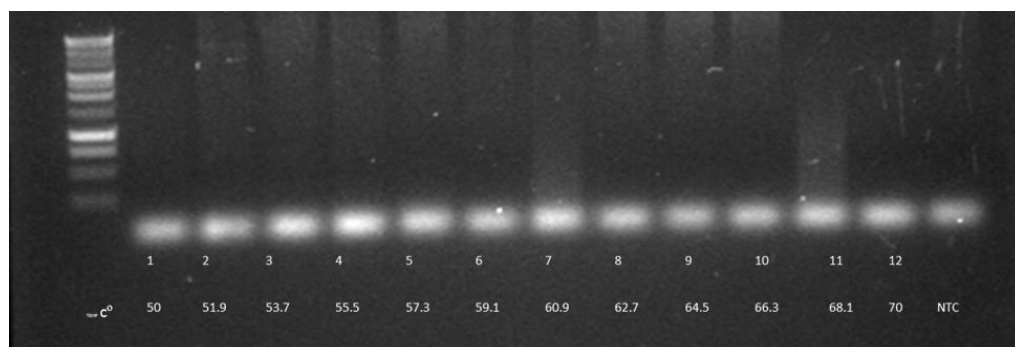


Figure 44: N36 primer optimization.

For N36 mutant primer set, in order to know the optimal annealing temperature, temperature gradient PCR (50C $^{\circ}$ to 70C $^{\circ}$) was performed and the products were run on the agarose gel. However, the gel electrophoresis showed the absence of any specific band in all the 11 Lanes and none of the tested annealing temperatures was able to produce a specific band of the correct size. Most lanes including NTC (last lane on the gel), instead showed a single band of approx. 100-150bp and most likely represented primer dimers (**Figure 44**).

As one of the reasons for no amplification can be wrong primer sequence, it was double checked for sequence homology with the template and only had one codon changed in the middle of the forward primer and the reverse primer was without any mutation. Also, primer concentration and extension temperature were all according to recommended settings.

Another important reason for PCR failure is a suboptimal concentration of $MgCl_2$ in the PCR reaction mix. To trouble shoot this possibility three additional concentrations of $MgCl_2$ were tried including 2mm, 2.5mm and 3mm final concentration of $MgCl_2$ in the temperature gradient PCR was set up but still with no amplification. Lastly, we also repeated the experiment was with *Pfu* polymerase by stratagene® but got no amplification

Figure 44.

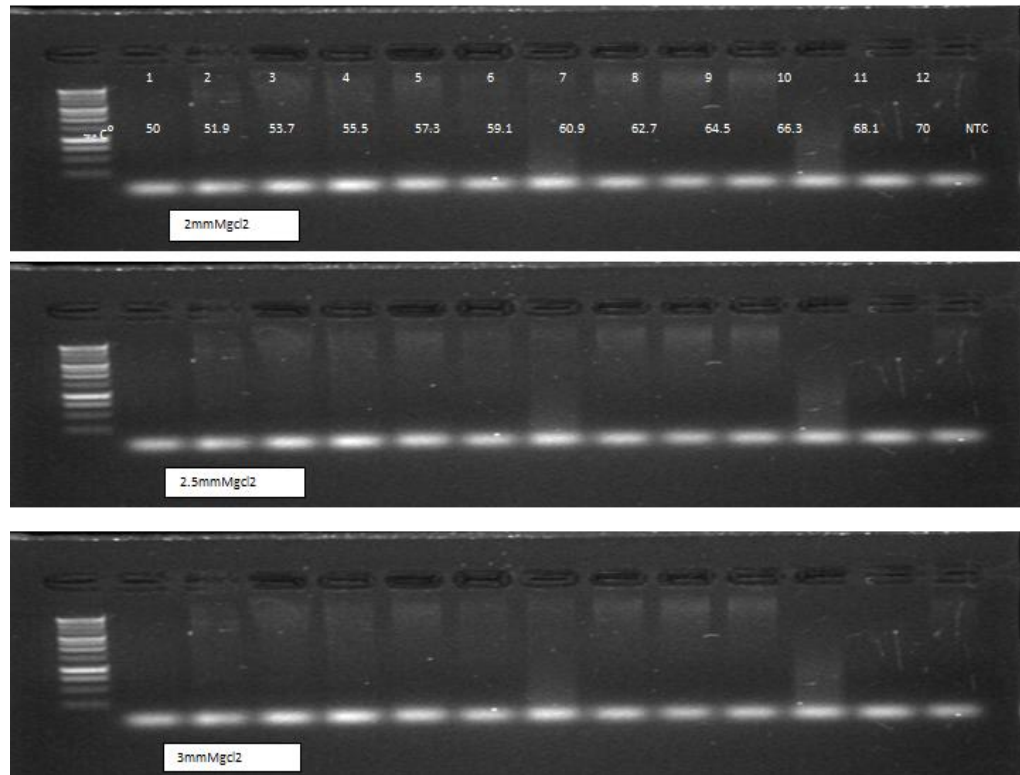


Figure 45: N36 primer optimization with added MgCl₂.

PCR optimization experiment was performed using three different concentrations of MgCl₂ (2mM, 2.5mM and 3mM) for N36 mutant primer. However, gel electrophoresis revealed that none of the concentrations could amplify the template at any temperature. Only primer dimers were observed including the NTC (no template control) lane.

We decided to redesign our N-36 forward primer and in the redesigned primer six new complementary bases were included to improve the annealing of primers to the template.

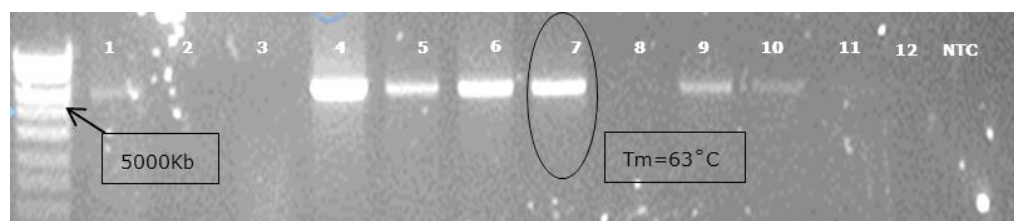


Figure 46: Temperature gradient for N36 Redesigned primer.

Gel electrophoresis of PCR products from temperature gradient PCR using redesigned primer for N36 site showed specific single bands of the correct size for 6 of the tested temperature range (52°C to 72 °C) and the annealing temperature of 63°C was chosen for our next experiments. There was no amplification seen in NTC (no template control) lane.

The newly synthesized primers were tested for their optimal annealing temperature using a range of 52°C to 72°C in a gradient PCR reaction. The redesigned N36 primer product was run on agarose gel for electrophoresis and revealed discrete single bands at the required band size with 7 out of 12 temperatures and with no band in NTC (no template control) lane thereby indicating no DNA contamination of PCR reaction **(Figure 46)**.

Similar to the first set we next aimed at sorting the optimal temperature for our N52 mutant primer pair using temperature gradient PCR and the recommended PCR settings as described in the materials and methods section. For this primer pair gel electrophoresis showed clean and specific bands at the expected band position in all of the temperatures tested (52°C to 72°C) but no band in negative control lane hence indicating no DNA contamination of reaction mix **(Figure 47)**.

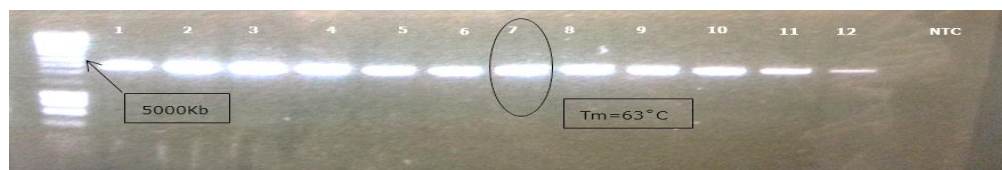


Figure 47: N52 primer optimisation.

Gel electrophoresis of PCR products from temperature gradient PCR using primer for the N52 site. It showed specific single bands of the correct size for all of the tested temperature range (52°C to 72 °C) and the annealing temperature of 63°C was chosen for our next experiments. There was no amplification seen in NTC (no template control) lane.

In any PCR, too much or too little template can have a profound influence on the results. A reaction with too little template

typically produces weak or non-existent bands when the reaction is run on a gel. Too much template can suppress the PCR or result in the production of unwanted end products that may appear as smears on the gel. For most PCR-based applications, high-quality plasmid DNA is recommended to be used at a concentration of 1–10 ng. This was particularly important for these PCRs, as, these were aimed at mutagenesis and not just amplification of the template.

Hence, as the aim of these PCR reactions was not just an amplification of the product. This experiment actually aimed at making the mutant copies of the template using specific mutant primers so later we can remove the wild type Template DNA and use the mutant plasmids. It was important to know the optimal (minimal) amount of template DNA that would be sufficient to produce the mutant product as not only it would give better PCR product but also easier to clean out by DpnI enzyme digestion.

To achieve that we decided to try different template plasmid concentrations for both N36 and N52 mutant primers and we also ran a positive control PCR using template plasmid and wildtype CD24 primers. We tried 1ng, 2ng, 500pg, 100pg and 50pg of template plasmid concentrations and the products were ran on the agarose gel. For the mutant primer N36 best band was produced by the PCR having 1ng plasmid template and for

N52 mutant 2ng was the lane that showed brightest band **(Figure 48/Figure 49)**.

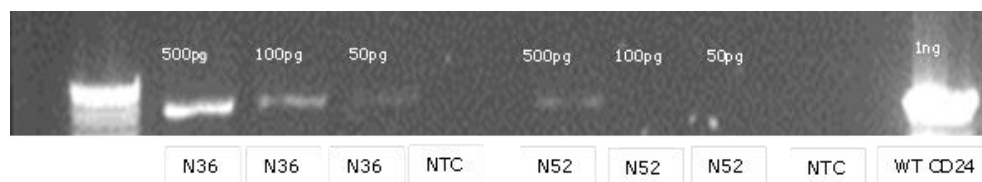


Figure 48: Template concentration optimisation.

Gel electrophoresis of PCR products using varying concentration of template revealed that for the N36 template as low as 100pg gave a clean band but for N52 even 500pg gave a faint band. However, both of these mutant products gave a band of the same size as a wild type CD24 PCR positive control. Both NTC (no template control) lanes showed no product hence indicating the absence of contamination of PCR reaction mix.

Our next step was to gel extract the mutant PCR product and the bands of the 1ng lane for N36 and the 2ng lane for N52 mutant primer were excised under UV light for this purpose. The extracted PCR products were purified and then digested using DpnI enzyme. This enzyme selectively digests only the template DNA as it attacks the methylated sites. As only the DNA grown inside the bacteria (template plasmid) gets methylated whereas the fresh PCR products are non-methylated the enzyme selectively digests these methylated DNA strands from parental template plasmid leaving in principle only the mutant PCR product. Appropriate controls were used at each experimental step as stated above.

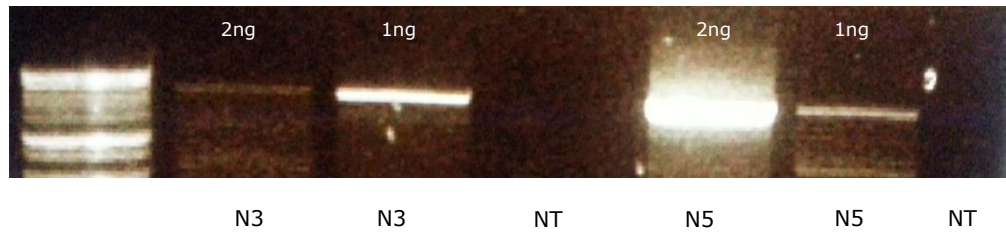


Figure 49: Template concentration optimisation.

Gel electrophoresis of PCR products using varying concentration of template revealed that for N36 template 2ng was too much and it gave a weaker band compared to sharp and bright seen in the 1ng lane. For N52 2ng gave the strongest band. Both NTC (no template control) lanes showed no product hence indicating the absence of contamination of PCR reaction mix.

After the DpnI digestion, the mutant products were ligated using DNA-Ligase4 from Invitrogen® overnight. Finally, ligated products were transformed into NEB 5-alpha Competent E. coli (High Efficiency Cat# C2987P) for multiplication of the mutant plasmids produced. The procedure is described in detail above in the material and methods section.

Following transformation combinations were performed

Transformation outcomes for N36 mutant:

1. Reaction mix without polymerase → Digested → Ligated → No colony.
2. N36-Mutant PCR product → Ligation alone → 600 colonies.
3. N36-Mutant PCR product → No ligation and No DpnI digestion → 6 colonies.
4. Cells alone without any PCR product → No colony.
5. N36 -Mutant PCR product → Digested → Ligated → 100 colonies.

Conclusions of transformation reactions:

Transformation Reaction 1 was our negative control as only had template plasmid but no PCR product as no polymerase was added to the reaction and absence of colonies showed complete digestion of the template plasmid by DpnI enzyme. Transformation Reaction 2 was the control for the back ground as both the template and the mutant plasmid will be present in the reaction, being a DpnI negative control it was expected to have 5-100 times more colonies compared to reaction 5. Transformation Reaction 3 was again as a control and showed back ground colonies produced by template plasmid. Transformation Reaction 4 Cells only was the control for contamination. As the agar media plates were made with ampicillin antibiotic, only the E.coli possessing Ampicillin resistance should be able to grow (E.coli transformed with plasmid vector because vector has ampicillin resistance gene). Transformation Reaction 5 was our expected mutant selecting setting as digestion was expected to remove all the template plasmid leaving a mutant product that was ligated for transformation and amplification inside E.coli. We selected 9 clones from these for gene sequencing analysis of plasmids.

Transformation outcomes for N52 mutant:

1. Reaction mix without polymerase → Digested → Ligated → No colony.
2. N52-Mutant PCR product → Ligation alone → 200 colonies.
3. N52-Mutant PCR product → No ligation and No DpnI digestion → No colony.
4. Cells alone without any PCR product → No colony.
5. N52 -Mutant PCR product → Digested → Ligated → 10 colonies.

Conclusions:

The N52 mutant transformations were analysed as well and in this case also, we got no growth in negative controls (Reactions 1, 3 and 4), Transformation Reaction 2 was Ligation alone and hence was an indication of both template and mutant clones but gave fewer colonies compared to N-36 transformants. Transformation Reaction 5 we can only get 10 colonies this indicated a lower transformation efficiency compared to N-36. We selected 7 clones for further analysis by gene sequencing.

Need for Gene Sequencing:

Although as described above, prior to transformation in *E. coli*, digestion with DpnI (NEB, UK), an enzyme that degrades methylated DNA, was used to reduce the amount of wild type template. However, this digestion is often incomplete and traces of template result in recovery of wild type plasmids that

can only be distinguished from mutant DNA through sequencing. These transformants were selected using ampicillin selection and appropriate controls were used to help identify colonies with highest probabilities of mutant clones being present.

Colonies were picked for each mutant primer and plasmids were extracted and quantified using mini-preps and nano drop as discussed above in materials and methods section. These were then sent for gene sequencing analysis using Universal priming sites present in our vector i.e T 7p forward and BGH reverse, in order to ensure the presence of correct change at the intended site and absence of any non-specific mutations introduced during the mutagenesis process.

Our wild type CD24 PCR product was a positive control. In order to analyse the effects of loss of specific N-glycosylation site (N36/ N52) and the resultant effects on the functionality of CD24 molecules, it was vital to analyse our mutant plasmids generated by site directed mutagenesis described above.

The clones fulfilling all of the three selection criteria mentioned below could only be used for next steps of the experimental plan.

- 1) The presence of complete CD24 sequence in the mutant plasmid vectors.
- 2) The presence of specific mutation i-e AAC→CAA for N-36 mutant clone and presence of AAT→CAA at site 52 in the case of the N-52 mutant clone.
- 3) The absence of undesired and non-specific mutation at any other site in the both mutant clones.

More over gene sequencing will also help us in confirmation of the presence of CD24 gene in our wild type CD24 plasmid vector and absence of any mutations compared to the reference CD24 sequence.

As described above we used Chromas lite, Mega 6 alignment tool and BLAST 2 software from NCBI to analyse the gene sequencing results. It was observed that our wild type CD24 plasmid had 100% homology with the CD24 reference gene from the NCBI library (cDNA clone MGC: 75043 IMAGE: 5591617) and there were no gaps or mismatches present **(Figure 50)**. The sequence of wild type CD24 also showed complete alignment with Reference CD24 sequence when analysed with Mega 6 alignment software **(Figure 51)**.

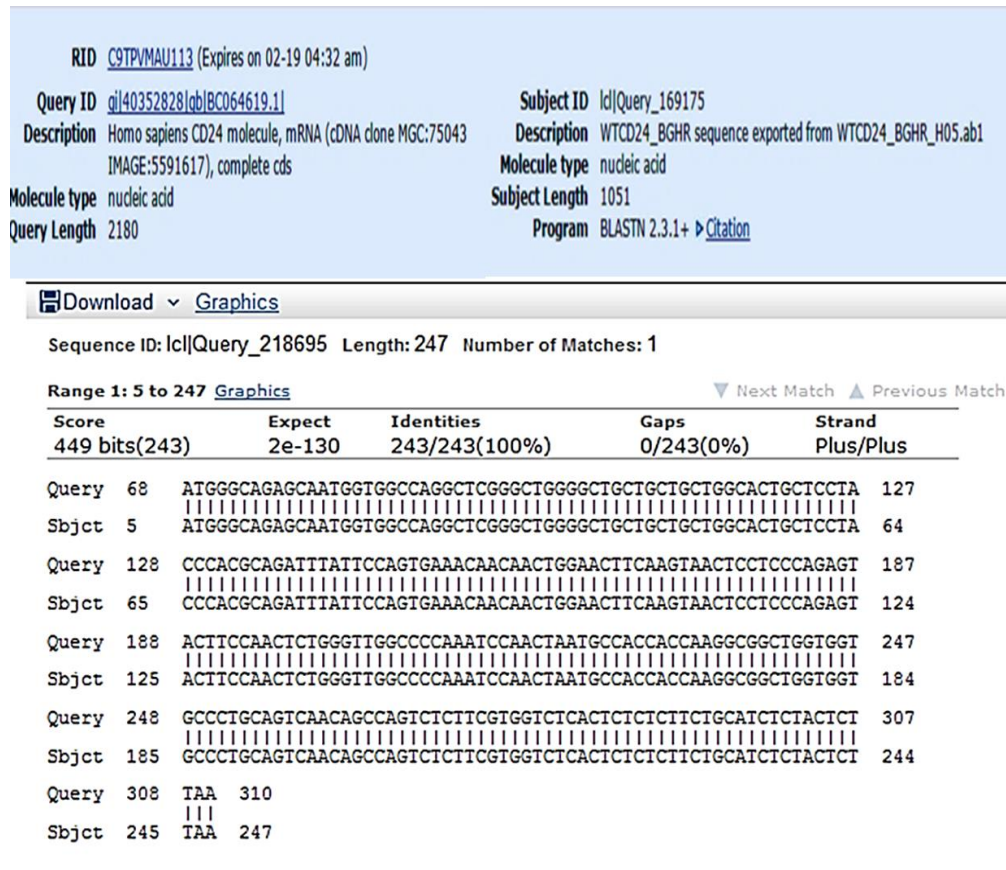


Figure 50: BLAST 2 analyses of CD24 reference gene and WT CD24 clone

The Chromaslite software was used to analyse the sequencing results of the CD24 pcDNA3.1 plasmid using the T7 forward primer and BGH reverse primer. The results showed 100 % sequence similarity between the resultant sequences and CD24 coding sequence when aligned using the NCBI alignment tool.

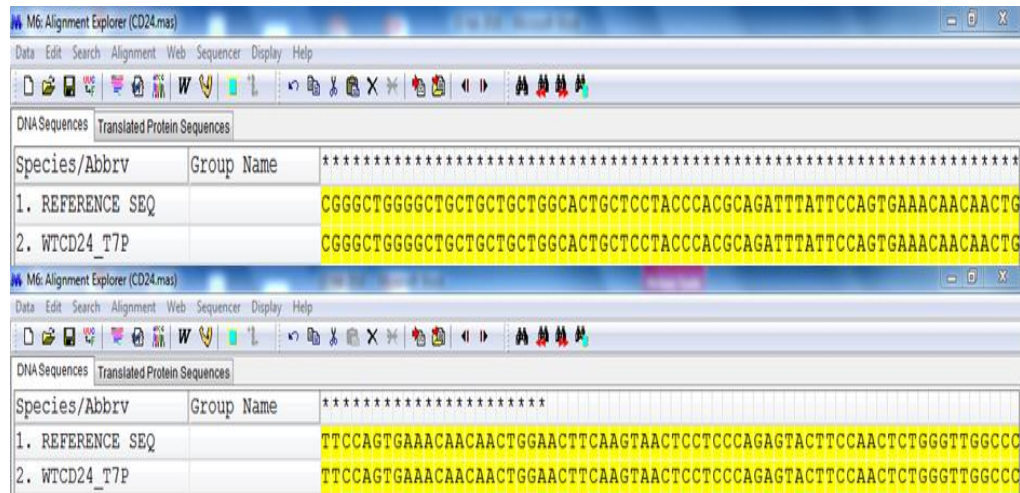


Figure 51: Sequence alignment of CD24 reference gene and WT CD24.

Mega6 alignment software was used to compare the sequence homology of our wild type CD24 vector plasmid and CD24 reference gene from NCBI gene bank (Accession # BC064619.1). The analysis showed complete alignment.

Sequence analysis of N36 mutant clones:

As stated above the clones were examined to get a clone that fulfills all three criteria mentioned earlier in order enable us to study the distinctive outcomes of N-glycosylation site mutations at both of the sites respectively.

The gene sequencing analysis of 9 clones for the N-36 site using Mega6 software revealed presence of CD24 gene sequence in the plasmids. Out of nine, 8 clones either had no mutation at the desired site or had undesired and nonspecific mutations. The required target mutation i-e ACC-->CAA at position 36 was observed only in one clone i-e Clone 5, however besides the presence of this specific mutation, there were extra

undesired mutations present along the sequence hence making it unfit for selection (**Figure 52**).

Sequence analysis of N52 mutant clones:

The Mega6 analysis for N-52 mutant clones revealed a mixture of results. Few clones showing the fulfillment of two criteria i.e presence of CD24 gene in the plasmid vector, and absence of undesired mutations but unfortunately none of these clones had the required mutation at N-52 glycosylation site (**Figure 53**).

Three clones besides having no mutation at N-36 or N-52 site had missing ORF sequence of CD24 gene in them compared to the reference with some gaps (**Figure 54**).

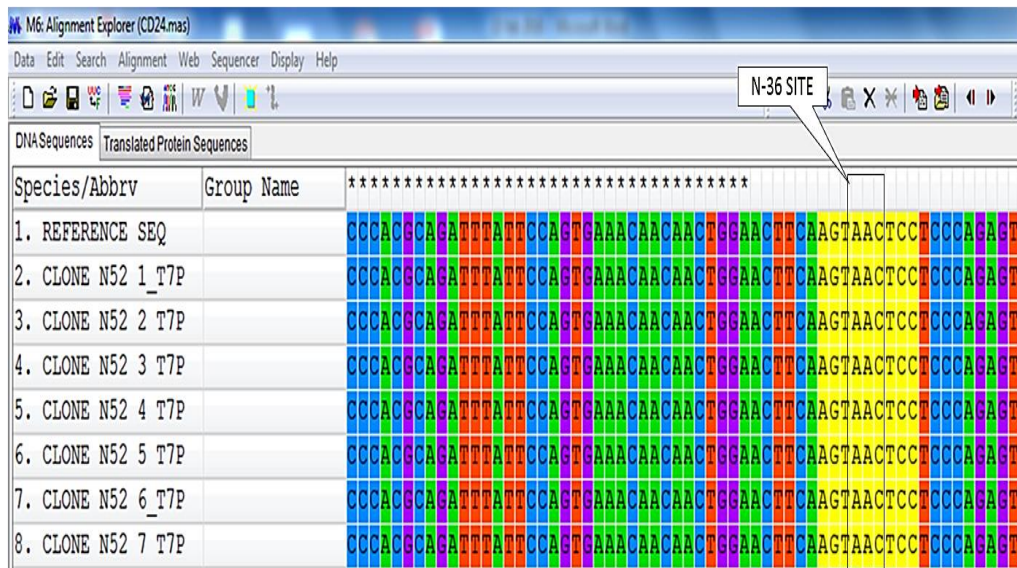
Hence, at this occasion, we could not select any clone for further experiments as none of these met the full criteria.



Figure 52: Mega6 alignment analysis of N-36 clones.

Screen shot of alignment results using Mega 6 software for N-36 clones. These results were sequenced using a T7p primer. The clones were analysed for the presence of sequence homology to CD24 Reference sequence (row1).The N-glycosylation sites are marked in boxes. (A) analysis of the sequences revealed misalignment and presence of unwanted changes instead of specifically required mutation. (B) Although the N-36 mutant primers were not expected to affect the N-52 site, sequencing showed disturbed sequence in all clones at the N-52 site as well.

A



B

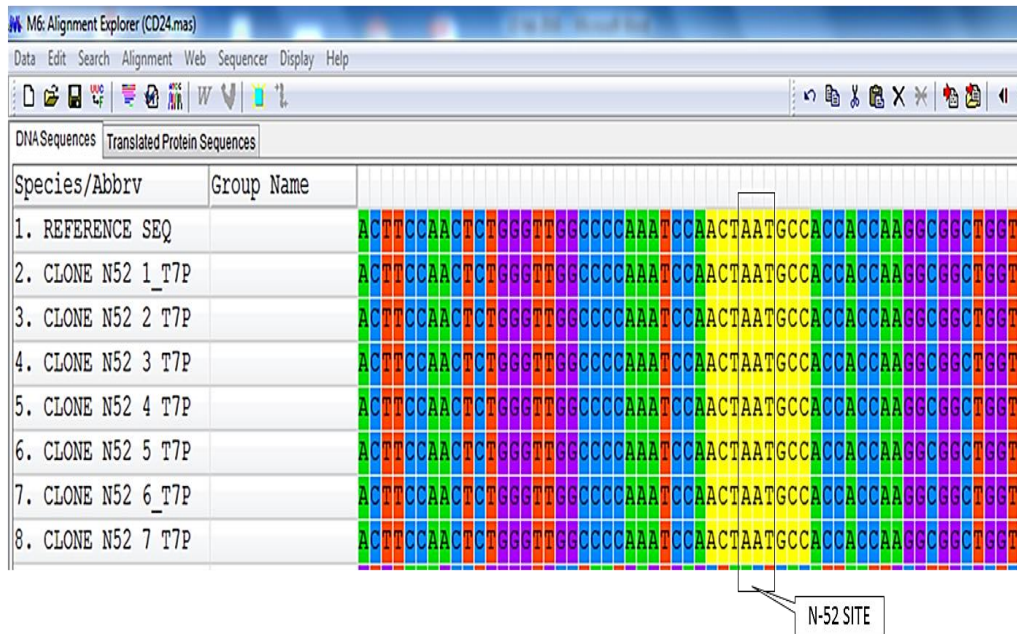


Figure 53: Mega6 analysis of N-52 Mutant clones.

The gene sequencing analysis of 7 clones for N-52 , using Mega6 software, revealed presence of CD24 gene in the plasmid in all clones with no mutation at any site including the N-glycosylation site i-e AAC-->CAA at position 36(site indicated in red box),this was the expected outcome of this primer set (A).

However, all the clones also had exactly the same sequence compared to reference CD24 including the N-glycosylation target mutation site i-e AAT-->CAA at position 52(site indicated in the red box). And none of the clones showed the desired mutation that was expected to be generated by the mutant primers (B).

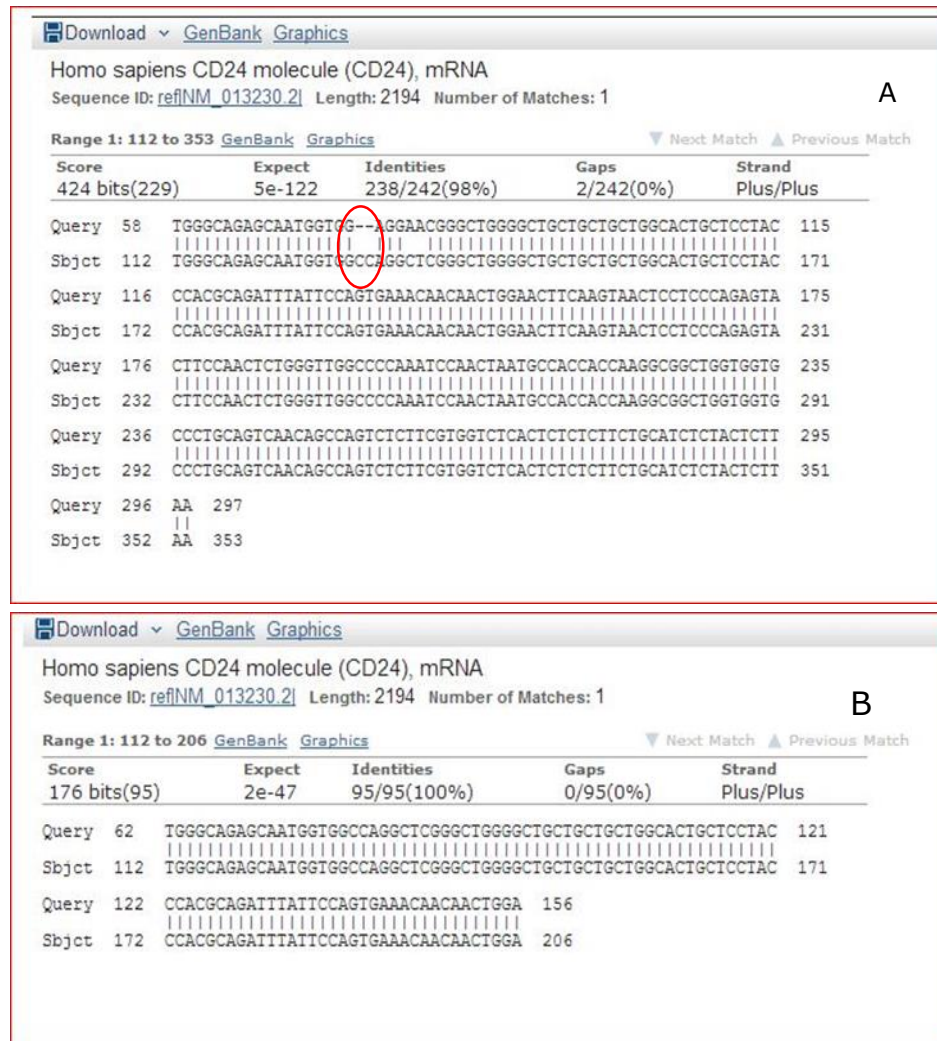


Figure 54: Screen shot of NCBI Blast2 of N-52 clone with CD24 ORF.

The comparison shows (A) shorter sequence and presence of missing bases at position 77,78 (encircled red). The remaining sequence had complete homology with the reference sequence.(B) Although the sequence showed 100% homology, only 95 bases from the ORF sequence were present in the mutant plasmid.

Results of HRM:

No product was shown on HRM as the machine read MAX LED reached meaning 100% reading for LC green whereas it should actually decrease and should be ideally around 25%. No melting curve was generated by all samples. Products were also run on the agarose gel but no product was seen on the gel either,

indicating that the experiment didn't work and needs optimisation. To overcome this the next possibility was to optimise the primers by repeating the PCRs using HF phusion enzyme (high fidelity) and temperature gradient.

Unfortunately, because of personal health and family issues, the study got interrupted at that point and this could not be tried.

SDM assist software designed primers:

On resumption of the study we tried once more the PCRs and sequencing but still failed to get the required clones. On reanalysis of all potential reasons of failure one possibility turned up as our primers were manually designed and were back to back with each other, based on Inverse PCR principle thereby generating blunt ends which were ligated later as directed by Phusion protocol. Although our PCR worked with our manually designed primers and HF Phusion polymerase and products appear specific and gave transformation results that seemed promising but the gene sequencing analysis revealed the failure of specific mutagenesis and resulted in a mixture of random and undesired mutations.

Hence, we next decided to try re-designing our primers, using software **SDM-assist** and the resultant primers are shown in **Table 13** as mentioned above.

Discussion:

This study aimed at mutating N-glycosylation sites present in CD24 molecule using site directed mutagenesis and to our knowledge will be the first study of its type.

Site-directed mutagenesis is a valuable tool for introducing specific nucleotide mutations based on PCR. The identification and construction of new commercial polymerases and advances in oligonucleotide synthesis have dramatically increased its efficiency. Primers designed with mutations can introduce small sequence changes. This process has dramatically improved the speed and reduced the cost of mutagenesis experiments.

Mutagenesis provides a useful method to study explicitly functions of different residues or glycans in proteins. This is not straightforward if we use the traditional methods such as chemical or enzymic modification or addition of glycosylation inhibitors (151).

Many commercial kits are available for this purpose with few differences and most widely used ones are Quick Change™ by Stratagene and it uses overlapping mutant primers to introduce the change in the plasmid-based gene sequence.

In this type of site-directed mutagenesis uses PCR primers designed to contain the desired change in the middle of the sequence. The PCR primer sequence simply replaces the original sequence. We used Phusion site directed mutated kit

that is another widely available tool using High fidelity polymerase II.

It requires back to back primer set with one or both of the primers having the mutation at the centre of the oligonucleotide. Inverse PCR is used for mutating plasmids. These back-to-back primers amplify the whole plasmid and the linear product is then ligated back to the circular form.

One potential reason for getting unwanted mutations could be the higher number of cycles although the estimated percentage of PCR products having an unwanted secondary mutation after 25 PCR cycles is only 5.5%(152).

Despite the common view that DpnI digestion is adequate to exclude the wild type plasmid DNA, a detailed study by Karnik *et al.* revealed that a rescue of 20-30% of un-mutated, wildtype plasmids after DpnI digest was inevitable and this could be one reason of getting the wild type clones in our N-52 primer set (150).

Another possible reasoning was given for the failure of site directed mutagenesis efficiency is primer impurity and a comparative study by Acevedo *et al.* showed that this played a critical role, with HPLC libraries enabling significantly higher yield on average than the ones, not HPLC purified but cleaned by conventional methods. However, the same study also showed that High fidelity Phusion hotstart II enzyme, that was

used in the current study, had the best outcome amongst the conventionally purified primers(153).

While PCR for substitutions is a way to introduce a mutation, it is restricted by the fact that the mutation can only be introduced in the sequence covered by the primers rather than the sequence that is present between the primers.

The guidelines given by Phusion site directed mutagenesis kit protocol for designing the primers were as follows:

For generating point mutations, there can be either one mismatch/mutagenic primer or both forward and reverse may have the mutation. The length of the correctly matched sequence in the mutagenic primers should be in average 24–30 nucleotides. The desired mutation should be in the middle of the primer with 10–15 perfectly matched nucleotides on each side. Complementarity between the primers should be avoided to prevent primer-dimer formation. Similarly inverted repeats (self-complementarity) should be avoided. The CG-content of the primer should be around 50%.And G's and C's at the 3'-end of the primers should be avoided(152).

Although we tried to follow as much of the above as possible, however, meeting the criteria of avoiding G's and C's near ends wasn't possible and the overall G C-content was around 47% in our manual primers. Trying to overcome these limitations

manually was cumbersome and time consuming hence, we decided to use a very helpful tool for redesigning our primers.

SDM- ASSIST SOFTWARE:

The SDM assist software provides an optimised strategy using partially overlapping primer pair which increases the likelihood of primer-template annealing over primer self-annealing. Although there are separate helpful web-based soft wares available both to design primers, SDM assist is unique as it allows the user to create all possible combinations of sequences encompassing the desired mutations.

The sequences can then be narrowed down to a single sequence that is used as the source for the downstream primer design. At the same time the program lists all physical properties of the DNA sequence that are relevant for optimal primer design such as melting temperature, the number of nucleotides exchanged, GC content and more. This feature alleviates the need to use a separate programme to choose the best option from the available primer combinations (154).

The plug-in also provides the plasticity of specifying just the amino acid required for mutation. Since the genetic code allows some level of redundancy (e.g. serine can be represented by six different codons), the program displays all possible candidate sequences.

Once the DNA sequence is pasted it automatically gets translated into an amino acid sequence including a ruler for easier identification of target sites. Simple drag and drop feature permits selection of amino acid to be replaced with required one. In addition, right-click on any amino acid shifts through the different codons of that specific amino acid. This option provides the control to select specific codon to represent the amino acid.

Keeping the fact that SDM primers are long, it is vital to have the best possible thermodynamic characteristics (such as GC content, melting temperature etc.) to warrant that they would work successfully in an SDM reaction. And above mentioned features of SDM assist tool encouraged us to use it and the primers were designed and selected in very short span with promising success based on the selected feature and previous experimental studies(150).

In brief new primers were successfully re-designed and these were partially overlapping primers (proposed to be better than both fully complementary primers and back to back primers in a recent study). They were shown to be compatible with Phusion site directed mutagenesis kit , but with an additional advantage of avoiding the requirement of Phosphorylation of primers and ligation step before transformation(150).

However because of time limitations, the project was handed over to the next Ph.D. candidate who have successfully obtained the mutant clones by using these SDM primers. And have found very interesting and significant outcomes by mutation of each of the N-glycosylation site, showing effects both on signalling and functional characteristics of the CD24 molecule as hypothesised by this project.

Chapter six: General Discussion.

General discussion:

The yet unsolved mysteries of cancer pathogenesis, development and progression stand in the way of finding its cure. Intensive research is being carried out to uncover and hence target, the abnormal molecular mechanisms operating within the malignant cellular machinery. This molecular targeting approach appears promising as seen in some haematological and solid malignancies.

CD24 molecule has relatively newer emergence on the scientific horizon. As an attribute to its significance, one finds this molecule in association with a diverse range of human pathologies including a growing list of cancers.

CD24 also called Heat stable antigen was first discovered by Springer *et al.* in 1978 in mice (155). Later human CD24 was cloned in 1990 by Kay R *et al.* (6). The location of CD24 gene is agreed to be on chromosome 6q21 (156) and exhibits an allelic polymorphism (Val to Ala exchange) (9). The CD24 protein is encoded by a 243 base pair coding sequence and the mature peptide is just 27-31 amino acids (5, 6).

In normal adult human tissues, CD24 is expressed on B cells, T cells, neutrophils, eosinophils, dendritic cells and macrophages. It is also seen on the epithelial cells, keratinocyte, muscle cells, pancreas, developing brain and stem cells (7).

In general, CD24 exhibits a higher expression on the progenitor cells and metabolically active cells with a gradual reduction in expression as the cell differentiates. It is not usually expressed on the adult human tissues. However, abnormal CD24 overexpression has been documented in a large variety of human cancers including squamous cell carcinoma, breast carcinoma, colorectal carcinoma, renal cell carcinoma, bladder carcinoma, ovarian carcinoma, gliomas, non-small-cell lung cancer, prostate cancer and primary neuroendocrine carcinomas (7, 9, 13, 32, 36, 88, 157). Similarly, CD24 polymorphisms are documented to be associated with the risk and progression of autoimmune diseases, including multiple sclerosis, rheumatoid arthritis and systemic lupus erythematosus (SLE)(158). Ahmed *et al.* found CD24 upregulation in regenerative mucosa of both ulcerative colitis (UC) and Crohn's Disease (CD)(26). These observations indicate its role in immune regulation as well as cancer pathogenesis.

Moreover, CD24 was recently demonstrated to be associated with a variety of Danger-associated molecular patterns (DAMPs). These DAMPs are intracellular components such as HMGB1, HSP70, HSP90 and cellular RNA etc., released during cellular injury and are found to interact with the Toll like receptors (TLRs). However it's already known that the

Pathogen-associated molecular patterns (PAMPs) also interact with Toll-like receptors (TLRs) on innate immune cells to initiate protective immune responses. Whether the host is able to discriminate between DAMPs and PAMPs was not clear (41). Chen *et al* found CD24 to interact with a variety of DAMPs, such as high mobility group box protein1, heat-shock proteins and nucleolins, they also observed CD24's interaction with SiglecG (mouse)/ Siglec10 (human). They found that DAMPs interact with TLRs, CD24 and Siglecs leading to selective repression of the host immune response. Since the pathway does not affect the host response to pathogen-associated molecular patterns(PAMPs), they proposed that the CD24–Siglec G pathway discriminates DAMPs from PAMPs (21, 41).This pathway was also thought to contribute to the cancer immune escape hypothesis (158).

Considering these interactions of CD24 with DAMPs and taking into account that majority of tumours including colorectal carcinoma show considerable tissue necrosis and hence the release of DAMPs in the tumour microenvironment, we were intrigued to explore if CD24 also modulate tissue response to DAMPs in the setting of cancers. We tested our query by performing functional assays on the colorectal carcinoma cells after exposure to DAMPs in CD24 positive and negative cell lines.

Four colorectal cancer cell lines including SW620 and DLD1 (+ve for CD24 expression) and HCT116 and RKO (-ve for CD24) were exposed to autologous necrotic cell lysates (DAMPs). The results of wound healing assay showed significant inhibition of colorectal cell migration by DAMPs but this was independent of CD24 status. Furthermore our trans-well assays also displayed reduced trans-well migration in majority of the cell lines independent of CD24 status after exposure to necrotic cell lysates. These results were supported by the knockdown and forced expression experiments as well.

We also explored effects of DAMPs on cellular proliferation using autologous DAMPs in three colorectal cancer cell lines. Our results indicated a significant increase in cellular proliferation when exposed to DAMPs, irrespective of the CD24 status of the cell line. At an attempt to find the possible mechanism of inhibition of motility by DAMPs we exposed cells to DAMPs and these cells were analysed for the status of cellular motility mediators by western blots. We found down-regulation of molecules associated with increased motility including Cten, N-cadherin and Snail in cells exposed to DAMPs.

We suggested thereby that in epithelial cells, CD24 does not appear to modulate cellular response to DAMPs. However, DAMPs does show effects on epithelial cell migration and proliferation. We reasoned that in contrast to the experiments

on immune cells (41) we were trying to explore the epithelial cells (colorectal carcinoma cell lines) which may have quite a different glycosylation compared to immune cells and may be a reason for different interactions and signalling outcomes in different tissues. It may also be possible that epithelial CD24 does not interact with DAMPs and the results of Chen *et al.* may be specific to immune cells. And the reason for this lack of modulation could be due to the absence of Siglecs on epithelial cells that is the third prerequisite in the model presented by Chen *et al.* (88).

Although many new aspects of CD24 biology have emerged since its discovery, it is still uncertain how it mediates its effects without a transmembrane domain and much less is known about its exact signalling partners. Aberrant activation of Wnt signalling pathway is very well known and is found in almost 80% of colorectal carcinomas (52, 159).

The presence of TCF/LEF consensus sequences in promoter region of CD24 suggests that it is target gene of Wnt signalling pathway and a recent study by Ahmed *et al.* have shown the direct relationship between β -catenin and CD24 confirming thereby, CD24 as a target of Wnt signalling in colon (26). This association of CD24 and β -catenin has also been reported in hepatocellular carcinoma by Yang *et al.* (62).

Bauman *et al.* showed that CD24 ectopic expression in breast cancer cells resulted in increased proliferation rates and the activation of the $\alpha_3\beta_1$ and $\alpha_4\beta_1$ integrins, which induced binding to selectins, collagen, and laminin thus increasing cell migration(33).

Runz *et al.* showed that although no **β_1 integrin** localizes to lipid raft domains in CD24-negative cells, transfection of CD24 induced the recruitment of **β_1 integrin** into these, cholesterol and sphingolipid-enriched, membrane domains. Moreover, they also showed that these CD24-transfectants increased both the invasiveness into a cushion of mixed collagens as well as the transmigration through a monolayer of endothelial cells (83). In another study by the same group, it was observed that in CD24-positive cells, CXCR4 lost its association with lipid rafts, necessary for effective binding to its ligand SDF-1. This, in turn, resulted in a subsequent inhibition of downstream signalling, cell migration and invasion. Conclusively CD24 restricted the lipid raft localization of CXCR4 (23). Given that CD24 is a major GPI-anchored and lipid rafts associated protein in many cell types, it might , therefore, act as a general “**gate-keeper**” to lipid rafts. In an attempt to further explore the downstream targets of CD24, Baumann *et al.* in a very recent study found that CD24 interacts with and augments the kinase activity of c-src, this happens within and was dependent upon intact lipid

rafts. CD24-augmented c-src kinase activity led to increased formation of focal adhesion complexes, accelerated phosphorylation of FAK and paxillin and consequently enhanced integrin-mediated adhesion(33).

Another molecule that increases cellular characteristics quite similar to CD24 is Cten, also known as Tensin4. Recent research has shown Cten to bind with β integrin's cytoplasmic tail and to be present within the focal adhesions. Cten is also demonstrated to be modulating proteins containing phosphorylated tyrosine residues like Focal adhesion Kinase (FAK), ILK, p130Cas and P13 kinase(99). We hypothesized that CD24 is signalling through Cten. We tested the hypothesis by performing forced expression and knock down experiments and also by carrying out co transfections. The results supported our hypothesis as Cten levels followed CD24 expression levels and CD24 mediated cell motility was abrogated by knockdown of Cten. Our group has previously shown Cten to be mediating increased motility via ILK and we found that FAK and ILK were common downstream targets of both molecules as knock down of FAK or ILK both annihilated the effects of CD24 on motility. We observed there was no remarkable change in the protein levels of FAK by the change in CD24 levels, however, we did find that Cten affects FAK protein expression. Recent research has already shown an

increase in ILk levels by Cten (99) and that CD24 increases phosphorylation of FAK (33). Taken all these bits together, CD24 appears to increase cellular motility by recruiting β -integrins to lipid rafts, increasing c-src phosphorylation and activation. This in turn leads to increased Cten levels and activation. The Cten increases protein kinases such as ILK and FAK and increases their activation via its SH2 (Src homology domain) and PTB (Phospho-tyrosine binding domain) domain, resulting in epithelial to mesenchymal transition and hence increased cellular motility as also shown by our group (98).

The molecular weight of CD24 ranges from 30 to 70 kDa (5), most of its weight is due to extensive N- and O-linked glycosylation, as it has 16 potential O- and N-glycosylation sites. The extensive glycosylation renders to CD24 similarity to a mucin(7). Many studies have shown that glycosylation patterns vary widely between the tissues and these have been proposed as a factor responsible for the broad spectrum of roles linked to CD24 (160). There is evidence that fucosylated glycans present on CD24 enable CD24 to interact with P-selectins on endothelial cell and platelet surfaces and help in cancer cell metastasis (12, 160). Similarly, in neuronal tissue, the interaction between L1 and CD24 depends on α 2,3-sialic acid present on CD24, and this interaction determines the cell type-specific promotion or inhibition of neurite outgrowth(18).

TAG-1 and Contactin (lectin-like molecules present in lipid rafts) were also found to interact with CD24 in cerebellar and dorsal root ganglion (DRG) neurons through Lewis x glycan present on CD24 (17).

Another very recent evidence signifying role of sugars is the amelioration of sepsis by inhibition of bacterial sialidases. These bacterial sialidases result in the annihilation of interaction between CD24-siglec-DAMP complex and destroy the negative feedback mechanism for the release of interleukins and cytokines leading to sepsis (66). Moreover increasing research have proposed a role of N-glycans in cancers (161).

The current study aimed at exploring the glycosylation aspect of CD24. We reasoned that being a heavily glycosylated molecule CD24 may also mediate its functions through its sugars as indicated by the studies above. Analysis of current information regarding the process of protein glycosylation and CD24 amino acid structure revealed two potential N-glycosylation sites to be present in the CD24 molecule but multiple O-glycosylation sites. We decided to remove the sugars from these N-glycosylation sites by mutating the amino acid sequence required for the N-glycosylation to occur. Our aim was to construct mutant CD24 plasmids with both N-glycosylation sites mutated, individually as well as simultaneously. These mutant plasmids were then to be transfected in cancer cell lines

and analysed for their effects by performing relevant functional studies compared to the wild type CD24 plasmid. To achieve that, we selected Site-directed mutagenesis technique. Site-directed mutagenesis (SDM) has proven itself as a quick reliable and relatively cheaper method to generate such point mutations and hence quite helpful to probe the function-structure relationship of proteins. There are other approaches available to remove the sugars from the molecules i-e using digestive enzymes that cleave off sugars or blocking the synthesis of these sugars by knocking down fucosyl-transferases. However for the current study, mutagenesis technique was preferred because it would allow us to mutate a particular N-glycosylation site using PCR and the resultant absence of N-sugar from that specific site only. This is not the case in enzymatic de-glycosylation as that would remove N-sugars from all N-sugar sites. Similarly the knock down of fucosyl transferases will block synthesis of these glycans non-specifically. Once the clone with the desired mutation is obtained and verified via sequencing, these plasmids can be used easily in further experiments.

Although our SDM technique didn't work successfully in this attempt but the repeated attempt by the next Ph.D member was successful and is yielding interesting data that will help in our understanding of this molecule.

Conclusions:

In summary the study aimed at investigating three aspects of CD24 biology including modulation effects of DAMPs response, signalling partners and structural significance of CD24. From our set of experiments we hereby conclude.

- Autologous DAMPs have inhibitory effects on colorectal cancer cell lines and both directional and non-directional motility is inhibited as appreciated by transwell and wound healing assay. This inhibition appears to be independent of CD24 status and seems to be mediated by downregulation of molecules associated with increased motility including Cten, N-cadherin, and Snail.
- As opposed motility, investigations involving three different colorectal cancer cell lines indicated an increase in cellular proliferation when exposed to autologous DAMPs and this effect was even more pronounced after 48 hours of exposure. However, once again this appeared independent of CD24.
- The study found CD24 to be having a direct regulatory effect on Cten protein levels and CD24 appears upstream of Cten. It was also observed that Cten, FAK, and ILK are indispensable for CD24 mediated increase of cell motility.
- The last part of the study was aimed at mutating N-glycosylation sites present in CD24 in order to see its

functional and signalling impact on CD24 biology. We employed site-directed mutagenesis technique and although the attempt was not successful this time but still provides a valuable approach to explore the yet unclear mechanism of the functionality of this molecule.

Potential strengths:

- This was the first study exploring CD24 and DAMPs interaction in autologous colorectal cancer cells (epithelial cells). And it also explored if dead cancer cells could signal remaining alive cells directly.
- Most experiments were carried out at least in three cell lines to avoid cell line specific effects in addition dual approach of knockdown and forced expression was also used to validate findings.
- A dual approach of knockdown and ectopic expression was employed for studying the signalling relationships of CD24 supported by co-transfections.
- This study has found the regulatory effect of CD24 on Cten levels and shown it to be functionally relevant as well.

Study limitations:

- Western blots were used in our study to compare and quantitate protein levels. Proteins have documented

molecular weights and appear as discrete single bands on the western blots. These bands are identified against a colour coded protein ladder with known molecular weights used as a marker. However, in case of CD24 the protein is heavily glycosylated with a variety of sugars attached to small amino acid backbone and produced a smear instead of a discrete band on the western blots with a size range from 37-75kDa.

Equal protein loading of all wells is vital in order to make sure that the differences appearing in different bands are actual dissimilarities of expression levels and not merely a result of unequal protein sample being used. One solution to that is to compare the lanes for a protein that is ubiquitously expressed by the cells and not affected by the experimental conditions. β -actin protein (molecular weight 42kDa) is a common example used as loading control, as β -actin is ubiquitously expressed by all cell lines, is quite stable under most experimental conditions and expressed in high amounts. We also used β -actin as our loading control in our initial set of experiments (Figure 15) we had to use parallel lanes on the same gel to detect β -actin because of overlapping molecular weight of CD24 and β -actin. However, we acknowledge that this is not a true reflection of loading control. The issue was sorted in

the next set of experiments, where comparative quantification was needed, by stripping and re-probing technique. Whereby after detection of CD24 protein, the SWA11 antibody was stripped off and the membranes were re-blotted with β -actin antibody hence reflecting protein loading of the same wells. Another approach could be using Histone3 (molecular weight 19kDa) as loading control as oppose to b-actin which will allow cutting of membrane and simultaneous blotting of both CD24 and H3 instead of stripping and re-blotting.

- The results of the DAMPs study will become more convincing if the effects on motility and proliferation by DAMPs (Necrotic cell lysates) could be reproduced by using purified DAMPs such as HMGB1. And if the reversal of effects could be shown by the addition of HMGB1 blocking antibody.
- Moreover, performing the experiments in a macrophage – epithelial coculture will be interesting to further clarify if the presence of Siglecs on macrophages will affect the response modulation of DAMPs by CD24. As it might be the case of completing the triad of **CD24-Siglec-DAMPs** to modulate cellular characteristics, as seen in immune cells.

- These experiments were performed in vitro and on cancer cell lines and this bear limitation of being not a true representation of in vivo conditions.
- Due to personal health and family constraints, experiments exploring the mechanism of increased Cten protein levels by CD24 could not be repeated. So was the case with re-trial of mutating N-glycosylation experiments.

Future Suggestions and Recommendations:

- As mentioned earlier, it will be interesting to expand the DAMPs project to include co-culture technique with immune cells as actual tumour microenvironment consists of immune cells, necrotic cells mesenchymal and epithelial cells with potential effects on each other. Extending these experiments to animal models will be further helpful in validating study results.
- Being heavily and differentially glycosylated, there is quite a possibility that CD24 performs so diverse functions albeit absence of a transmembrane domain, via these sugar moieties. Hence mutating its glycosylation sites is a very novel model. As it will indicate the specific effect and significance of each site. We started off with N-glycosylation sites as there are only two potential sites for

N-glycosylation and more than 16 O-glycosylation sites. The next Ph.D. student who took over this project has already found some interesting effects of mutating of both N-glycosylation sites individually. This can further be extended by creating a mutant having both mutations in one plasmid and also extending these to O-glycosylation sites. This study will provide novel information that has not yet attempted by any other group to our knowledge.

- Another very interesting aspect of CD24 biology is its presence in lipid rafts. These lipid rafts are specialised areas of cell membrane highly enriched in cholesterol and sphingolipids. These detergent resistant membrane areas have been further characterised into different domains associated with signalling pathways, endocytosis and increasingly associated to be involved in multiple important cellular characteristics in recent literature. It has already been seen that CD24 mediates some of its functions by regulating trafficking of molecules in and out of these lipid rafts. However, the exact location of CD24 and mechanism of this traffic regulation by CD24 is still unknown. We propose CD24 is present in **Reggie microdomains** that are independent of caveolin and dynamin domains and are identified by flotillin 2 proteins. This hypothesis is based on the studies in drosophila

indicating Reggie domains to be associated with Wnt signalling. Furthermore, in prostate cancer cells, that were caveolin1 and PTEN negative , lipid rafts mediated effects through AKT and STAT3 and both of these molecules are linked to CD24 hence again pointing towards the possibility of CD24 being present in these domains. This could be explored further and will be an addition to the further understanding of CD24 biology.

Study hypothesis:

CD24 is present in Reggie microdomains (a subtype of lipid rafts) and flotillin 2 is involved in its signal transduction across the membrane.

Possible Work plan for lipid rafts project:

- Using Immunofluorescence for flotillin, caveolin and CD24 to see if they co- localize,
- Co-immune-precipitation for CD24, caveolin, Flotillin2 and CD24.
- Investigate effects of blocking flotillin 2 / caveolin on CD24 localization, amount and its downstream targets (Cten/ FAK/Ilk/c-src/Snail).
- Blocking Flotillin-2 by antibodies in both CD24 positive and negative lines and performing functional assays and

to see if results are reversible by reversing F2 blockade
will be interesting.

References.

References.

References:

1. Hough MR, Rosten PM, Sexton TL, Kay R, Humphries RK. Mapping of CD24 and homologous sequences to multiple chromosomal loci. *Genomics*. 1994 Jul;22(1):154-61.
2. Pass MK, Quintini G, Zarn JA, Zimmermann SM, Sigrist JA, Stahel RA. The 5'-flanking region of human CD24 gene has cell-type-specific promoter activity in small-cell lung cancer. *Int J Cancer*. 1998 Nov 9;78(4):496-502.
3. Wang L, Lin S, Rammohan KW, Liu Z, Liu JQ, Liu RH, et al. A dinucleotide deletion in CD24 confers protection against autoimmune diseases. *PLoS Genet*. 2007 Apr 6;3(4):e49.
4. Shulewitz M, Soloviev I, Wu T, Koeppen H, Polakis P, Sakanaka C. Repressor roles for TCF-4 and Sfrp1 in Wnt signaling in breast cancer. *Oncogene*. 2006 Jul;25(31):4361-9.
5. Henniker A. CD24. *Journal of biological regulators and homeostatic agents*. 2001;15(2):182-4.
6. Kay R, Takei F, Humphries R. Expression cloning of a cDNA encoding M1/69-J11d heat-stable antigens. *The Journal of Immunology*. 1990;145(6):1952.
7. Fang X, Zheng P, Tang J, Liu Y. CD24: from A to Z. *Cellular & molecular immunology*. 2010;7(2):100-3.
8. Sagiv E, Arber N. The novel oncogene CD24 and its arising role in the carcinogenesis of the GI tract: from research to therapy. *Expert Review of Gastroenterology and Hepatology*. 2008;2(1):125-33.
9. Kristiansen G, Sammar M, Altevogt P. Tumour biological aspects of CD24, a mucin-like adhesion molecule. *Journal of Molecular Histology*. 2004;35(3):255-62.
10. Ohl C, Albach C, Altevogt P, Schmitz B. N-glycosylation patterns of HSA/CD24 from different cell lines and brain homogenates: a comparison. *Biochimie*. 2003 6//;85(6):565-73.
11. Ohl C, Albach C, Altevogt P, Schmitz B. < i> N</i>-glycosylation patterns of HSA/CD24 from different cell lines and brain homogenates: a comparison. *Biochimie*. 2003;85(6):565-73.
12. Aigner S, Sthoeger ZM, Fogel M, Weber E, Zarn J, Ruppert M, et al. CD24, a mucin-type glycoprotein, is a ligand for P-selectin on human tumor cells. *Blood*. 1997;89(9):3385-95.
13. Kneuer C, Ehrhardt C, Radomski MW, Bakowsky U. Selectins-potential pharmacological targets? *Drug discovery today*. 2006;11(21-22):1034-40.
14. Aigner S, Ramos CL, Hafezi-moghadam A, Lawrence MB, Friederichs J, Altevogt P, et al. CD24 mediates rolling of breast carcinoma cells on P-selectin. *The FASEB journal*. 1998;12(12):1241-51.
15. Baumann P, Cremers N, Kroese F, Orend G, Chiquet-Ehrismann R, Uede T, et al. CD24 expression causes the acquisition of multiple cellular properties associated with tumor growth and metastasis. *Cancer research*. 2005;65(23):10783.
16. Kadmon G, Halbach F, Horstkorte R, Eckert M, Altevogt P, Schachner M. Evidence for Cis Interaction and Cooperative Signalling by the Heat-stable Antigen Nectadrin (murine CD24) and the Cell Adhesion Molecule L1 in Neurons. *European Journal of Neuroscience*. 1995;7(5):993-1004.
17. Lieberoth A, Splittstoesser F, Katagihallimath N, Jakovcevski I, Loers G, Ranscht B, et al. Lewis(x) and alpha2,3-sialyl glycans and their receptors TAG-1, Contactin, and L1 mediate CD24-dependent neurite outgrowth. *J Neurosci*. 2009 May 20;29(20):6677-90.

References.

18. Kleene R, Yang H, Kutsche M, Schachner M. The Neural Recognition Molecule L1 Is a Sialic Acid-binding Lectin for CD24, Which Induces Promotion and Inhibition of Neurite Outgrowth. *Journal of Biological Chemistry*. 2001;276(24):21656-63.
19. Lieberoth A, Splittstoesser F, Katagihallimath N, Jakovcevski I, Loers G, Ranscht B, et al. Lewisx and α 2,3-Sialyl Glycans and Their Receptors TAG-1, Contactin, and L1 Mediate CD24-Dependent Neurite Outgrowth. *The Journal of Neuroscience*. 2009;29(20):6677-90.
20. Varki A, Angata T. Siglecs—the major subfamily of I-type lectins. *Glycobiology*. 2006 January 2006;16(1):1R-27R.
21. Liu Y, Chen GY, Zheng P. CD24-Siglec G/10 discriminates danger-from pathogen-associated molecular patterns. *Trends in immunology*. 2009;30(12):557-61.
22. Kay R, Rosten P, Humphries R. CD24, a signal transducer modulating B cell activation responses, is a very short peptide with a glycosyl phosphatidylinositol membrane anchor. *The Journal of Immunology*. 1991 August 15, 1991;147(4):1412-6.
23. Schabath H, Runz S, Joumaa S, Altevogt P. CD24 affects CXCR4 function in pre-B lymphocytes and breast carcinoma cells. *Journal of Cell Science*. 2006 January 15, 2006;119(2):314-25.
24. Tan Y, Zhao M, Xiang B, Chang C, Lu Q. CD24: from a Hematopoietic Differentiation Antigen to a Genetic Risk Factor for Multiple Autoimmune Diseases. *Clin Rev Allergy Immunol*. 2016 Feb;50(1):70-83.
25. Fang X, Zheng P, Tang J, Liu Y. CD24: from A to Z. *Cellular & molecular immunology*. 2010;7(2):100-3.
26. Ahmed MAH, Jackson D, Seth R, Robins A, Lobo DN, Tomlinson IPM, et al. CD24 is upregulated in inflammatory bowel disease and stimulates cell motility and colony formation. *Inflammatory Bowel Diseases*. 2010;16(5):795-803.
27. Zhang C, Li C, He F, Cai Y, Yang H. Identification of CD44+CD24+ gastric cancer stem cells. *Journal of cancer research and clinical oncology*. 2011;137(11):1679-86.
28. Duckworth CA, Clyde D, Pritchard DM. CD24 is expressed in gastric parietal cells and regulates apoptosis and the response to *Helicobacter felis* infection in the murine stomach. *Am J Physiol Gastrointest Liver Physiol*. 2012 Oct;303(8):G915-26.
29. Ahmed M, Al-Attar A, Kim J, Watson N, Scholefield J, Durrant L, et al. CD24 shows early upregulation and nuclear expression but is not a prognostic marker in colorectal cancer. *Journal of clinical pathology*. 2009;62(12):1117.
30. Keeratichamroen S, Leelawat K, Thongtawee T, Narong S, Aegem U, Tujinda S, et al. Expression of CD24 in cholangiocarcinoma cells is associated with disease progression and reduced patient survival. *International journal of oncology*. 2011;39(4):873-81.
31. Hurt EM, Kawasaki BT, Klarmann GJ, Thomas SB, Farrar WL. CD44+ CD24- prostate cells are early cancer progenitor/stem cells that provide a model for patients with poor prognosis. *British journal of cancer*. 2008;98(4):756-65.
32. Overdevest JB, Thomas S, Kristiansen G, Hansel DE, Smith SC, Theodorescu D. CD24 offers a therapeutic target for control of bladder cancer metastasis based on a requirement for lung colonization. *Cancer Research*. 2011;71(11):3802-11.
33. Baumann P, Thiele W, Cremers N, Muppala S, Krachulec J, Diefenbacher M, et al. CD24 interacts with and promotes the activity of c-src within lipid rafts in breast cancer cells, thereby increasing integrin-dependent adhesion. *Cellular and molecular life sciences : CMLS*. 2011.

References.

34. Kitaura Y, Chikazawa N, Tasaka T, Nakano K, Tanaka M, Onishi H, et al. Transforming growth factor β 1 contributes to the invasiveness of pancreatic ductal adenocarcinoma cells through the regulation of CD24 expression. *Pancreas*. 2011;40(7):1034-42.
35. Sagiv E, Memeo L, Karin A, Kazanov D, Jacob-Hirsch J, Mansukhani M, et al. CD24 is a new oncogene, early at the multistep process of colorectal cancer carcinogenesis. *Gastroenterology*. 2006;131(2):630-9.
36. Sheng L, Shui Y. CD24 polymorphism and hepatocellular carcinoma. *Hepatology (Baltimore, Md)*. 2011.
37. Gao MQ, Choi YP, Kang S, Youn JH, Cho NH. CD24+ cells from hierarchically organized ovarian cancer are enriched in cancer stem cells. *Oncogene*. 2010;29(18):2672-80.
38. Zhu D, McCarthy H, Ottensmeier CH, Johnson P, Hamblin TJ, Stevenson FK. Acquisition of potential N-glycosylation sites in the immunoglobulin variable region by somatic mutation is a distinctive feature of follicular lymphoma. *Blood*. 2002 Apr;99(7):2562-8.
39. Suzuki T, Kiyokawa N, Taguchi T, Sekino T, Katagiri YU, Fujimoto J. CD24 Induces Apoptosis in Human B Cells Via the Glycolipid-Enriched Membrane Domains/Rafts-Mediated Signaling System. *The Journal of Immunology*. 2001 May 1, 2001;166(9):5567-77.
40. Li O, Zheng P, Liu Y. CD24 expression on T cells is required for optimal T cell proliferation in lymphopenic host. *The Journal of experimental medicine*. 2004;200(8):1083.
41. Chen GY, Tang J, Zheng P, Liu Y. CD24 and Siglec-10 Selectively Repress Tissue Damage-Induced Immune Responses. *Science*. 2009;323(5922):1722.
42. Liu JQ, Carl JW, Joshi PS, RayChaudhury A, Pu XA, Shi FD, et al. CD24 on the resident cells of the central nervous system enhances experimental autoimmune encephalomyelitis. *J Immunol*. 2007 May;178(10):6227-35.
43. Sammar M, Aigner S, Altevogt P. Heat-stable antigen (mouse CD24) in the brain: dual but distinct interaction with P-selectin and L1. *Biochim Biophys Acta*. 1997 Feb 8;1337(2):287-94.
44. Diaz-Gallo LM, Medrano LM, Gómez-García M, Cardeña C, Rodrigo L, Mendoza JL, et al. Analysis of the influence of two CD24 genetic variants in Crohn's disease and ulcerative colitis. *Human immunology*. 2011;72(10):969-72.
45. Lee YH, Bae SC. Association between functional CD24 polymorphisms and susceptibility to autoimmune diseases: A meta-analysis. *Cell Mol Biol (Noisy-le-grand)*. 2015;61(8):97-104.
46. González SJ, Rojas JI, Redal MA, Patrucco L, Correale J, Argibay PF, et al. CD24 as a genetic modifier of disease progression in multiple sclerosis in Argentinean patients. *Journal of the neurological sciences*. 2011;307(1-2):18-21.
47. Huang XL, Xu DH, Wang GP, Zhang S, Yu CG. Associations between CD24 gene polymorphisms and inflammatory bowel disease: A meta-analysis. *World J Gastroenterol*. 2015 May 21;21(19):6052-9.
48. Dalerba P, Cho RW, Clarke MF. Cancer stem cells: models and concepts. *Annu Rev Med*. 2007;58:267-84.
49. Vermeulen L, Todaro M, de Sousa Mello F, Sprick MR, Kemper K, Perez Alea M, et al. Single-cell cloning of colon cancer stem cells reveals a multi-lineage differentiation capacity. *Proceedings of the National Academy of Sciences of the United States of America*. 2008;105(36):13427-32.
50. Reya T, Morrison SJ, Clarke MF, Weissman IL. Stem cells, cancer, and cancer stem cells. 2001.
51. Kemper K, Grandela C, Medema JP. Molecular identification and targeting of colorectal cancer stem cells. *Oncotarget*. 2010;1(6):396-404.

References.

52. Takahashi-Yanaga F, Kahn M. Targeting Wnt signaling: can we safely eradicate cancer stem cells? *Clinical Cancer Research*. 2010;16(12):3153.
53. O'Brien CA, Pollett A, Gallinger S, Dick JE. A human colon cancer cell capable of initiating tumour growth in immunodeficient mice. *Nature*. 2006;445(7123):106-10.
54. Li C, Heidt DG, Dalerba P, Burant CF, Zhang L, Adsay V, et al. Identification of pancreatic cancer stem cells. *Cancer research*. 2007;67(3):1030.
55. Bretz N, Noske A, Keller S, Erbe-Hofmann N, Schlange T, Salnikow AV, et al. CD24 promotes tumor cell invasion by suppressing tissue factor pathway inhibitor-2 (TFPI-2) in a c-Src-dependent fashion. *Clinical & Experimental Metastasis*. 2011.
56. Lee KM, Ju JH, Jang K, Yang W, Yi JY, Noh DY, et al. CD24 regulates cell proliferation and transforming growth factor β -induced epithelial to mesenchymal transition through modulation of integrin β 1 stability. *Cell Signal*. 2012 Nov;24(11):2132-42.
57. Su N, Peng L, Xia B, Zhao Y, Xu A, Wang J, et al. Lyn is involved in CD24-induced ERK1/2 activation in colorectal cancer. *Mol Cancer*. 2012;11:43.
58. Zheng J, Li Y, Yang J, Liu Q, Shi M, Zhang R, et al. NDRG2 inhibits hepatocellular carcinoma adhesion, migration and invasion by regulating CD24 expression. *BMC cancer*. 2011;11(1):251.
59. Friederichs J, Zeller Y, Hafezi-Moghadam A, Gröne H-J, Ley K, Altevogt P. The CD24/P-selectin Binding Pathway Initiates Lung Arrest of Human A125 Adenocarcinoma Cells. *Cancer Research*. 2000 December 1, 2000;60(23):6714-22.
60. Jiao XL, Zhao C, Niu M, Chen D. Downregulation of CD24 inhibits invasive growth, facilitates apoptosis and enhances chemosensitivity in gastric cancer AGS cells. *Eur Rev Med Pharmacol Sci*. 2013 Jul;17(13):1709-15.
61. Lee SH, Kim H, Hwang JH, Shin E, Lee HS, Hwang DW, et al. CD24 and S100A4 expression in resectable pancreatic cancers with earlier disease recurrence and poor survival. *Pancreas*. 2014 Apr;43(3):380-8.
62. Yang XR, Xu Y, Yu B, Zhou J, Li JC, Qiu SJ, et al. CD24 is a novel predictor for poor prognosis of hepatocellular carcinoma after surgery. *Clinical Cancer Research*. 2009;15(17):5518-27.
63. Sagiv E, Starr A, Rozovski U, Khosravi R, Altevogt P, Wang T, et al. Targeting CD24 for treatment of colorectal and pancreatic cancer by monoclonal antibodies or small interfering RNA. *Cancer research*. 2008;68(8):2803.
64. Grützmann J, Allinger I, Kristiansen CPMDG. Expression of CD24 in adenocarcinomas of the pancreas correlates with higher tumor grades. *Pancreatology*. 2004;4:454-60.
65. Shapira S, Shapira A, Starr A, Kazanov D, Kraus S, Benhar I, et al. An immunoconjugate of anti-CD24 and Pseudomonas exotoxin selectively kills human colorectal tumors in mice. *Gastroenterology*. 2011;140(3):935-46.
66. Paulson JC, Kawasaki N. Sialidase inhibitors DAMPen sepsis. *Nat Biotech*. [News and Views]. 2011 05//print;29(5):406-7.
67. Liu Y, Zheng P, Chen G-Y, Zheng X, Cheng X, Kunkel S, et al., inventors; Treatment of drug-related side effect and tissue damage by targeting the CD24-HMGB1-Siglec10 axis patent U.S. Pat. No. 8,163,281. 2014 2014-1-28.
68. Kristiansen G, Machado E, Bretz N, Rupp C, Winzer KJ, König AK, et al. Molecular and clinical dissection of CD24 antibody specificity by a comprehensive comparative analysis. *Laboratory Investigation*. 2010;90(7):1102-16.

References.

69. Lieu CH, Klauck PJ, Henthorn PK, Tentler JJ, Tan AC, Spreafico A, et al. Antitumor activity of a potent MEK inhibitor, TAK-733, against colorectal cancer cell lines and patient derived xenografts. *Oncotarget*. 2015 Oct 27;6(33):34561-72.
70. Kim TK, Eberwine JH. Mammalian cell transfection: the present and the future. *Anal Bioanal Chem*. 2010;397(8):3173-8.
71. Dalby B, Cates S, Harris A, Ohki EC, Tilkins ML, Price PJ, et al. Advanced transfection with Lipofectamine 2000 reagent: primary neurons, siRNA, and high-throughput applications. *Methods*. 2004 2004/06/01/;33(2):95-103.
72. Geback T, Schulz MM, Koumoutsakos P, Detmar M. TScratch: a novel and simple software tool for automated analysis of monolayer wound healing assays. *Biotechniques*. 2009 Apr;46(4):265-74.
73. Bianchi ME. DAMPs, PAMPs and alarmins: all we need to know about danger. *Journal of Leukocyte Biology*. 2007 January 1, 2007;81(1):1-5.
74. Dai S, Sodhi C, Cetin S, Richardson W, Branca M, Neal MD, et al. Extracellular High Mobility Group Box-1 (HMGB1) Inhibits Enterocyte Migration via Activation of Toll-like Receptor-4 and Increased Cell-Matrix Adhesiveness. *Journal of Biological Chemistry*. 2010 February 12, 2010;285(7):4995-5002.
75. Ulloa L, Messmer D. High-mobility group box 1 (HMGB1) protein: Friend and foe. *Cytokine & Growth Factor Reviews*. 2006 6//;17(3):189-201.
76. Kono H, Rock KL. How dying cells alert the immune system to danger. *Nat Rev Immunol*. [10.1038/nri2215]. 2008 04//print;8(4):279-89.
77. Schindelmann S, Windisch J, Grundmann R, Kreienberg R, Zeillinger R, Deissler H. Expression profiling of mammary carcinoma cell lines: correlation of in vitro invasiveness with expression of CD24. *Tumor biology*. 2002;23(3):139-45.
78. Mossanen JC, Tacke F. Acetaminophen-induced acute liver injury in mice. *Laboratory Animals*. 2015 2015/04/01;49(1_suppl):30-6.
79. Lee JY, Zhao L, Hwang DH. Modulation of pattern recognition receptor-mediated inflammation and risk of chronic diseases by dietary fatty acids. *Nutrition Reviews*. [10.1111/j.1753-4887.2009.00259.x]. 2010;68(1):38-61.
80. Lotfi R, Eisenbacher J, Solgi G, Fuchs K, Yildiz T, Nienhaus C, et al. Human mesenchymal stem cells respond to native but not oxidized damage associated molecular pattern molecules from necrotic (tumor) material. *Eur J Immunol*. 2011 Jul;41(7):2021-8.
81. Rovere-Querini P, Capobianco A, Scaffidi P, Valentinis B, Catalanotti F, Giazzon M, et al. HMGB1 is an endogenous immune adjuvant released by necrotic cells. *EMBO Reports*. 2004;5(8):825-30.
82. Yang D, Chen Q, Yang H, Tracey KJ, Bustin M, Oppenheim JJ. High mobility group box-1 protein induces the migration and activation of human dendritic cells and acts as an alarmin. *J Leukoc Biol*. 2007 Jan;81(1):59-66.
83. Runz S, Mierke CT, Joumaa S, Behrens J, Fabry B, Altevogt P. CD24 induces localization of beta1 integrin to lipid raft domains. *Biochemical and biophysical research communications*. [Research Support, Non-U.S. Gov't]. 2008 Jan 4;365(1):35-41.
84. Pistoia V, Raffaghello L. Damage-associated molecular patterns (DAMPs) and mesenchymal stem cells: a matter of attraction and excitement. *Eur J Immunol*. 2011 Jul;41(7):1828-31.
85. Smith SC, Oxford G, Wu Z, Nitz MD, Conaway M, Frierson HF, et al. The Metastasis-Associated Gene CD24 Is Regulated by Ral GTPase and Is a Mediator of Cell Proliferation and Survival in Human Cancer. *Cancer research*. 2006 February 15, 2006;66(4):1917-22.
86. Kang R, Tang D, Schapiro NE, Loux T, Livesey KM, Billiar TR, et al. The HMGB1/RAGE inflammatory pathway promotes pancreatic tumor growth

References.

- by regulating mitochondrial bioenergetics. *Oncogene*. 2014 Jan;33(5):567-77.
87. Shapira S, Kazanov D, Weisblatt S, Starr A, Arber N, Kraus S. The CD24 Protein Inducible Expression System Is an Ideal Tool to Explore the Potential of CD24 as an Oncogene and a Target for Immunotherapy in Vitro and in Vivo. *Journal of Biological Chemistry*. 2011 November 25, 2011;286(47):40548-55.
88. Liu B, Zhang Y, Liao M, Deng Z, Gong L, Jiang J, et al. Clinicopathologic and prognostic significance of CD24 in gallbladder carcinoma. *Pathology oncology research : POR*. 2011;17(1):45-50.
89. Goldman Steven A, Sim F, Auvergne Romane M, inventors; CD24 as a Brain Tumor Stem Cell Marker and a Diagnostic and Therapeutic Target in Primary Neural And Glial Tumors of the Brain. 2011.
90. Aigner S, Ramos CL, Hafezi-Moghadam A, Lawrence MB, Friederichs J, Altevogt P, et al. CD24 mediates rolling of breast carcinoma cells on P-selectin. *Faseb j*. 1998 Sep;12(12):1241-51.
91. Levental I, Grzybek M, Simons K. Greasing Their Way: Lipid Modifications Determine Protein Association with Membrane Rafts. *Biochemistry*. 2010 2010/08/03;49(30):6305-16.
92. Mierke CT, Bretz N, Altevogt P. Contractile forces contribute to increased glycosylphosphatidylinositol-anchored receptor CD24-facilitated cancer cell invasion. *The Journal of biological chemistry*. 2011;286(40):34858-71.
93. Burridge K, Fath K, Kelly T, Nuckolls G, Turner C. Focal Adhesions - Transmembrane Junctions Between The Extracellular-Matrix And The Cytoskeleton. *Annual Review of Cell Biology*. 1988;4:487-525.
94. Elad N, Volberg T, Patla I, Hirschfeld-Warneken V, Grashoff C, Spatz JP, et al. The role of integrin-linked kinase in the molecular architecture of focal adhesions. *J Cell Sci*. 2013 Sep 15;126(Pt 18):4099-107.
95. Yam JW, Tse EY, Ng IO. Role and significance of focal adhesion proteins in hepatocellular carcinoma. *J Gastroenterol Hepatol*. 2009 Apr;24(4):520-30.
96. Hynes RO. Integrins: Bidirectional, allosteric signaling machines. *Cell*. 2002 Sep;110(6):673-87.
97. Stupack DG, Cheresh DA. Get a ligand, get a life: integrins, signaling and cell survival. *J Cell Sci*. 2002 Oct;115(Pt 19):3729-38.
98. Albasri A, Seth R, Jackson D, Benhasouna A, Crook S, Nateri AS, et al. C-terminal Tensin-like (CTEN) is an oncogene which alters cell motility possibly through repression of E-cadherin in colorectal cancer. *J Pathol*. 2009 May;218(1):57-65.
99. Albasri A, Al-Ghamdi S, Fadhil W, Aleskandarany M, Liao YC, Jackson D, et al. Cten signals through integrin-linked kinase (ILK) and may promote metastasis in colorectal cancer. *Oncogene*. 2011 06/30/print;30(26):2997-3002.
100. Al-Ghamdi S, Albasri A, Cachat J, Ibrahim S, Muhammad BA, Jackson D, et al. Cten Is Targeted by Kras Signalling to Regulate Cell Motility in the Colon and Pancreas. *PLoS ONE*. 2011;6(6):e20919.
101. Bretz NP, Salnikov AV, Perne C, Keller S, Wang X, Mierke CT, et al. CD24 controls Src/STAT3 activity in human tumors. *Cellular and Molecular Life Sciences*. 2012:1-17.
102. Lee TK, Castilho A, Cheung VC, Tang KH, Ma S, Ng IO. CD24(+) liver tumor-initiating cells drive self-renewal and tumor initiation through STAT3-mediated NANOG regulation. *Cell Stem Cell*. 2011;9(1):50-63.
103. Barbieri I, Pensa S, Pannellini T, Quaglino E, Maritano D, Demaria M, et al. Constitutively active Stat3 enhances neu-mediated migration and

References.

- metastasis in mammary tumors via upregulation of Cten. *Cancer Res.* 2010 Mar 15;70(6):2558-67.
104. Schaller MD, Borgman CA, Cobb BS, Vines RR, Reynolds AB, Parsons JT. pp125FAK a structurally distinctive protein-tyrosine kinase associated with focal adhesions. *Proc Natl Acad Sci U S A.* 1992 Jun 1;89(11):5192-6.
105. Scheswohl DM, Harrell JR, Rajfur Z, Gao G, Campbell SL, Schaller MD. Multiple paxillin binding sites regulate FAK function. *J Mol Signal.* 2008;3:1.
106. Wade R, Brimer N, Lyons C, Vande Pol S. Paxillin enables attachment-independent tyrosine phosphorylation of focal adhesion kinase and transformation by RAS. *J Biol Chem.* 2011 Nov 4;286(44):37932-44.
107. Lark AL, Livasy CA, Calvo B, Caskey L, Moore DT, Yang X, et al. Overexpression of focal adhesion kinase in primary colorectal carcinomas and colorectal liver metastases: immunohistochemistry and real-time PCR analyses. *Clin Cancer Res.* 2003 Jan;9(1):215-22.
108. Sulzmaier FJ, Jean C, Schlaepfer DD. FAK in cancer: mechanistic findings and clinical applications. *Nat Rev Cancer.* 2014 Sep;14(9):598-610.
109. Hannigan G, Troussard AA, Dedhar S. Integrin-linked kinase: a cancer therapeutic target unique among its ILK. *Nat Rev Cancer.* [10.1038/nrc1524]. 2005 01//print;5(1):51-63.
110. Persad S, Dedhar S. The role of integrin-linked kinase (ILK) in cancer progression. *Cancer and Metastasis Reviews.* 2003 2003/12/01;22(4):375-84.
111. Han KS, Li N, Raven PA, Fazli L, Ettinger S, Hong SJ, et al. Targeting Integrin-Linked Kinase Suppresses Invasion and Metastasis through Downregulation of Epithelial-to-Mesenchymal Transition in Renal Cell Carcinoma. *Mol Cancer Ther.* 2015 Apr;14(4):1024-34.
112. Bravou V, Klironomos G, Papadaki E, Taraviras S, Varakis J. ILK overexpression in human colon cancer progression correlates with activation of beta-catenin, down-regulation of E-cadherin and activation of the Akt-FKHR pathway. *J Pathol.* 2006 Jan;208(1):91-9.
113. Dai DL, Makretsov N, Campos EI, Huang C, Zhou Y, Huntsman D, et al. Increased expression of integrin-linked kinase is correlated with melanoma progression and poor patient survival. *Clin Cancer Res.* 2003 Oct 1;9(12):4409-14.
114. Bravou V, Klironomos G, Papadaki E, Stefanou D, Varakis J. Integrin-linked kinase (ILK) expression in human colon cancer. *Br J Cancer.* England; 2003. p. 2340-1.
115. Al-Ghamdi S, Cachat J, Albasri A, Ahmed M, Jackson D, Zaitoun A, et al. C-terminal tensin-like gene functions as an oncogene and promotes cell motility in pancreatic cancer. *Pancreas.* 2013 Jan;42(1):135-40.
116. Zhao J, Guan JL. Signal transduction by focal adhesion kinase in cancer. *Cancer Metastasis Rev.* 2009 Jun;28(1-2):35-49.
117. Wu JC, Chen YC, Kuo CT, Yu HW, Chen YQ, Chiou A, et al. Focal adhesion kinase-dependent focal adhesion recruitment of SH2 domains directs SRC into focal adhesions to regulate cell adhesion and migration. *Scientific Reports.* 2015 Dec;5.
118. Nikolopoulos SN, Turner CE. Integrin-linked kinase (ILK) binding to paxillin LD1 motif regulates ILK localization to focal adhesions. *J Biol Chem.* 2001 Jun 29;276(26):23499-505.
119. Liao Y-C, Chen N-T, Shih Y-P, Dong Y, Lo SH. Up-regulation of C-terminal tensin-like molecule promotes the tumorigenicity of colon cancer through β -catenin. *Cancer research.* 2009;69(11):4563-6.
120. Varelas X, Bouchie MP, Kukuruzinska MA. Protein N-glycosylation in oral cancer: dysregulated cellular networks among DPAGT1, E-cadherin adhesion and canonical Wnt signaling. *Glycobiology.* 2014 Jul;24(7):579-91.

References.

121. Lisowska E, Jaskiewicz E. Protein Glycosylation, an Overview. eLS: John Wiley & Sons, Ltd; 2001.
122. Drickamer K TM. Introduction to Glycobiology. (2nd ed.) ed. USA.: Oxford University Press; 2006.
123. Bause E, Legler G. The role of the hydroxy amino acid in the triplet sequence Asn-Xaa-Thr(Ser) for the N-glycosylation step during glycoprotein biosynthesis. *Biochem J.* 1981 Jun 1;195(3):639-44.
124. Rao RS, Bernd W. Do N-glycoproteins have preference for specific sequons? *Bioinformatics.* 2010;5(5):208-12.
125. Shakin-Eshleman SH, Spitalnik SL, Kasturi L. The amino acid at the X position of an Asn-X-Ser sequon is an important determinant of N-linked core-glycosylation efficiency. *J Biol Chem.* 1996 Mar 15;271(11):6363-6.
126. Drake RR, Jones EE, Powers TW, Nyalwidhe JO. Altered glycosylation in prostate cancer. *Adv Cancer Res.* 2015;126:345-82.
127. Hang I, Lin CW, Grant OC, Fleurkens S, Villiger TK, Soos M, et al. Analysis of site-specific N-glycan remodelling in the ER and the Golgi. *Glycobiology.* 2015 Aug.
128. Han M, Wang X, Ding H, Jin M, Yu L, Wang J, et al. The role of N-glycosylation sites in the activity, stability, and expression of the recombinant elastase expressed by *Pichia pastoris*. *Enzyme Microb Technol.* 2014 Jan;54:32-7.
129. Bhatia PK, Mukhopadhyay A. Protein glycosylation: implications for in vivo functions and therapeutic applications. *Adv Biochem Eng Biotechnol.* 1999;64:155-201.
130. Kukuruzinska MA, Lennon K. Protein N-glycosylation: molecular genetics and functional significance. *Crit Rev Oral Biol Med.* 1998;9(4):415-48.
131. Brockhausen I, Schutzbach J, Kuhns W. Glycoproteins and their relationship to human disease. *Acta Anat (Basel).* 1998;161(1-4):36-78.
132. Brockhausen I. Pathways of O-glycan biosynthesis in cancer cells. *Biochim Biophys Acta.* 1999 Dec;1473(1):67-95.
133. Irimura T, Denda K, Iida S, Takeuchi H, Kato K. Diverse glycosylation of MUC1 and MUC2: potential significance in tumor immunity. *J Biochem.* 1999 Dec;126(6):975-85.
134. Sethi MK, Kim H, Park CK, Baker MS, Paik YK, Packer NH, et al. In-depth N-glycome profiling of paired colorectal cancer and non-tumorigenic tissues reveals cancer-, stage- and EGFR-specific protein N-glycosylation. *Glycobiology.* 2015 Oct;25(10):1064-78.
135. Kaprio T, Satomaa T, Heiskanen A, Hokke CH, Deelder AM, Mustonen H, et al. N-glycomic profiling as a tool to separate rectal adenomas from carcinomas. *Mol Cell Proteomics.* 2015 Feb;14(2):277-88.
136. Padler-Karavani V. Aiming at the sweet side of cancer: aberrant glycosylation as possible target for personalized-medicine. *Cancer Lett.* 2014 Sep;352(1):102-12.
137. Haakensen VD, Steinfeld I, Saldova R, Shehni AA, Kifer I, Naume B, et al. Serum N-glycan analysis in breast cancer patients - Relation to tumour biology and clinical outcome. *Mol Oncol.* 2015 Aug.
138. Friederichs J, Zeller Y, Hafezi-Moghadam A, Grone HJ, Ley K, Altevogt P. The CD24/P-selectin binding pathway initiates lung arrest of human A125 adenocarcinoma cells. *Cancer Res.* 2000 Dec 1;60(23):6714-22.
139. Choi YL, Lee SH, Kwon GY, Park CK, Han JJ, Choi JS, et al. Overexpression of CD24: association with invasiveness in urothelial carcinoma of the bladder. 2009.
140. Gerger A, Zhang W, Yang D, Bohanes P, Ning Y, Winder T, et al. Common cancer stem cell gene variants predict colon cancer recurrence. *Clinical cancer research : an official journal of the American Association for Cancer Research.* 2011;17(21):6934-43.

References.

141. Poncet C, Frances V, Gristina R, Scheiner C, Pellissier JF, Figarella-Branger D. CD24, a glycosylphosphatidylinositol-anchored molecules is transiently expressed during the development of human central nervous system and is a marker of human neural cell lineage tumors. *Acta Neuropathol.* 1996;91(4):400-8.
142. Bleckmann C, Geyer H, Reinhold V, Lieberoth A, Schachner M, Kleene R, et al. Glycomic analysis of N-linked carbohydrate epitopes from CD24 of mouse brain. *Journal of Proteome Research.* 2009 //;8(2):567-82.
143. Kobata A. A journey to the world of glycobiology. *Glycoconj J.* 2000 Jul-Sep;17(7-9):443-64.
144. Bleckmann C, Geyer H, Lieberoth A, Splittstoesser F, Liu Y, Feizi T, et al. O-glycosylation pattern of CD24 from mouse brain. *Biological chemistry.* 2009;390(7):627-45.
145. Motari E, Zheng X, Su X, Liu Y, Kvaratskhelia M, Freitas M, et al. Analysis of Recombinant CD24 Glycans by MALDI-TOF-MS Reveals Prevalence of Sialyl-T Antigen. *American journal of biomedical sciences.* 2009;1(1):1-11.
146. Biolabs NE. Glycosaminoglycan Chains (GAGs) and Glycolipids.
147. Hart GW. The role of asparagine-linked oligosaccharides in cellular recognition by thymic lymphocytes. Effects of tunicamycin on the mixed lymphocyte reaction. *Journal of Biological Chemistry.* 1982;257(1):151-8.
148. Amino Acids. 2017 [updated 2017; cited]; Available from: http://www.biochem.umd.edu/biochem/kahn/teach_res/amino_acids/.
149. Reikofski J, Tao BY. Polymerase chain reaction (PCR) techniques for site-directed mutagenesis. *Biotechnol Adv.* 1992;10(4):535-47.
150. Xia Y, Chu W, Qi Q, Xun L. New insights into the QuikChange™ process guide the use of Phusion DNA polymerase for site-directed mutagenesis. *Nucleic Acids Research.* 2014.
151. Chen HM, Ford C, Reilly PJ. Substitution of asparagine residues in *Aspergillus awamori* glucoamylase by site-directed mutagenesis to eliminate N-glycosylation and inactivation by deamidation. *Biochem J.* 1994 Jul 1;301 (Pt 1):275-81.
152. Sabel J, Clore A, Reinertson B, Rose S. Ultramer™ Oligonucleotides Experimental Overview, Protocol, Troubleshooting.: Integrated DNA Technologies; 2011 [cited. Available from: <http://www.idtdna.com/site>.
153. Acevedo-Rocha CG, Reetz MT, Nov Y. Economical analysis of saturation mutagenesis experiments. *Scientific Reports.* [Article]. 2015 07/20/online;5:10654.
154. Karnik A, Karnik R, Grefen C. SDM-Assist software to design site-directed mutagenesis primers introducing "silent" restriction sites. *BMC Bioinformatics.* 2013 2013//;14(1):1-9.
155. Springer T, Galfre G, Secher D, Milstein C. Monoclonal xenogeneic antibodies to murine cell surface antigens: identification of novel leukocyte differentiation antigens. *European Journal of Immunology.* 1978;8(8):539-51.
156. Hough MR, Rosten PM, Sexton TL, Kay R, Humphries RK. Mapping of CD24 and homologous sequences to multiple chromosomal loci. *Genomics.* 1994;22(1):154-61.
157. Chou YY, Jeng YM, Lee TT, Hu FC, Kao HL, Lin WC, et al. Cytoplasmic CD24 expression is a novel prognostic factor in diffuse-type gastric adenocarcinoma. *Annals of surgical oncology.* 2007;14(10):2748-58.
158. Fang X, Zheng P, Tang J, Liu Y. CD24: from A to Z. *Cellular and Molecular Immunology.* 2010;7(2):100-3.
159. Lambert R, Provenzale D, Ectors N, Vainio H, Dixon M, Atkin W, et al. Early diagnosis and prevention of sporadic colorectal cancers. *Endoscopy.* 2001;33(12):1042-64.

References.

160. Motari E, Zheng X, Su X, Liu Y, Kvaratskhelia M, Freitas M, et al. Analysis of Recombinant CD24 Glycans by MALDI-TOF-MS Reveals Prevalence of Sialyl-T Antigen. *American journal of biomedical sciences*. 2009;1(1):1.
161. Bironaite D, Nesland JM, Dalen H, Risberg B, Bryne M. N-Glycans influence the in vitro adhesive and invasive behaviour of three metastatic cell lines. *Tumour Biol*. 2000 2000 May-Jun;21(3):165-75.

Appendix.

Appendix.

Appendix:

Appendix i. Brief Intro to CD24.

CD24 antigen (small cell lung carcinoma cluster 4 antigen)
CD24 molecule Synonyms : CD24A ; FLJ22950 ; FLJ43543 ; MGC75043 ;
CD24 antigen;
Locus ID: 100133941 Cytogenetic: 6q21
RefSeq: BC064619.1, AAH64619
RefSeq Size: 2180
RefSeq ORF: 243
[RefSeq, Jul 2008].
CD24 ORF sequence:

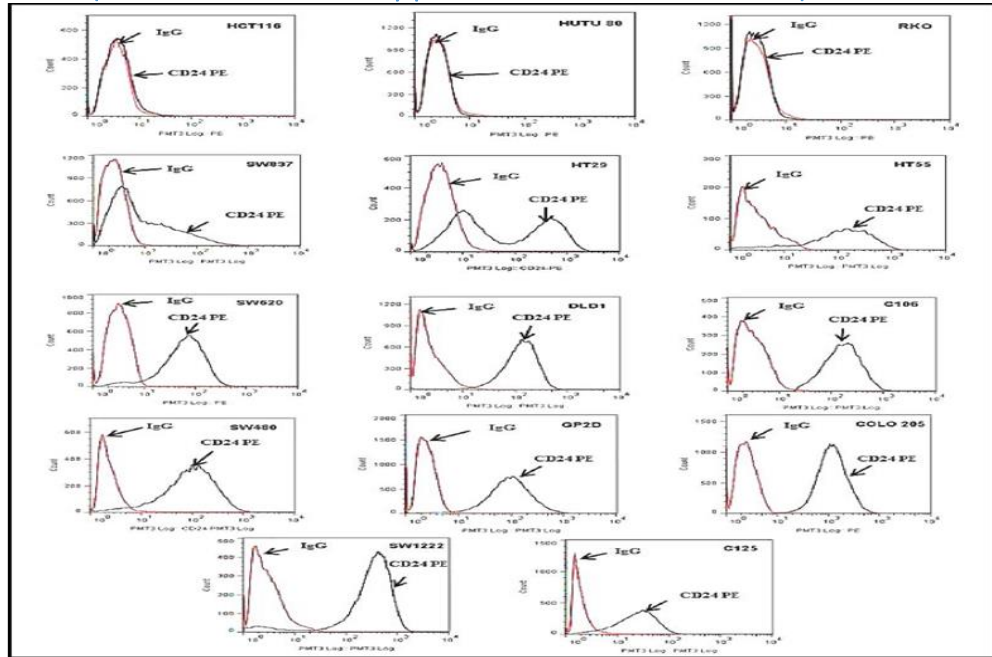
[NCBI RefSeq Nucleic](#) | NM_013230 | XM_001725629 | Homo sapiens CD24 molecule (CD24), mRNA

Appendix ii. CD24 (BC064619) Human cDNA.

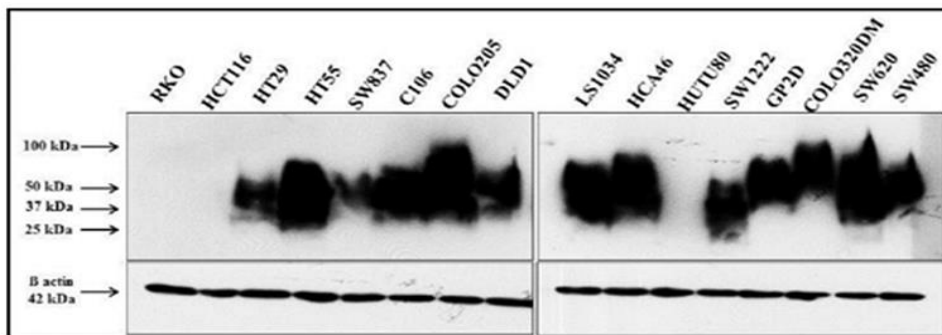
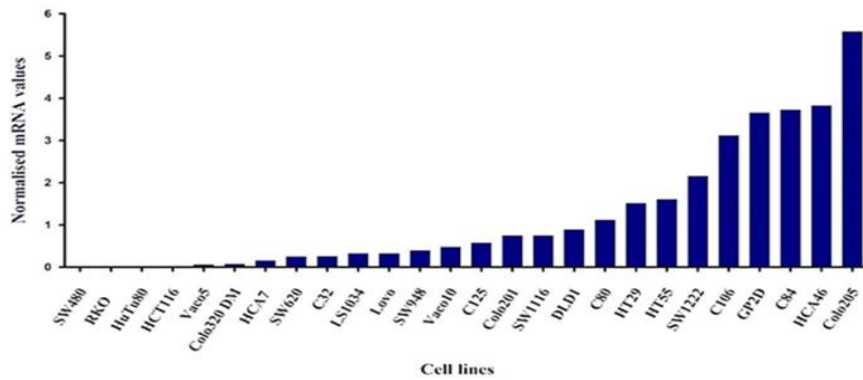
Clonehttp://www.origene.com/human_cdna/BC064619/SC126016.aspx

```
CCCCGAGCCAGCGGTTCTCCAAGCACCAGCATCCTGCTAGACGCGCCGCGCACCCGACGG
AGGGGACATGGGCAGAGCAATGGTGGCCAGGCTCGGGCTGGGGCTGCTGCTGGCACT
GCTCCTACCCACGCAGATTTATTCCAGTGAAACAACAACCTGGAACCTCAAGTAACCTCCTC
CCAGAGTACTTCCAACCTCTGGGTTGGCCCCAAATCCAACATAATGCCACCACCAAGCGGC
TGGTGGTGCCTGCAGTCAACAGCCAGTCTCTTCGTGGTCTCACTCTCTCTTCTGCATCT
CTACTCTTAAGAGACTCAGGCCAAGAAACGTCTTCTAAATTTCCCATCTTCTAAACCCA
ATCCAAATGGCGTCTGGAAGTCCAATGTGGCAAGGAAAAACAGGTCTTCATCGAATCTAC
TAATTCACACCTTTTATTGACACAGAAAATGTTGAGAATCCCAAATTTGATTGATTTGA
AGAACATGTGAGAGGTTTGACTAGATGATGGATGCCAATATTAATCTGCTGGAGTTTCA
TGTACAAGATGAAGGAGAGGCAACATCCAAAATAGTTAAGACATGATTTCTTGAATGTG
GCTTGAGAAATATGGACACTTAATACTACCTTGAAAATAAGAATAGAAAATAAGGATGGG
ATTGTGGAATGGAGATTCAGTTTTTCATTTGGTTCATTAATTTCTATAAGGCCATAAAACAG
GTAATATAAAAAGCTTCCATGATTTCTATTTATATGTACATGAGAAGGAACTTCCAGGTGT
TACTGTAATTCCTCAACGTATTGTTTCGACAGCCTAATTTAATGCCGATATACTCTAGA
TGAAGTTTTACATTTGAGCTATTGCTGTTCTCTTGGGAAGTGAACCTCACTTTCTCCT
GAGGCTTTGGATTTGACATTTGCATTTGACCTTTTATGTAGTAATTGACATGTGCCAGGGC
AATGATGAATGAGAATCTACCCAGATCCAAGCATCCTGAGCAACTCTTGATTATCCAT
ATTGAGTCAAATGGTAGGCATTTCTATCACCTGTTTCCATTCAACAAGAGCACTACATT
CATTAGCTAAACGGATTCCAAAGAGTAGAATTGCATTGACCGGACTAATTTCAAATG
CTTTTTATTATTATTTTTTTTTAGACAGTCTCACTTTGTGCGCCAGGCCGGAGTGCAGTG
GTGCGATCTCAGATCAGTGTACCATTTGCCTCCCGGGCTCAAGCGATTCTCCTGCCTCAG
CTCCCAAGTAGCTGGGATTACAGGCACCTGCCACCATGCCCGGCTAATTTTTGTAATTT
TAGTAGAGACAGGGTTTCACCATGTTGCCAGGCTGGTTTCGAACCTCTGACCTCAGGTG
ATCCACCCGCTCGGCCTCCCAAAGTGCTGGGATTACAGGCTTGAGCCCCGCGCCACG
CATCAAAATGCTTTTTATTTCTGCATATGTTGAATACTTTTTACAATTTAAAAAATGAT
CTGTTTTGAAGGCAAAATTGCAAATCTTGAAATTAAGAAGGCAAAAATGTAAAGGAGTCA
AACTATAAATCAAGTATTTGGGAAGTGAAGACGAAGCTAATTTGCATTAATTTACAAA
CTTTTATACTCTTTCTGTATATACATTTTTTTCTTTAAAAAACAACATATGGATCAGAAT
AGCCACATTTGGAACACTTTTTGTTATCAGTCAATATTTTTAGATAGTTAGAACCCTGGTC
CTAAGCCTAAAAGTGGGCTTGATTTCTGCAGTAAATCTTTTACAACCTGCCTCGACACACAT
AAACCTTTTTAAAAATAGACACTCCCCGAAGTCTTTTGTTCGCATGGTCACACACTGATG
CTTAGATGTTCCAGTAATCTAATATGGCCACAGTAGTCTTGATGACCAAAGTCCTTTTTT
TCCATCTTTAGAAAACATACATGGGAACAAACAGATCGAACAGTTTTTGAAGCTACTGTGTG
TGTGAATGAACACTCTTTTGCTTTATTTCCAGAATGCTGTACATCTATTTGGATTGTATA
TTGTGTTTGTATTTACGCTTTGATTATAGTAACTCTTATGGAATTGATTTGCATTG
AACACAAACTGTAAATAAAAAAGAAATGGCTGAAAGAGCAAAAAAAAAAAAAAAAAAAAA
AAAAAAAAAAAAAAAAAAAA
```

Appendix iii. CD24 expression levels in colorectal carcinoma cell lines (Data from work done by previous PhD student on CD24).



Flow cytometry analysis of CD24 in different colorectal cancer cell lines. The figure shows the differential cell surface expression of CD24 in 14 CRC cell lines. Notably, HCT116, RKO, HUTU 80 were CD24 negative, SW837 and HT29 showed intermediate expression, while SW480, SW620, DLD1, GP2D and most of the remaining cell lines showed high CD24 positivity.



Appendix iv. BCA protein assay Kit standard preparation guidelines.

Preparation of Standards and Working Reagent (required for both assay procedures)**A. Preparation of Diluted Albumin (BSA) Standards**

Use Table 1 as a guide to prepare a set of protein standards. Dilute the contents of one Albumin Standard (BSA) ampule into several clean vials, preferably using the same diluent as the sample(s). Each 1mL ampule of 2mg/mL Albumin Standard is sufficient to prepare a set of diluted standards for either working range suggested in Table 1. There will be sufficient volume for three replications of each diluted standard.

Table 1. Preparation of Diluted Albumin (BSA) Standards

Dilution Scheme for Standard Test Tube Protocol and Microplate Procedure (Working Range = 20-2,000µg/mL)			
<u>Vial</u>	<u>Volume of Diluent</u> (µL)	<u>Volume and Source of BSA</u> (µL)	<u>Final BSA Concentration</u> (µg/mL)
A	0	300 of Stock	2000
B	125	375 of Stock	1500
C	325	325 of Stock	1000
D	175	175 of vial B dilution	750
E	325	325 of vial C dilution	500
F	325	325 of vial E dilution	250
G	325	325 of vial F dilution	125
H	400	100 of vial G dilution	25
I	400	0	0 = Blank

Dilution Scheme for Enhanced Test Tube Protocol (Working Range = 5-250µg/mL)			
<u>Vial</u>	<u>Volume of Diluent</u> (µL)	<u>Volume and Source of BSA</u> (µL)	<u>Final BSA Concentration</u> (µg/mL)
A	700	100 of Stock	250
B	400	400 of vial A dilution	125
C	450	300 of vial B dilution	50
D	400	400 of vial C dilution	25
E	400	100 of vial D dilution	5
F	400	0	0 = Blank

B. Preparation of the BCA Working Reagent (WR)

1. Use the following formula to determine the total volume of WR required:

$$(\# \text{ standards} + \# \text{ unknowns}) \times (\# \text{ replicates}) \times (\text{volume of WR per sample}) = \text{total volume WR required}$$

Example: for the standard test-tube procedure with 3 unknowns and 2 replicates of each sample:

$$(9 \text{ standards} + 3 \text{ unknowns}) \times (2 \text{ replicates}) \times (2\text{mL}) = 48\text{mL WR required}$$

Note: 2.0mL of the WR is required for each sample in the test-tube procedure, while only 200µL of WR reagent is required for each sample in the microplate procedure.

2. Prepare WR by mixing 50 parts of BCA Reagent A with 1 part of BCA Reagent B (50:1, Reagent A:B). For the above example, combine 50mL of Reagent A with 1mL of Reagent B.

Appendix v. BCA microplate procedure for protein quantification.

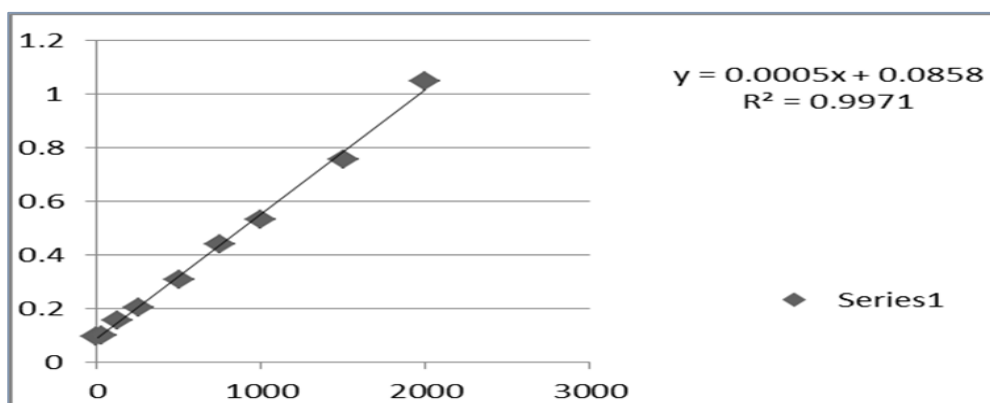
Microplate Procedure (Sample to WR ratio = 1:8)

1. Pipette 25 μ L of each standard or unknown sample replicate into a microplate well (working range = 20-2000 μ g/mL) (e.g., Thermo Scientific™ Pierce™ 96-Well Plates, Product No. 15041).

Note: If sample size is limited, 10 μ L of each unknown sample and standard can be used (sample to WR ratio = 1:20). However, the working range of the assay in this case will be limited to 125-2000 μ g/mL.

2. Add 200 μ L of the WR to each well and mix plate thoroughly on a plate shaker for 30 seconds.
3. Cover plate and incubate at 37°C for 30 minutes.
4. Cool plate to RT. Measure the absorbance at or near 562nm on a plate reader.

Appendix vi. BCA standard curve for protein quantification.



Appendix.

Appendix vii. SDS Polyacrylamide gel recipe.

Solutions for Tris/Glycine SDS-Polyacrylamide Gel Electrophoresis

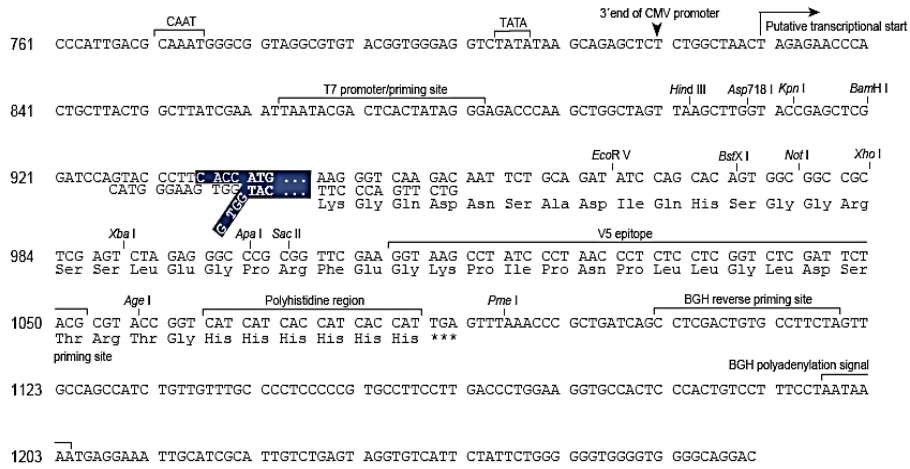
6%	5 ml	10 ml	15 ml	20 ml	25 ml	30 ml	40 ml	50 ml
H ₂ O	2.7	5.3	8.0	10.6	13.3	15.9	21.1	26.5
30% Acrylamide mix ^a	1.0	2.0	3.0	4.0	5.0	6.0	8.0	10.0
1.5 M Tris (pH 8.8)	1.3	2.5	3.8	5.0	6.3	7.5	10.0	12.5
10% SDS ^b	0.05	0.1	0.15	0.2	0.25	0.3	0.4	0.5
10% APS ^c	0.05	0.1	0.15	0.2	0.25	0.3	0.4	0.5
TEMED ^d	0.004	0.008	0.012	0.016	0.02	0.024	0.032	0.04
8%	5 ml	10 ml	15 ml	20 ml	25 ml	30 ml	40 ml	50 ml
H ₂ O	2.3	4.6	7.0	9.3	11.6	13.9	18.6	23.2
30% Acrylamide mix	1.3	2.7	4.0	5.3	6.7	8.0	10.7	13.4
1.5 M Tris (pH 8.8)	1.3	2.5	3.8	5.0	6.3	7.5	10.0	12.5
10% SDS	0.05	0.1	0.15	0.2	0.25	0.3	0.4	0.5
10% APS	0.05	0.1	0.15	0.2	0.25	0.3	0.4	0.5
TEMED	0.003	0.006	0.009	0.012	0.015	0.018	0.024	0.03
10% ↓	5 ml	10 ml	15 ml	20 ml	25 ml	30 ml	40 ml	50 ml
H ₂ O	2.0	4.0	5.9	7.9	9.9	11.9	15.8	20
30% Acrylamide mix	1.7	3.3	5	6.7	8.3	10.0	13.3	16.6
1.5 M Tris (pH 8.8)	1.3	2.5	3.8	5.0	6.3	7.5	10.0	12.5
10% SDS	0.05	0.1	0.15	0.2	0.25	0.3	0.4	0.5
10% APS	0.05	0.1	0.15	0.2	0.25	0.3	0.4	0.5
TEMED	0.002	0.004	0.006	0.008	0.01	0.012	0.016	0.02
12%	5 ml	10 ml	15 ml	20 ml	25 ml	30 ml	40 ml	50 ml
H ₂ O	1.7	3.3	5.0	6.6	8.3	9.9	13.2	16.4
30% Acrylamide mix	2.0	4.0	6.0	8.0	10.0	12.0	14.0	20.0
1.5 M Tris (pH 8.8)	1.3	2.5	3.8	5.0	6.3	7.5	10.0	12.5
10% SDS	0.05	0.1	0.15	0.2	0.25	0.3	0.4	0.5
10% APS	0.05	0.1	0.15	0.2	0.25	0.3	0.4	0.5
TEMED	0.002	0.004	0.006	0.008	0.01	0.012	0.016	0.02
15%	5 ml	10 ml	15 ml	20 ml	25 ml	30 ml	40 ml	50 ml
H ₂ O	1.2	2.3	3.5	4.6	5.7	6.9	9.2	11.4
30% Acrylamide mix	2.5	5.0	7.5	10.0	12.5	15.0	20.0	25.0
1.5 M Tris (pH 8.8)	1.3	2.5	3.8	5.0	6.3	7.5	10.0	12.5
10% SDS	0.05	0.1	0.15	0.2	0.25	0.3	0.4	0.5
10% APS	0.05	0.1	0.15	0.2	0.25	0.3	0.4	0.5
TEMED	0.002	0.004	0.006	0.008	0.01	0.012	0.016	0.02

STACK	1 ml	2 ml	3 ml	4 ml	5 ml	6 ml	8 ml	10 ml
H ₂ O	0.68	1.4	2.1	2.7	3.4	4.1	5.5	6.8
30% Acrylamide mix	0.17	0.33	0.5	0.67	0.83	1.0	1.3	1.7
1.0 M Tris (pH 6.8)	0.13	0.25	0.38	0.5	0.63	0.75	1.0	1.25
10% SDS	0.01	0.02	0.03	0.04	0.05	0.06	0.08	0.1
10% APS	0.01	0.02	0.03	0.04	0.05	0.06	0.08	0.1
TEMED	0.001	0.002	0.003	0.004	0.005	0.006	0.008	0.01

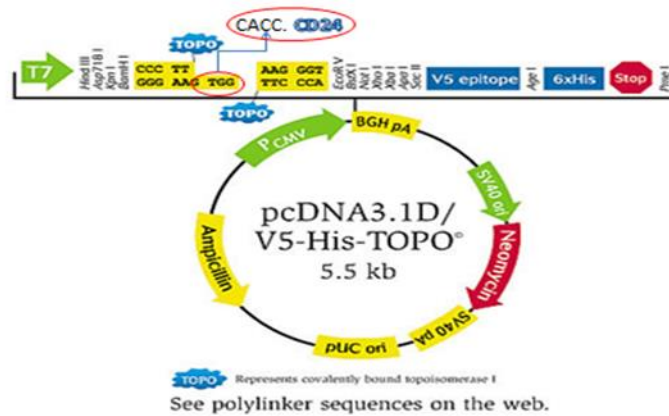
^aCommonly 29.2% acrylamide and 0.8% *N,N'*-methylene-bis-acrylamide; ^bSodium dodecyl sulfate; ^cAmmonium persulfate; ^d*N,N,N',N'*-Tetramethylethylenediamine.

Appendix.

Appendix viii. pcDNA3.1D/V5-His-TOPO vector map:



Appendix ix. Vector Map of His Topo Cloning vector 3.1.



Vector Map of pcDNA3.1 CD24

Appendix x. SOC media Recipe.

SOC media (1 liter total volume):

20 g Bacto Tryptone	10 mL 1M MgCl ₂
5 g Bacto Yeast Extract	10 mL 1M MgSO ₄
2 mL 5M NaCl	20 mL 1M glucose
2.5 mL 1M KCl	